RM No. L7D04

RESEARCH MEMORANDUM

INVESTIGATION OF THE LOADS ON A CONVENTIONAL FRONT AND REAR SLIDING CANOPY

By

Howard E. Dexter and Edward A. Rickey

Langley Memorial Aeronautical Laboratory
Langley Field, Va.

NATIONAL ADVISORY COMMITTEE FOR AERONAUTICS

WASHINGTON

July 9, 1947

NACA RM No. L7D04

NATIONAL ADVISORY COMMITTEE FOR AERONAUTICS

RESEARCH MEMORANDUM

INVESTIGATION OF THE LOADS ON A CONVENTIONAL FRONT AND REAR SLIDING CANOPY

By Howard E. Dexter and Edward A. Rickey

SUMMARY

As one phase of a comprehensive canopy load investigation, conventional front and rear sliding canopies which are typified by installation on the SB2C-4E airplane, were tested in the Langley full-scale tunnel to determine the pressure distributions and the aerodynamic loads on the canopies. A preliminary analysis of the results of these tests is presented in this report. Plots are presented that show the distribution of pressure at four longitudinal stations through each canopy for a range of conditions selected to determine the effects of varying canopy position, yaw, lift coefficient, and power. The results indicate that the maximum loads, based on the external-internal pressure differential, for the front and rear canopies were obtained with the airplane simulating the high speed flight condition. The highest loading on the front canopy was in the exploding direction for the configuration with the front and rear canopies closed. The highest loads on the rear canopy were in the crushing direction with the front canopy open and the rear canopy closed. For most of the simulated flight conditions, the highest loads on the front canopy, per unit area, were over twice as great as the highest loads on the rear canopy when the comparison was made for the most critical canopy configuration in each case. The external pressure distribution over the front and rear canopies, which were fairly symmetrical at 0° angle of yaw, were greatly distorted at other yaw attitudes, particularly for the propeller operating conditions. These distorted pressure distributions resulted in local exploding and crushing loads on both canopies which were often considerably higher than the average canopy loads.

INTRODUCTION

The occurence of canopy failures has indicated that present load requirements used in the design of canopies and their components may

not be adequate. As the current load requirements are based on wind-tunnel pressure distributions obtained over a range of pitch and yaw attitudes with the canopy closed and do not include accurate measurements of internal pressure or of the effects of canopy opening, it is desirable that these factors be investigated and the critical load condition be more accurately defined.

As a result, a general investigation has been conducted at the Langley Laboratory of the National Advisory Committee for Aeronautics to determine the critical load requirements by means of external and internal pressure measurements on airplanes employing three representative types of canopies. The three types of canopies selected for the tests were the conventional single sliding enclosure, conventional front and rear sliding enclosures, and the bubble-type enclosure which are typified by the installations on the Grumman F6F-3, Curtiss SB2C-4E, and Grumman F8F-1 airplane, respectively.

As the first phase of this investigation, tests have been made in the Langley full-scale tunnel to determine external and internal pressure distributions on the three types of canopies for an extensive range of simulated flight conditions with canopy position varied from closed to full open.

This report presents a preliminary analysis of the results obtained with the conventional front and rear sliding canopies on the SB2C-4E airplane. Additional reports have been prepared covering results of the conventional single sliding canopy and the bubble type canopy. (See references 1 and 2.)

SYMBOLS

C_L lift coefficient $\left(\frac{L}{q_o S}\right)$

P pressure coefficient $\left(\frac{p - p_o}{q_o}\right)$

T_o thrust coefficient $\left(\frac{T}{\rho V^2 D^2}\right)$

D propeller diameter, feet

L lift, pounds

p local static pressure, pounds per square foot

p_o free-stream static pressure, pounds per square foot

q_o free-stream dynamic pressure, pounds per square foot

S wing area, square feet

T thrust, pounds

V airspeed, feet per second

ρ mass denisty of air, slugs per cubic foot

Subscripts:

e external

f front of the canopy

i internal

r rear of the canopy

AIRPLANE AND CANOPIES

The Curtiss SB2C-4E airplane is a single-engine, two-place, low-wing scout and dive bomber for use aboard aircraft carriers. The airplane is equipped with a four-blade 12-foot 2-inch diameter Curtiss electric propeller, model C5423-A44, powered by an R-2600-20 Wright engine having a military rating of 1720 brake horsepower at 2600 rpm at sea level. The gross weight of the airplane is about 15,000 pounds; the wing area is about 422 square feet. A three-view drawing with the principal dimensions of the airplane is shown in figure 1.

The airplane is equipped with canopies each of which is mounted on four carriers that roll on tracks designed to raise the canopies slightly and at the same time direct them over the fuselage when opening. The front canopy slides to the rear while the rear canopy slides forward. The front canopy is subdivided into two large Plexiglas side panels and is equipped with a quick-release jettisoning latch. The rear canopy consists of a number of Plexiglas panels and has a built-in emergency hatch. The latter canopy also is equipped with a hinged deflector on each side of the canopy shown in figure 2, which extends outward from the canopy about 50° when the canopy is in the full-open position. With the rear canopy in the

closed position, the deflectors retract flush with the sides (fig. 2). A line drawing of the canopies showing the contours and the principal dimensions is presented in figure 3. As can be seen from this figure, the canopies have straight forward and aft sections. There was no effective partition separating the front and rear cockpits in this airplane.

METHODS AND TESTS

The SB2C-4E airplane is shown mounted on the tunnel balance in figure 4.

External pressures over the front and rear canopies, over the fuselage between the front and rear canopies, and behind the rear canopy were determined by means of static-pressure orifices installed flush with the surfaces. Internal pressures on the canopies were measured with static-pressure tubes fastened to the inner surface of the canopies. The locations of the static-pressure orifices and the static-pressure tubes are shown in figure 3.

The internal and external pressures were measured with the propeller operating and with the propeller removed for various canopy positions. The tests were made with the airplane set at angles of attack corresponding to lift coefficients of 0.17, 0.56, 0.98, and 1.33, which were determined from propeller-removed force test data (fig. 5). These lift coefficients cover the range of flight attitudes from take-off to high-speed level flight at sea level. The propeller-removed tests included the four lift coefficients at 0° and -7° angles of yaw and the two high lift coefficients at -15° angle of yaw. These tests were repeated with the propeller operating at military power and the range of yaw angles was extended to include 7° and 15°. In addition, with the propeller operating at idling power, tests were made at $C_L = 1.33$ for each yaw angle. Each test was made for the following six canopy arrangements; with the rear canopy full open, the front canopy was closed, 3-inches open, one-half open, and full open; and with the rear canopy closed, the front canopy was full open and closed.

All the tests were made with the cowl flaps closed in order to give the data a greater range of applicability among airplanes with different cowl flap arrangements.

The effects of the propeller operation and yaw on C_L were neglected in establishing the test program because slight changes in this variable were considered to be of secondary importance for these tests.

To simplify testing in the full-scale tunnel, the propeller blades were fixed at a blade angle of 26°, measured at the 0.75 radius, for all tests with the propeller operating. This blade angle very closely simulated the correct thrust-torque relationship for this airplane over the range of power conditions employed in these tests. Thrust coefficients, used in the tests to simulate constant military power operation in flight for each of the respective lift coefficients, were determined from the curve of T_c against C_L calculated for sea-level military power (fig. 5).

The idling power tests were made at the lowest possible smooth-running speed. The tests were made at a tunnel airspeed of approximately 62 miles per hour.

RESULTS AND DISCUSSION

All canopy pressures are expressed in this report in terms of the coefficient P, equal to $\frac{p - p_o}{q_o}$. The external pressure coefficients P_e are presented in lateral plots for four representative longitudinal stations on each canopy. The figures also include the internal pressure coefficients P_{i_f} and P_{i_r}, which are the average internal pressures at the front and at the rear of the canopies. These two internal pressure coefficients are presented because there was practically no variation among the individual internal pressures at either the front or the rear stations, but there was some variation between average pressures of the stations.

Front Canopy Pressures

The test results for the front canopy are presented in figures 6 to 13.

Canopy position effects.- Six canopy positions are presented in each figure to illustrate the variation of the pressures with canopy opening for each test condition. In general, regardless of yaw angle, lift coefficient, or power conditions, the external pressures over the front canopy were uniform longitudinally for the configuration with the front canopy closed and the rear canopy full open. Opening the front canopy 3 inches, with the rear canopy full-open, produced high negative external pressure peaks over the front of the canopy. Further opening of the front canopy caused a reduction in the high negative pressure peaks until at full-open the pressures

were again uniform longitudinally. The pressures over the rear part of the canopy were not appreciably affected by opening the front canopy, and consequently, the over-all external pressure increase with the front canopy 3 inches open and the rear canopy open was only moderate. Rear canopy position appears to have negligible effect on the front canopy external pressure distribution.

The internal pressures are directly dependent upon the external pressures surrounding the canopy and upon the amount of leakage between the two pressure fields. Opening the canopy has the effect of increasing the leakage area. Consequently, the configuration with the front canopy full-open and the rear canopy closed produced the highest negative internal pressures; the lowest negative internal pressures were produced with both canopies closed. To illustrate the magnitudes of the internal pressures for these two canopy settings, figure 9(d) shows the average internal pressure coefficients ranged from −1.01 with the front canopy full-open and the rear canopy closed to −0.10 with both canopies closed.

The configuration which produced the highest net loads on the canopy based on the differential of the external and internal pressure coefficients $(P_e - P_i)$ was that with the front and rear canopies closed, for which case the highest canopy loads were in the exploding direction.

Lift-coefficient effects.- Four lift coefficients ranging from 0.17 to 1.33, are shown in figure 6 for the propeller-removed condition at 0° angle of yaw. The external pressure distributions were symmetrical for each lift coefficient, with somewhat higher negative pressures appearing on the sides of the canopy than at the top. The average external pressure coefficient increased from approximately −0.3 to −0.5 when the lift coefficient was varied from 0.17 to 1.33, for the configuration with the front and rear canopies closed, and proportionate increases were observed for the other canopy positions.

Generally, the negative internal pressures increased slightly with increasing lift coefficient. An exception to this rule, however, is the condition with the front and rear canopies closed, for which the internal pressure coefficients appeared to retain their relatively low magnitudes over the entire range of lift coefficients.

Power effect.- The front canopy pressures are shown for the propeller operating conditions at 0° angle of yaw in figures 9(a) through 9(d) for military power at four different lift coefficients and in figure 9(e) for idling power. The pressures observed for the idling power condition were comparable to those shown previously in figure 6(d) for similar configurations with the propeller removed.

Propeller operation at military power did not cause much asymmetry in the distribution of the external pressures, even in the upper range of lift coefficients where the high torque coefficients produced the greatest rotation in the slipstream. The additional axial slipstream velocity, however, for all of the conditions tested produced high negative external pressures about the entire canopy. These pressure increases were greater at the high lift coefficients as a result of the higher thrust coefficients at these attitudes. A comparison of the pressures for the conditions with the propeller operating at military power with those for the conditions with the propeller removed (figs. 6(a) and 6(d)) showed the average external pressure coefficients at $C_L = 0.17$ were increased from approximately −0.3 to −0.4 and at $C_L = 1.33$ were increased from approximately −0.5 to −1.3 by the addition of power for the configuration with the front and rear canopies closed.

Most of the negative internal pressure coefficients, with the exception of the configuration with the front and rear canopies closed, were considerably higher for the military power conditions than those observed for the propeller-removed conditions. These pressure coefficients were further increased at the high lift coefficients. With the front and rear canopies closed, the internal pressure coefficients were only slightly increased for the propeller operating condition.

Although the differential of the external-internal pressure coefficients was very much larger at $C_L = 1.33$ than at $C_L = 0.17$, the net load on the canopy when based on the appropriate airspeed was considerably higher at $C_L = 0.17$ than at $C_L = 1.33$ for most of the canopy configurations. The load at $C_L = 0.17$, which corresponds to the high-speed flight condition, was in the exploding direction for the front canopy. It may be expected that the loads on the front canopy encountered for a high-speed pull-up will be somewhat higher than those for the level-flight high-speed condition, inasmuch as the net external-internal pressure coefficients are somewhat greater at the higher lift coefficients.

Yaw Effect.- The effects on the canopy pressures of yawing the airplane through a range of negative yaw attitudes (left wing retarded) with the propeller removed are shown in figure 7 and 8, for yaw angles of −7° and −15°, respectively. The results show that at yawed attitudes, the external pressure distributions were asymmetrical, with high negative pressure regions over the top and trailing side of the canopy. For the propeller operating conditions at the negative yaw attitudes (figs. 10 and 11) the negative external pressures were increased to a much greater extent at the sides of the canopy than over the top of the canopy. This

distribution was attributed to the opposition of the rotation of the propeller slipstream to the asymmetrical air flow over the top of the canopy and the resultant reduction of the local velocity in this region.

With the airplane yawed through the positive range of yaw attitudes (left wing advanced) and the propeller operating (figs. 12 and 13), higher negative external pressures were produced over the top and right side of the canopy because the asymmetrical air flow and the propeller slipstream rotation were in the additive direction at these attitudes.

The negative internal pressure coefficients generally increased with increasing yaw angle.

The asymmetrical external pressure distributions at the high yaw angles were responsible for high localized canopy loadings based on the net external-internal pressure coefficients which for some canopy configurations even resulted in net crushing loads over the top of the canopy at negative yaw angles, and on the left side of the canopy at positive yaw angle.

Rear Canopy Pressures

The test results for the rear canopy are presented in figures 14 to 22. For all conditions with the rear canopy closed the pressures on the sides of the canopy at lateral station 23 were extremely erratic due to the flow over the trailing edge of the deflectors in the flush position, and they are not shown in the figures.

Canopy-position effect.- Figure 14 illustrates the typical longitudinal pressure variations on the sides and top of the rear canopy for the configurations with the rear canopy closed and open. The deflectors, which protrude into the air stream on both sides of the canopy when the canopy is full open, caused the external pressures on the sides of the canopy to build up from the negative pressure region at the front of the canopy to fairly high positive pressures just ahead of the deflectors. Immediately behind the deflectors high negative pressures were observed. The typical longitudinal pressure distribution over the top of the canopy was more uniform, as were the distributions for the top and sides when the canopy was closed and the deflectors were in the flush position. It is believed that somewhat similar uniform pressure distributions would occur for the intermediate canopy positions for which the deflectors would remain in the flush position.

Figures 15 through 22 indicate the external pressures over the rear canopy were not effected by changes in the front canopy position.

Inasmuch as there was no effective partition separating the front and rear cockpits, the rear canopy internal pressures varied with canopy position in a manner similar to that of the front canopy internal pressures mentioned in a previous section of this report. In general, the highest negative internal pressures were obtained for the configuration with the front canopy full open and rear canopy closed, for which case the net external-internal canopy loads were in the crushing direction. The lowest negative internal pressures were measured with the front and rear canopies closed, for which case the net loads were in the exploding direction. Generally the maximum exploding loads on the rear canopy were very small. The magnitudes of the internal pressure coefficients for these two canopy configurations are shown in figure 18(d) for which case the average coefficient ranged from −0.82 with the front canopy full-open and the rear canopy closed to −0.11 with both canopies closed.

Lift-coefficient effect.- The rear canopy pressures for various lift coefficients are shown for the propeller-removed conditions in figures 15, 16, and 17 for yaw angles of 0°, −7°, and −15°, respectively. The external pressures appeared to be independent of lift coefficient inasmuch as similar distributions and magnitudes were observed throughout the range of lift coefficients for each yaw angle.

Generally the negative internal pressures, with the exception of the configuration with the front and rear canopies closed, increased slightly with increasing lift coefficient. This lift-coefficient effect on the rear canopy internal pressures was attributed to the variation of these pressures with the front canopy internal pressures.

Power effect.- Canopy pressures with the propeller operating are shown for 0° angle of yaw in figures 18(a) through 18(d) for military power at various lift coefficients and in figure 18(e) for idling power. The pressures observed for idling power were similar to those shown previously in figure 15(d) for the same configurations with the propeller removed. Military power did not cause much asymmetry in the distribution of the external pressures at the various lift coefficients. For the configurations with the rear canopy closed, the additional slipstream axial velocity produced somewhat higher negative external pressures over the entire canopy for the propeller-operating conditions than for the same configurations with propeller removed. These pressure increases were greater at the high lift coefficients as a result of the higher thrust coefficients at these attitudes. For the configurations with the rear canopy open, the longitudinal pressure variations across the extended deflectors were much greater for the military power conditions than for the propeller-removed conditions.

Most of the negative internal pressures, with the exception of the configuration with the front and rear canopies closed, were much higher for the military-power conditions than the propeller-removed conditions. The negative internal pressures were further increased at the high lift coefficients. With the front and rear canopies closed the internal pressures were only slightly increased for the propeller operating conditions.

The net crushing load on the rear canopy for the configuration with the front canopy open and the rear canopy closed was over twice as great at $C_L = 0.17$ as at $C_L = 1.33$ when based on the corresponding airspeeds, although the net external-internal pressure coefficients were very much larger at $C_L = 1.33$ than at $C_L = 0.17$. For most of the simulated flight conditions the net rear canopy crushing loads (per unit area) with the front canopy open and the rear canopy closed were less than one-half of the net front canopy exploding loads with the front and rear canopies closed.

Yaw effects.- The effects on the canopy pressures of yawing the airplane through a range of negative yaw attitudes (left wing retarded) are shown for the propeller-removed tests in figures 16 and 17 for yaw angles of -7° and -15°, respectively. In general, asymmetrical external pressure distributions were produced at the yawed attitudes, with somewhat higher negative external pressures over the top and trailing side of the canopy. For the configurations with the rear canopy open, the longitudinal pressure variations across the extended deflector on the leading side of the canopy were considerably higher at the yawed attitudes than at 0° angle of yaw. For the same configurations, with the propeller operating at military power at these yaw attitudes (figs. 19 and 20), large longitudinal pressure variations were produced over the extended deflector on the opposite (trailing) side of the canopy as a result of the interaction of the propeller slipstream and the asymmetrical air flow. For the configurations with the rear canopy closed, the pressures over the entire canopy were increased in the negative direction by the additional slipstream axial velocity.

With the airplane yawed in the positive direction (left wing advanced) and the propeller operating at military power (figs. 21 and 22), the asymmetry of the external pressures due to yaw did not change appreciably, but high negative external pressures were produced over the top of the canopy as a result of the propeller slipstream rotation and the asymmetrical air flow, which were in an additive direction.

CONCLUSIONS

A preliminary analysis of the results of the canopy loads tests on the conventional front and rear sliding canopies which are typified by the installation on the SB2C-4E airplane, conducted in the Langley full-scale tunnel, showed that for the range of conditions tested:

1. The maximum loading condition, based on the external-internal pressure differential, for the front and rear canopies were obtained for the high-speed flight condition of this airplane.

2. The highest loads on the front canopy were in the exploding direction and occurred for the configuration with the front and rear canopies closed.

3. The highest loads on the rear canopy were in the crushing direction and occurred with the front canopy open and the rear canopy closed. For most of the simulated flight conditions the highest rear canopy loads (per unit area) were less than one-half the highest front canopy loads.

4. The asymmetrical air flow about the airplane at yawed attitudes produced unbalanced external pressure distributions which resulted in local net exploding and crushing loads on both canopies that were often considerably higher than the average net canopy loads.

5. The negative external and internal pressure coefficients for both canopies were increased by the additional axial velocity of the propeller slipstream. The rotation of the propeller slipstream had negligible effect on the pressure distributions at 0° yaw angle; but at the positive and negative yaw attitudes the combined effects of the slipstream rotational velocity and the asymmetrical air flow produced distorted distributions over the canopies.

6. The external pressure coefficients over the front canopy and the internal pressure coefficients for both canopies increased slightly with increasing lift coefficient.

7. Large longitudinal external pressure variations were produced along the sides of the rear canopy by the deflectors which

extended into the air stream for all configurations with the rear canopy full open.

Langley Memorial Aeronautical Laboratory
National Advisory Committee for Aeronautics
Langley Field, Va.

REFERENCES

1. Cooke, Bennie W., Jr., and Czarnecki, K. R.: Canopy Loads Investigation for the F6F-3 Airplane. NACA RM No. L6L23a, 1946.

2. Cooke, Bennie W., Jr.: Investigation of the Loads on a Typical Bubble Type Canopy. NACA RM No. L7D07, 1947.

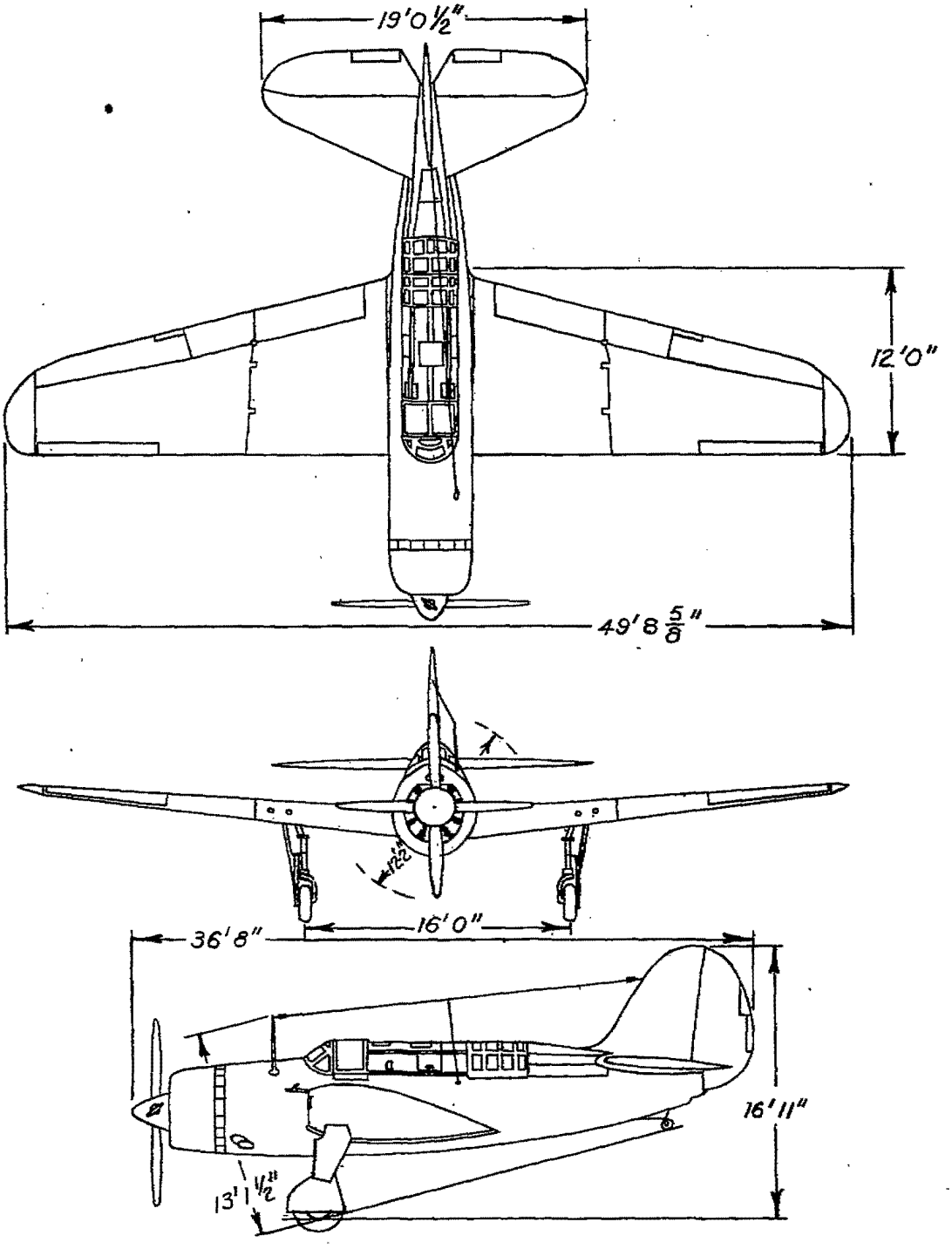

Figure 1.- The SB2C-4E airplane

NATIONAL ADVISORY
COMMITTEE FOR AERONAUTICS

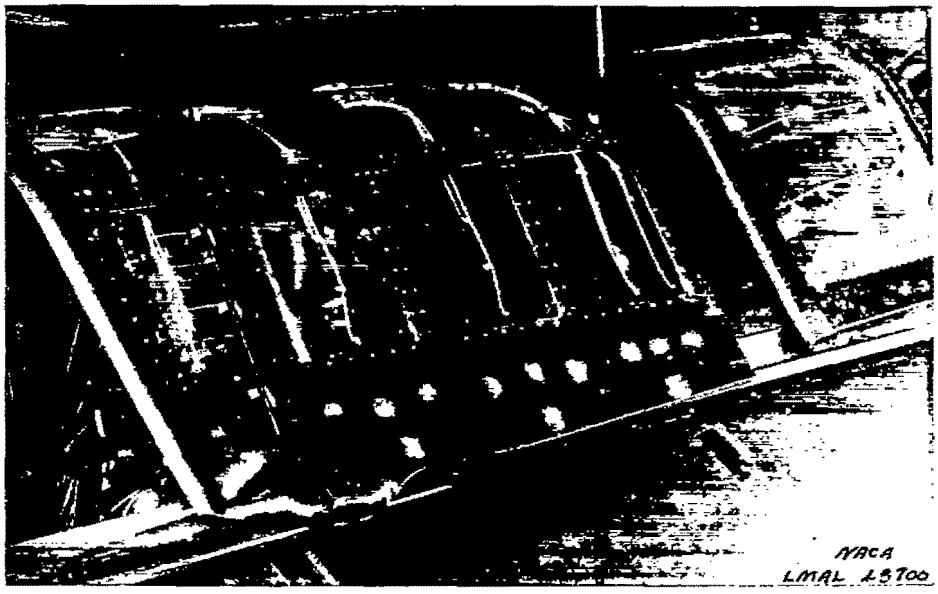

(a) Canopy and deflector open.

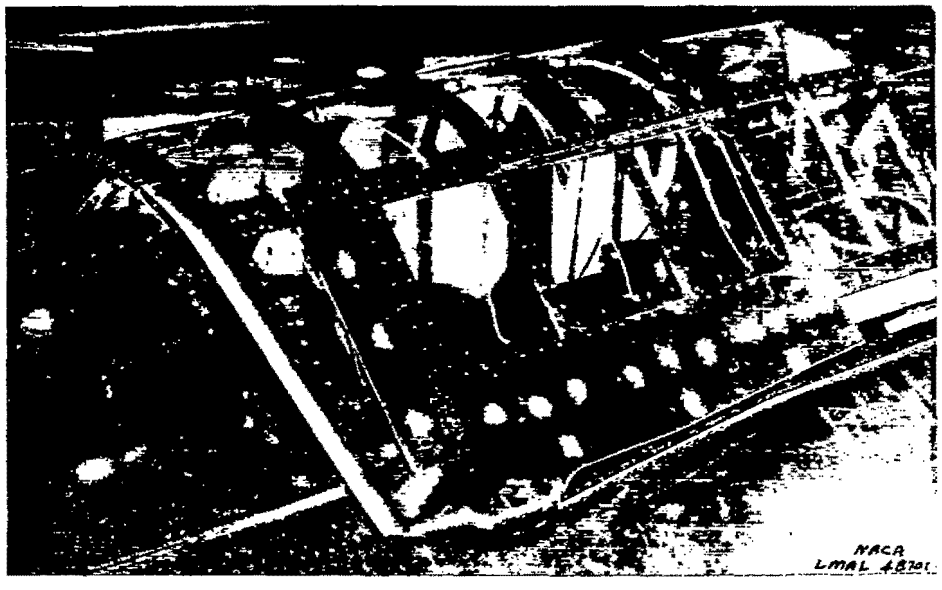

(b) Canopy and deflector closed.

Figure 2.- The rear canopy in the open and closed positions, showing the two positions of the deflectors.

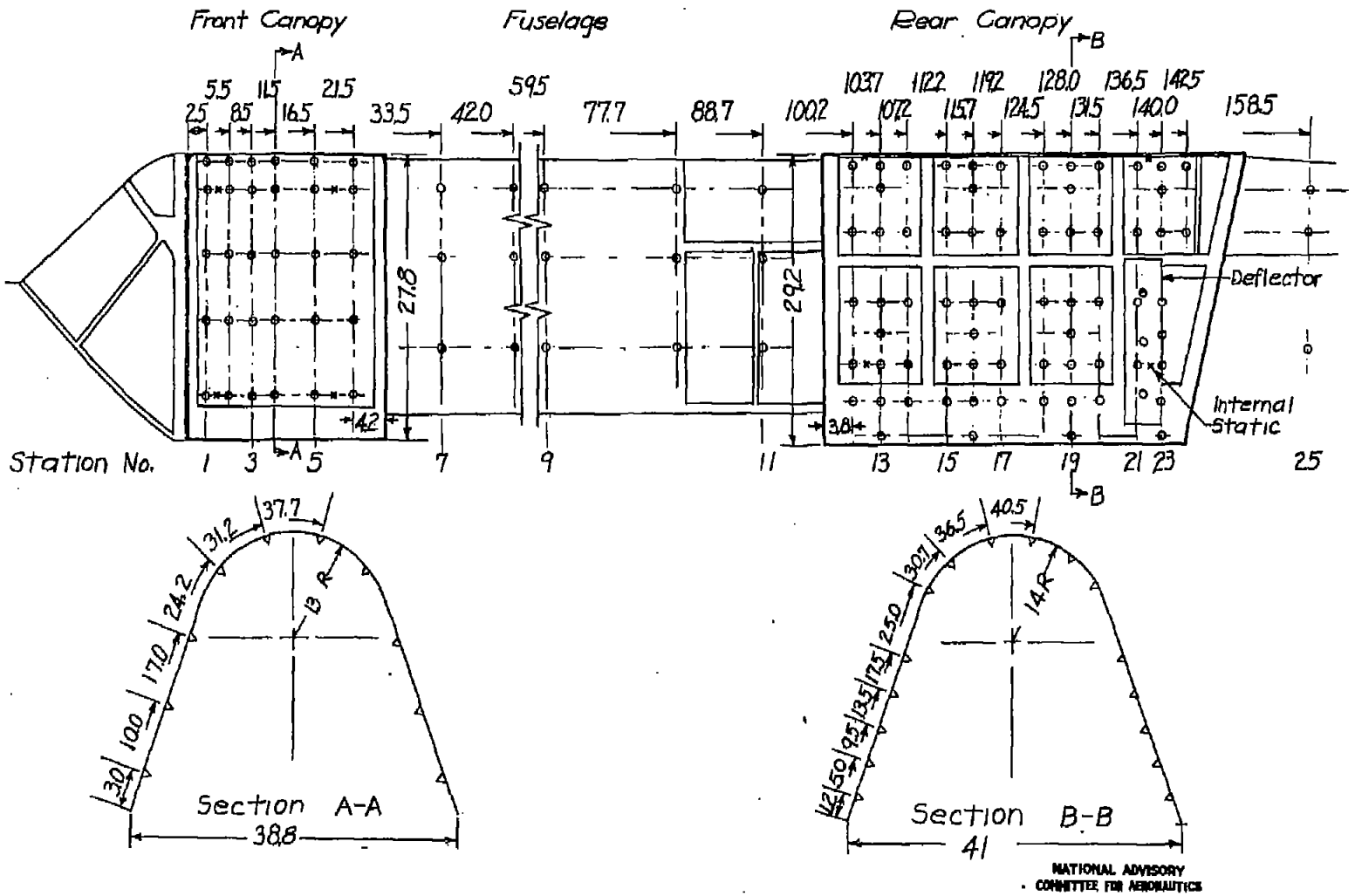

Figure 3. - Principle dimensions of the canopies with the transverse and longitudinal locations of the static pressure orifices. All dimensions are in inches.

Fig. 3

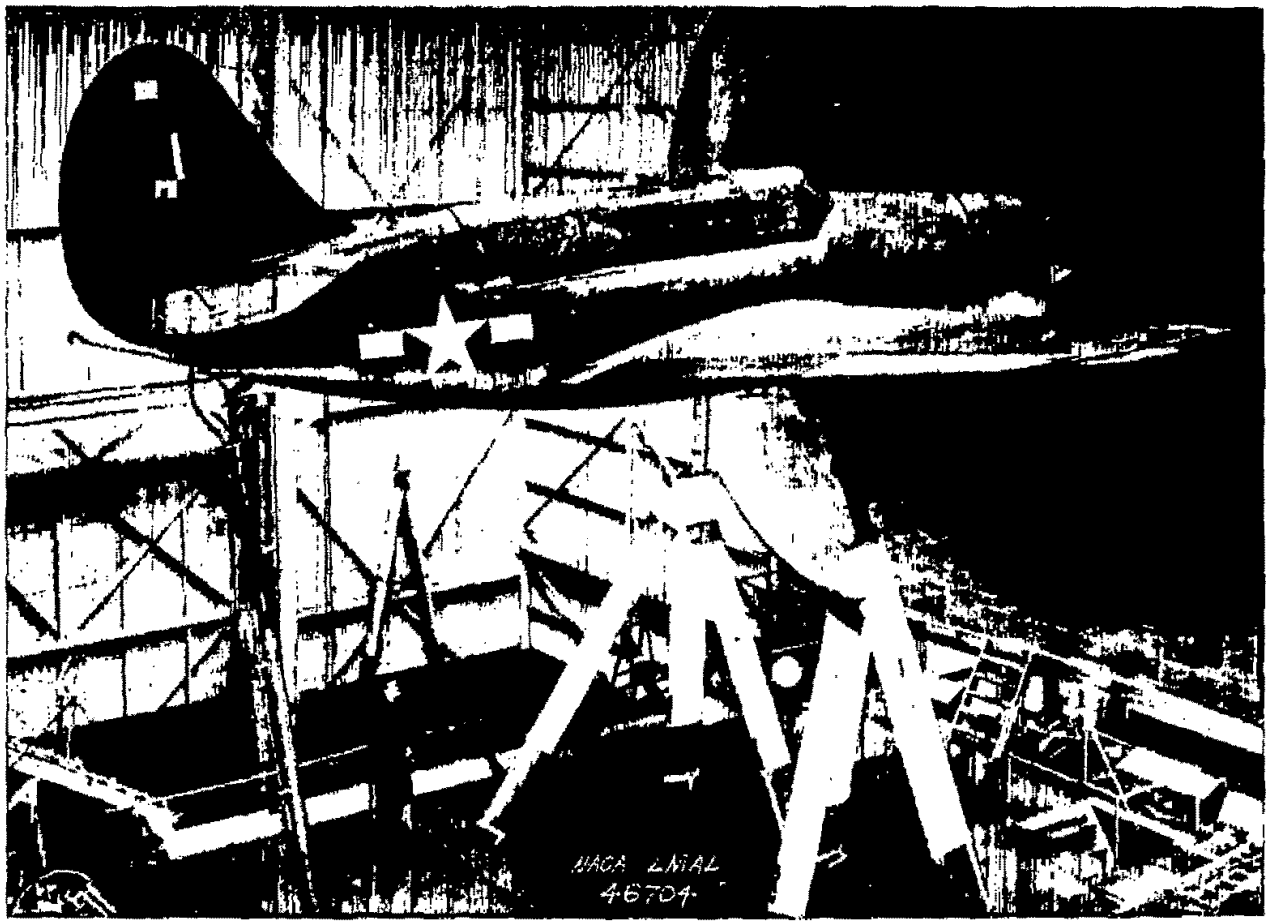

Figure 4.- The SB2C-4E airplane mounted in the Langley full-scale tunnel for canopy loads investigation.

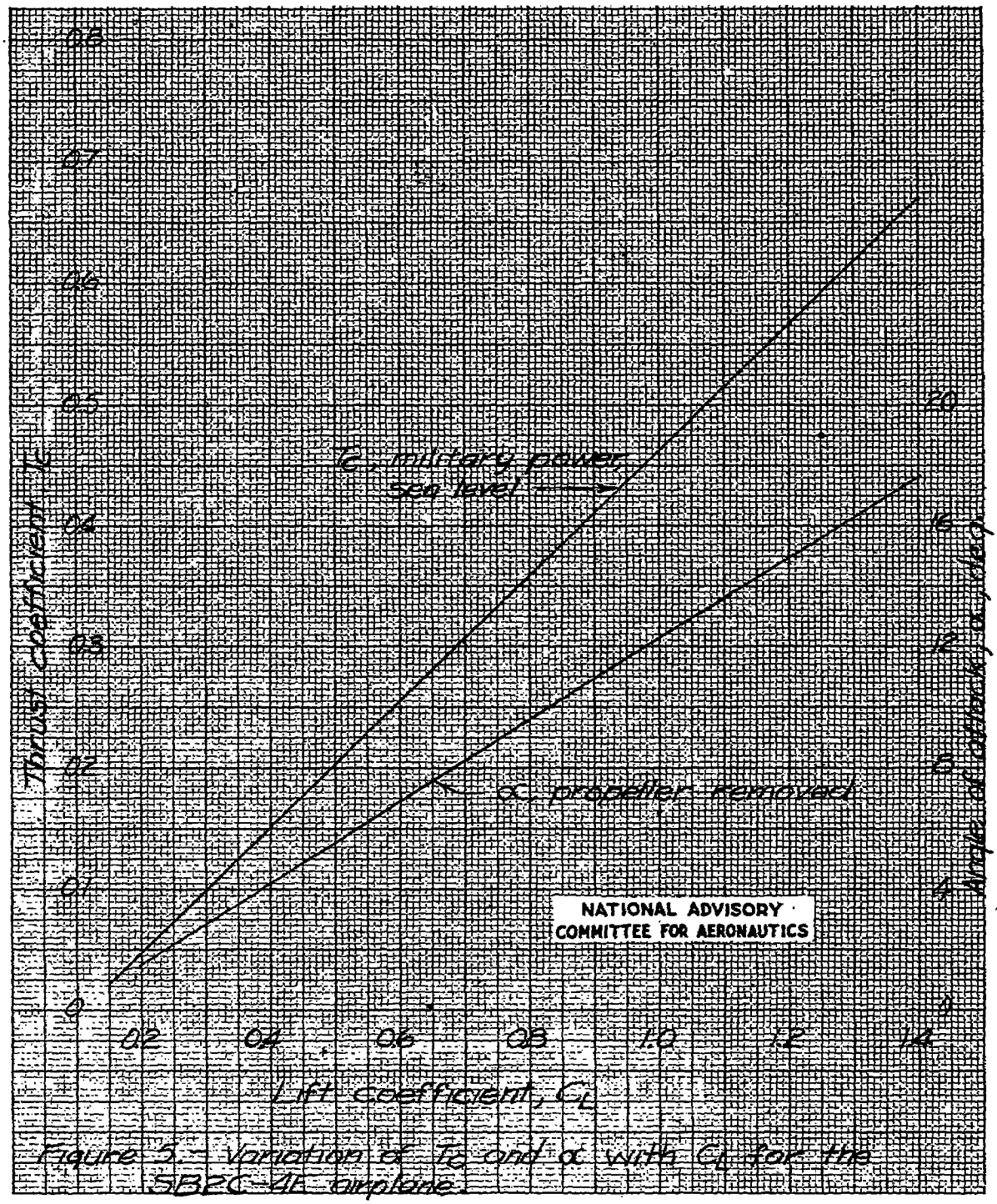

Figure 5.- Variation of T_c and α with C_L for the SB2C-4E airplane.

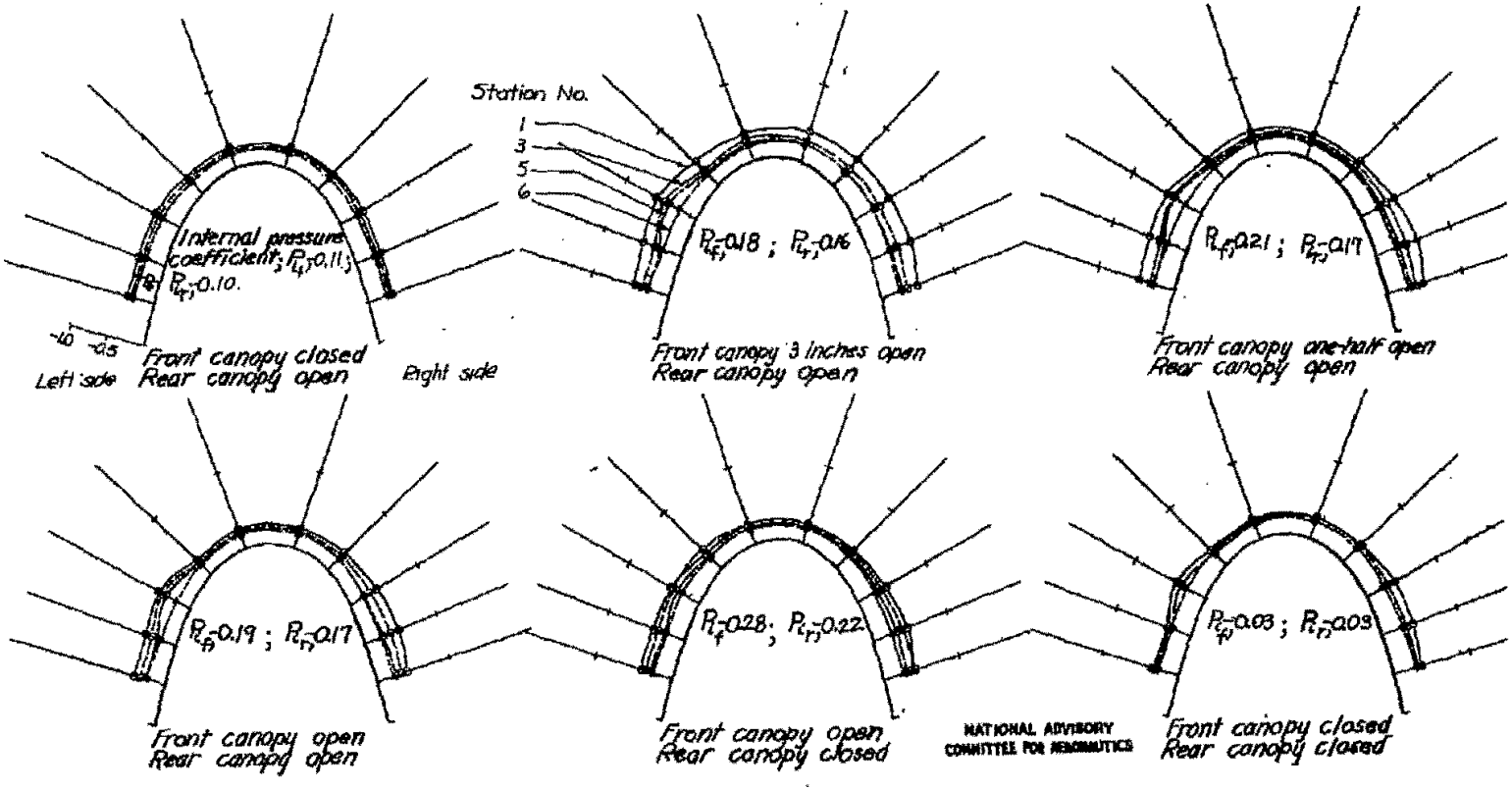

(c) Propeller removed; C_L, 0.17

Figure 6 .- Pressure distributions over the front canopy of the SB2C-4E airplane. ψ, 0 deg

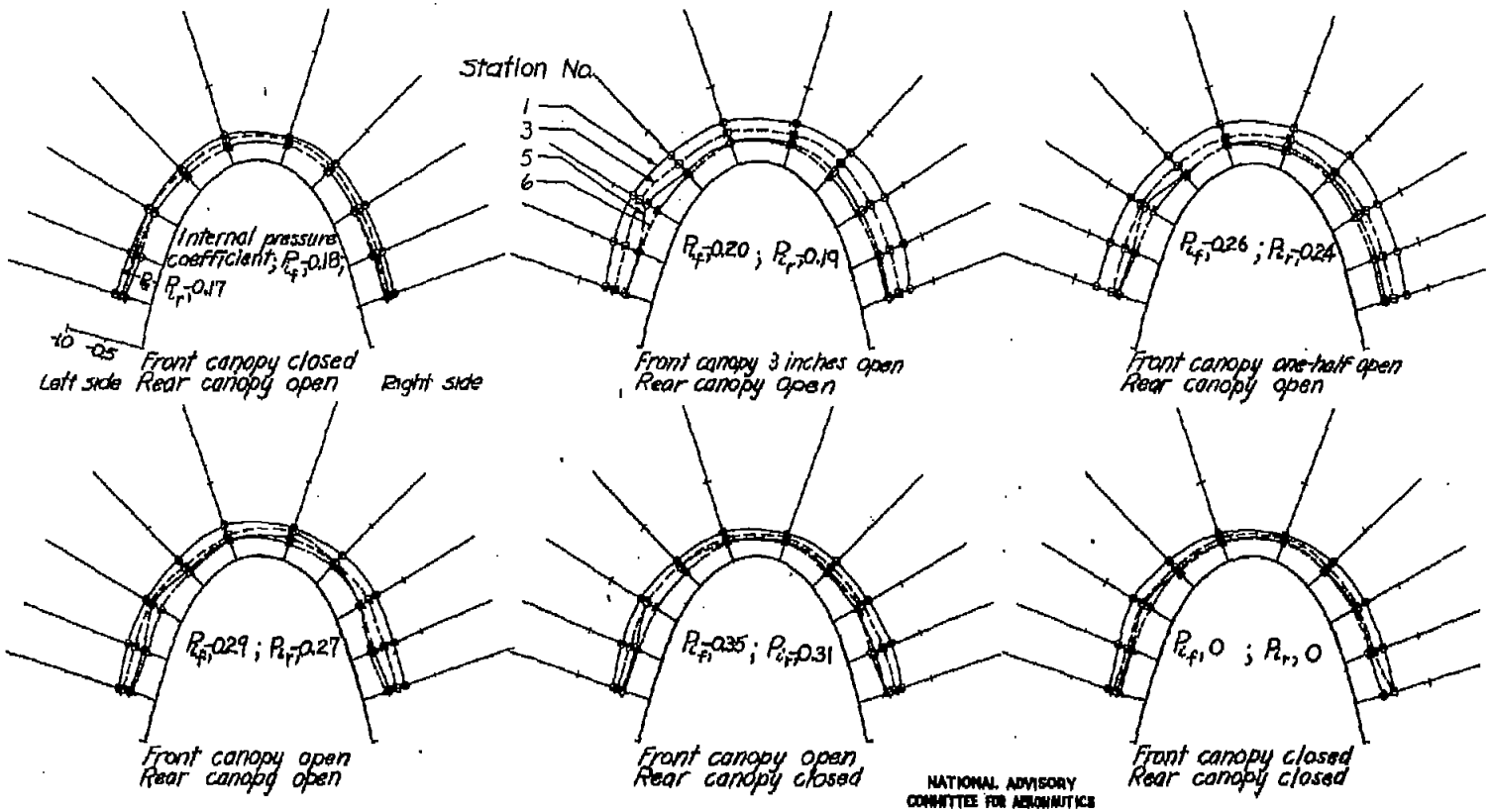

(b) **Propeller removed;** C_L, 0.56

Figure 6.- Continued.

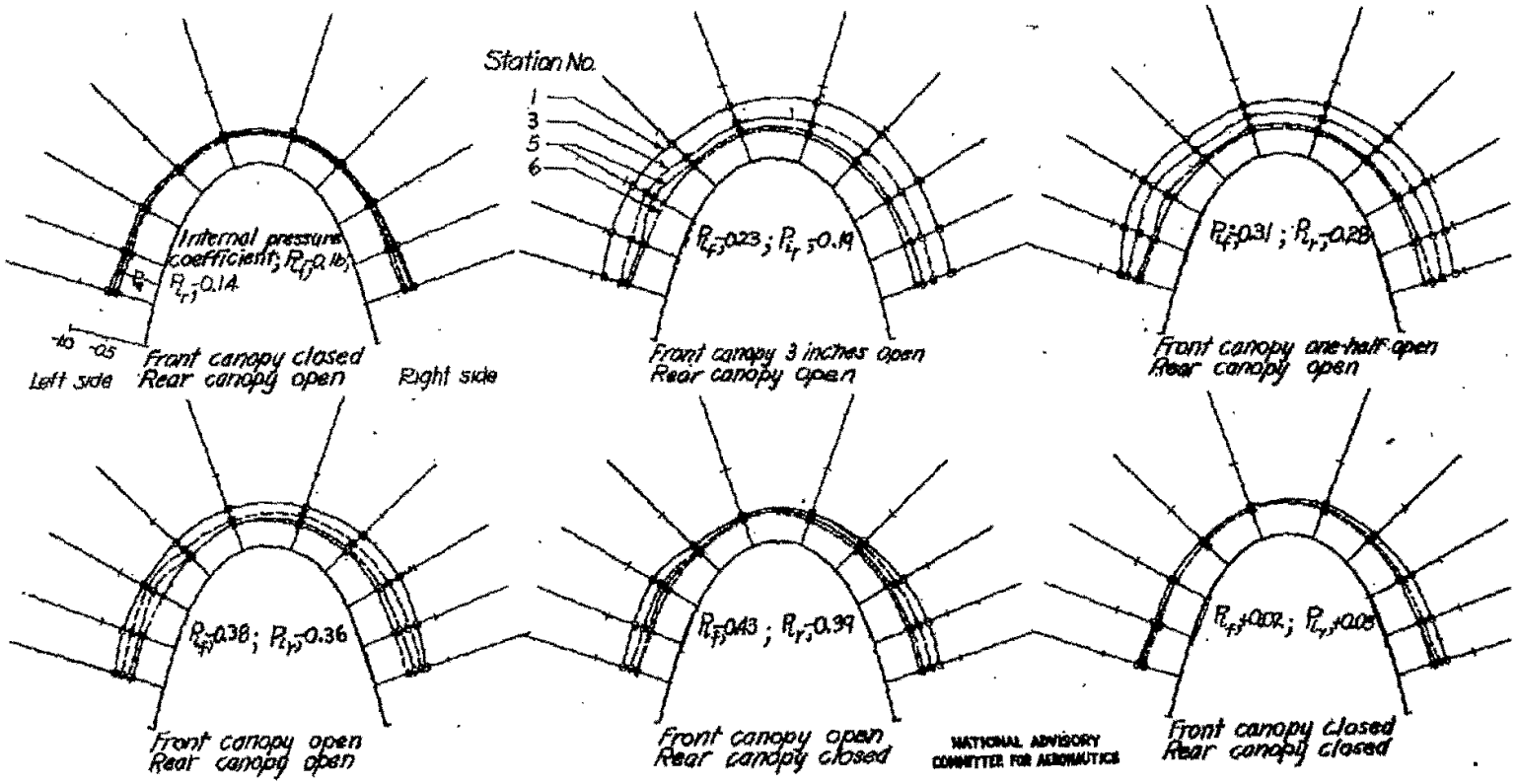

(c) **Propeller removed; C_L, 0.98**

Figure 6. - Continued.

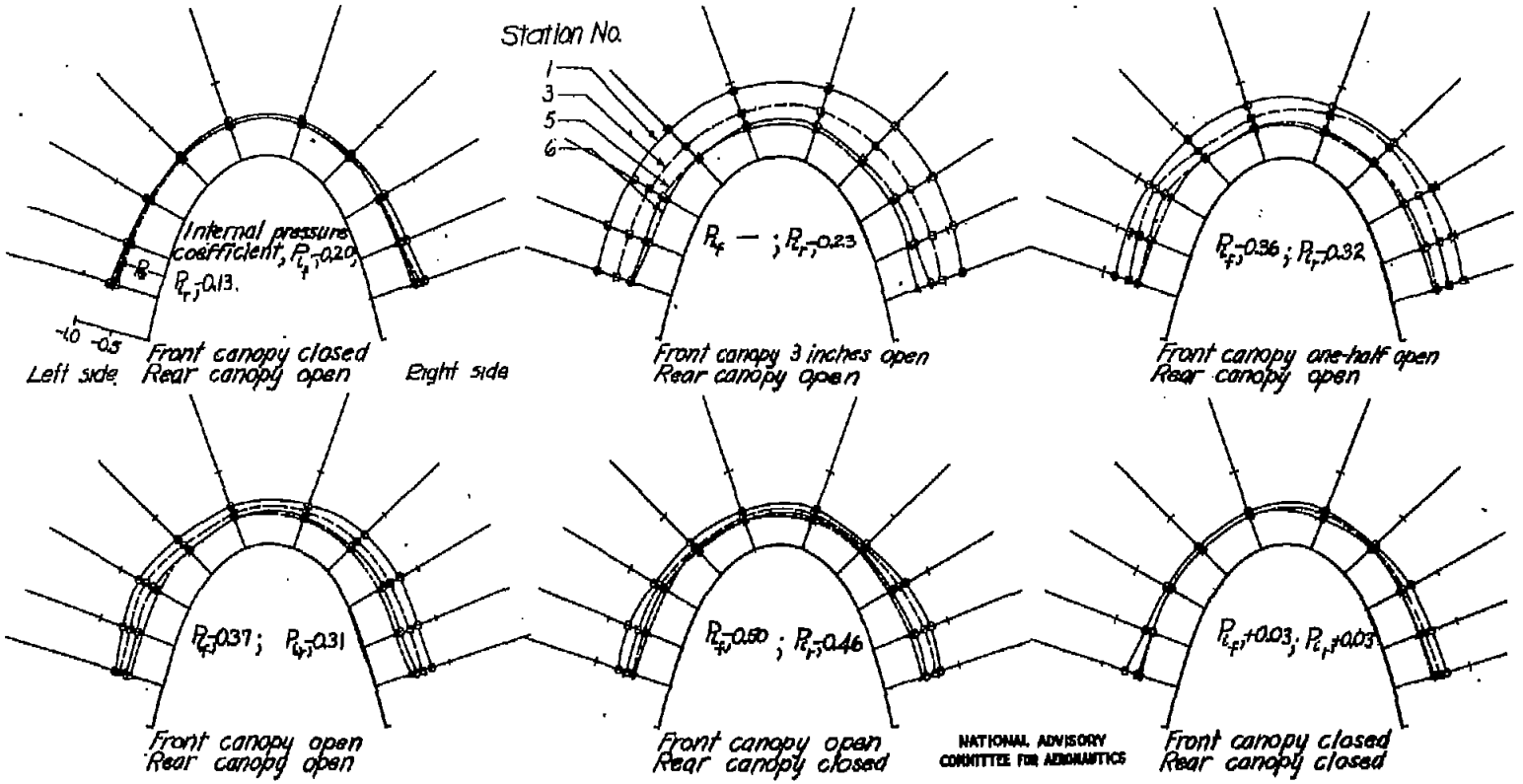

(d) Propeller removed; C_L, 1.33

Figure 6.-Concluded.

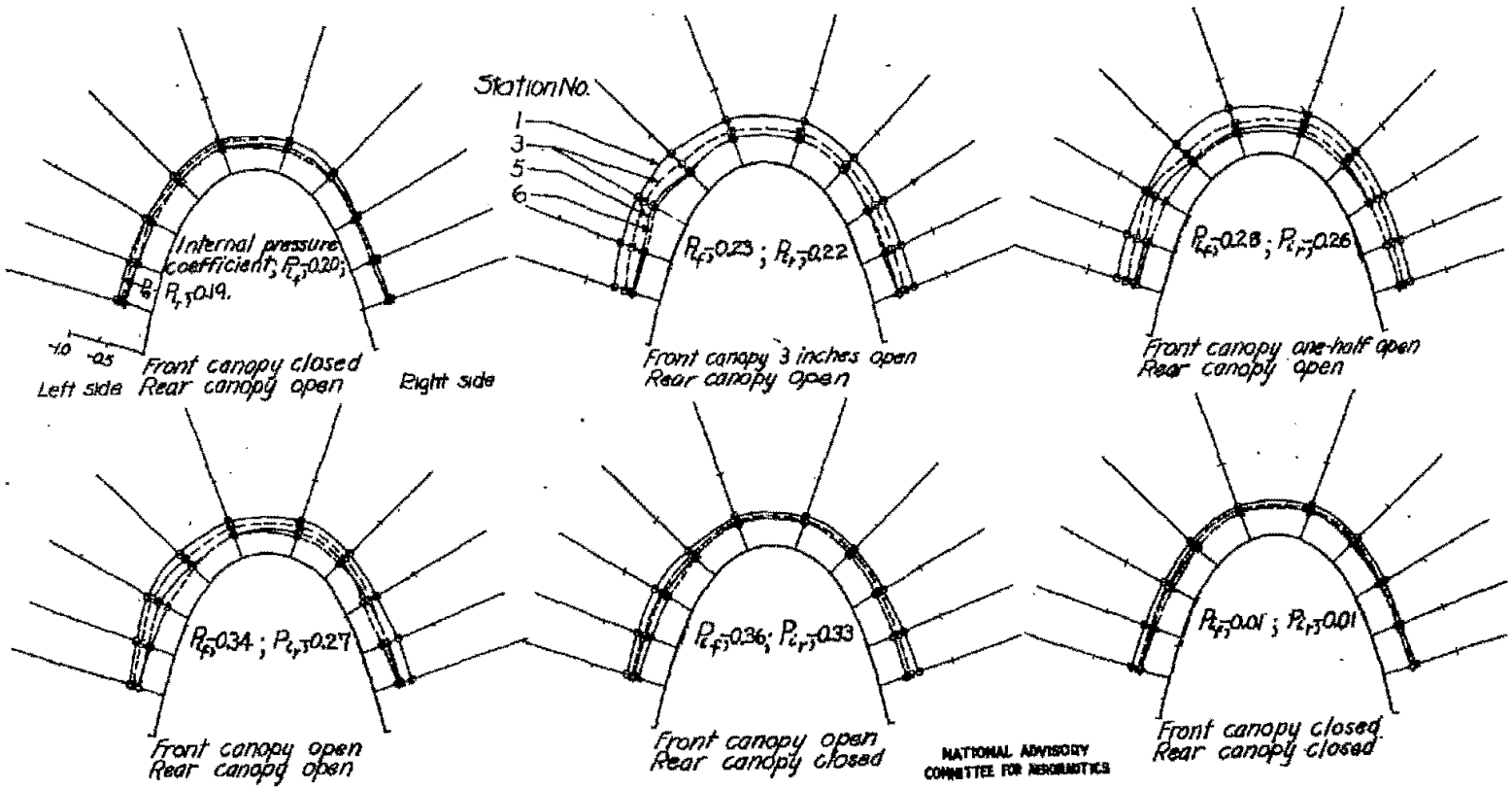

(a) Propeller removed; C_L, 0.56

Figure 7 .– Pressure distributions over the front canopy of the SB2C-4E airplane. α_i, -7 deg.

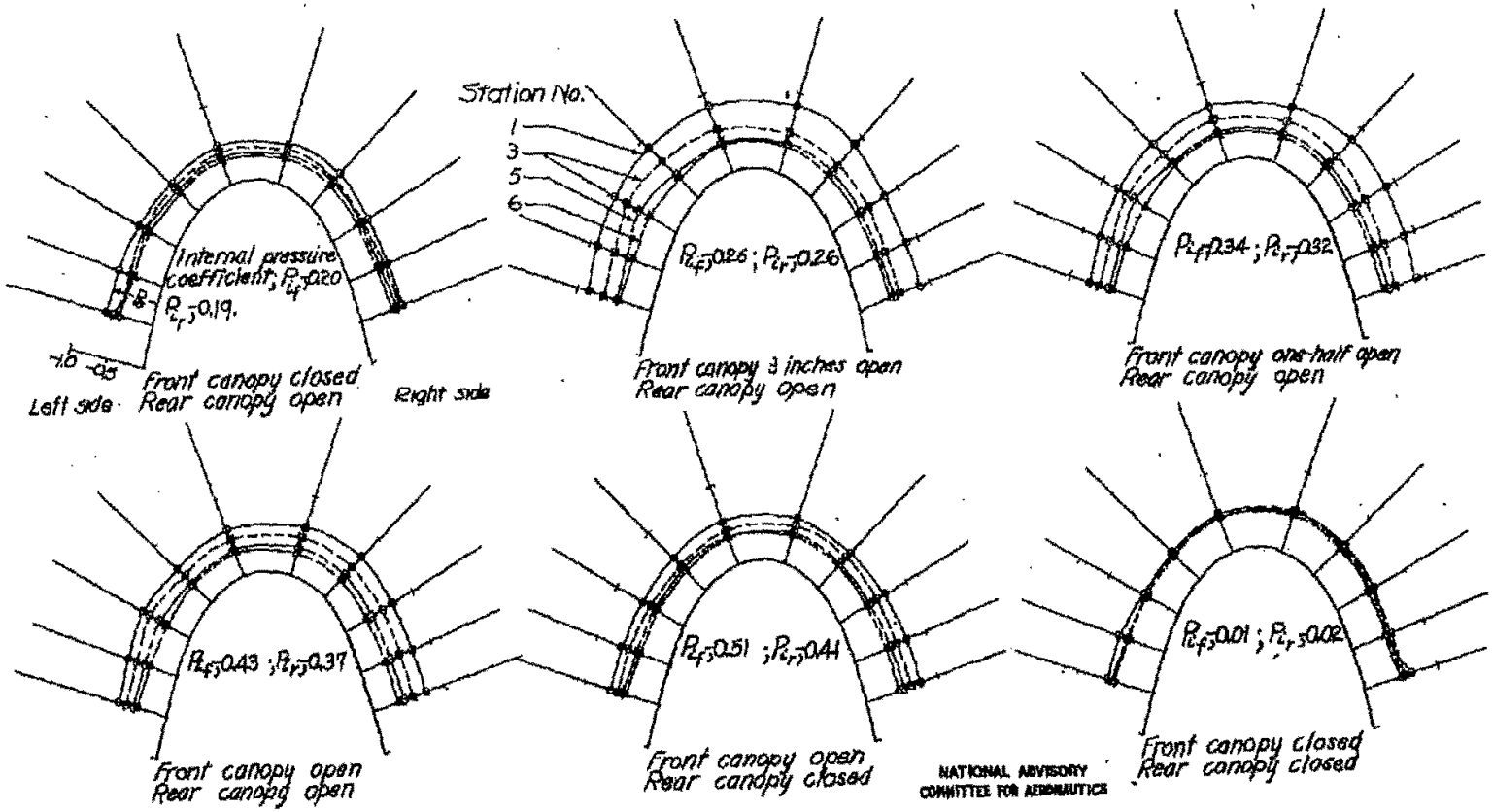

(b) Propeller removed, C_L, 0.98

Figure 7.- Continued.

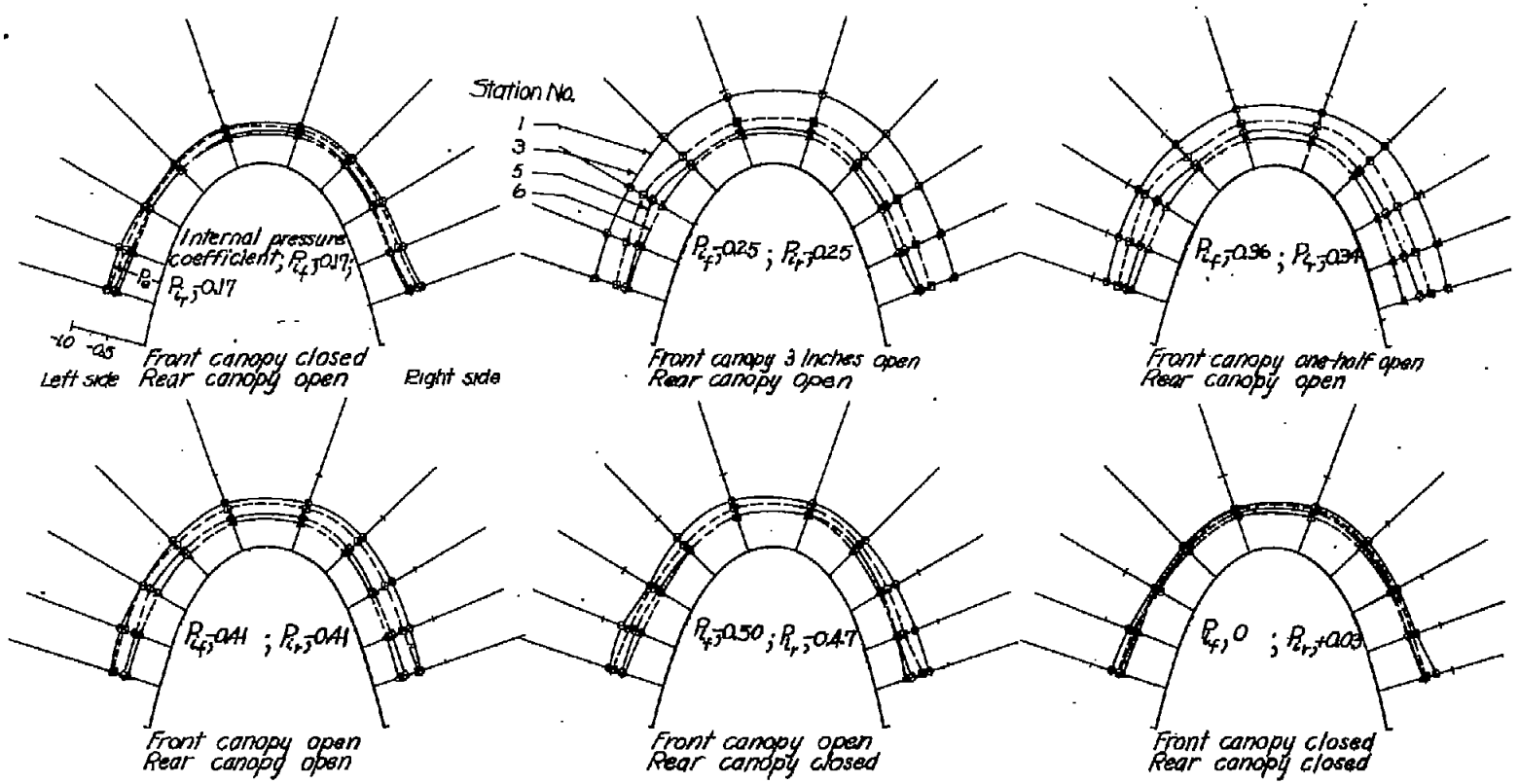

(c) **Propeller removed; C_L, 1.33**

NATIONAL ADVISORY COMMITTEE FOR AERONAUTICS

Figure 7. - Concluded.

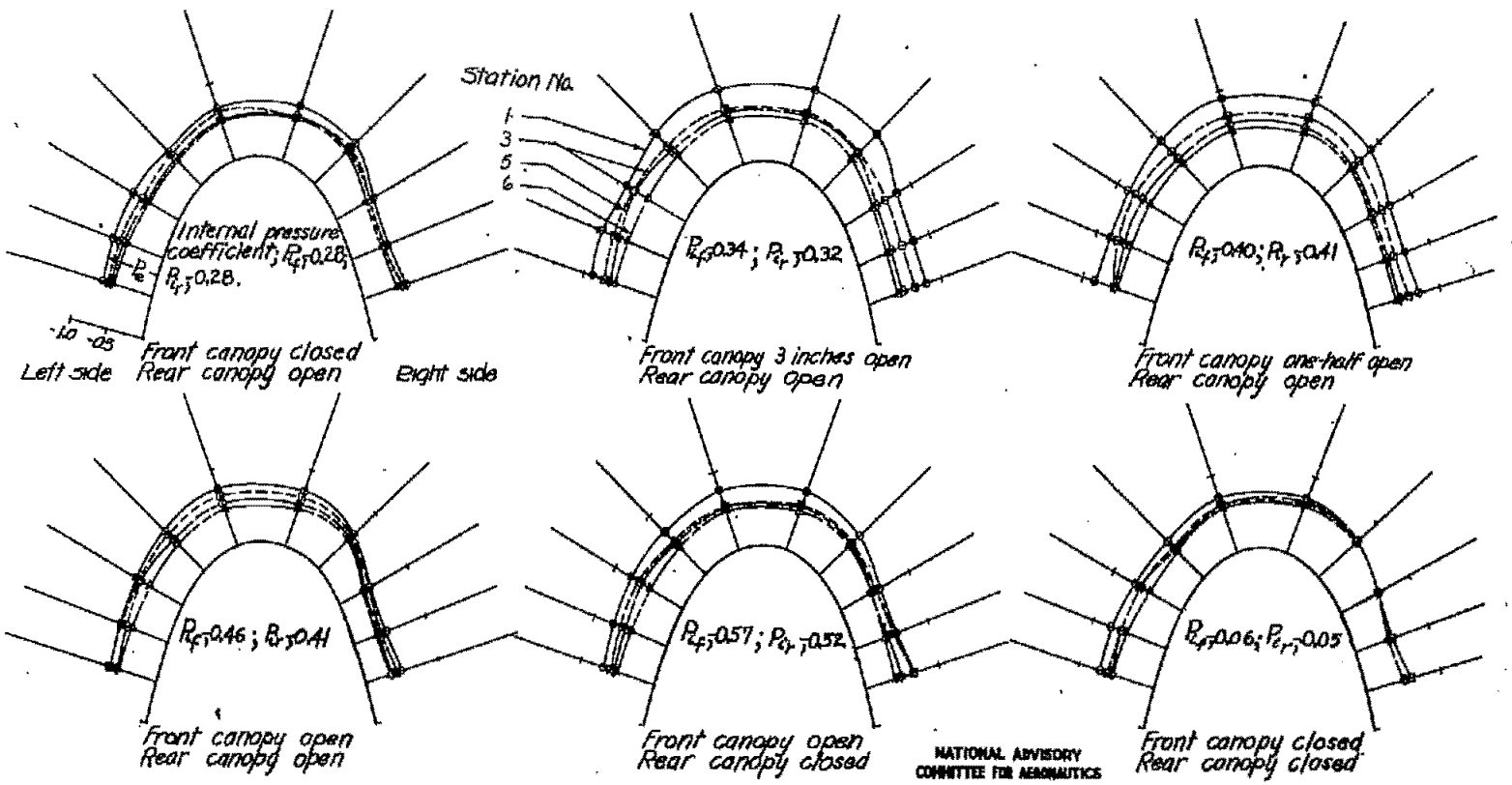

(a) Propeller removed; C_L, 0.98

Figure 8 .— Pressure distributions over the front canopy of the SB2C-4E airplane. V_i, -15 deg.

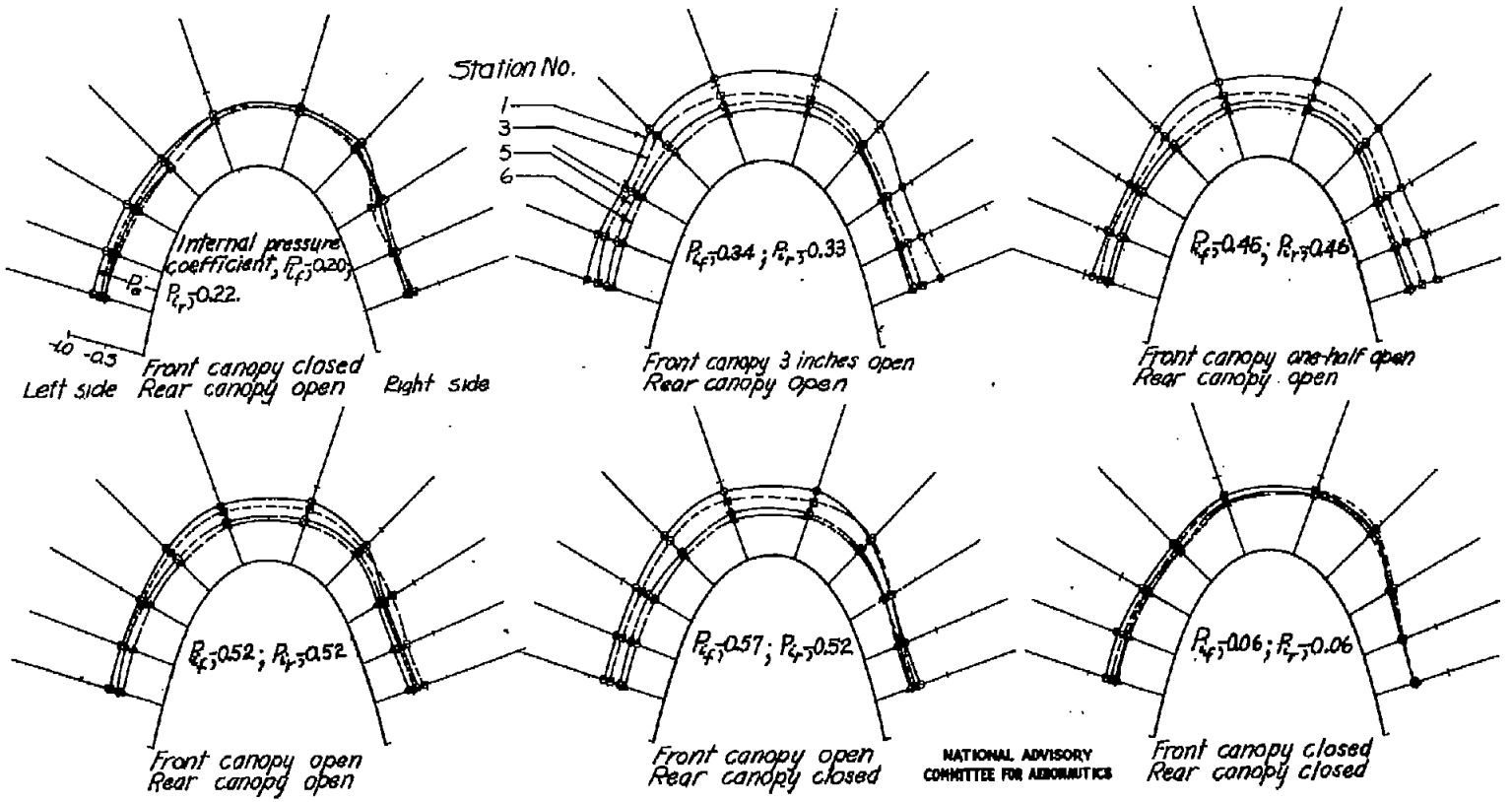

(b) **Propeller removed; C_L, 1.33**

Figure 8.- Concluded.

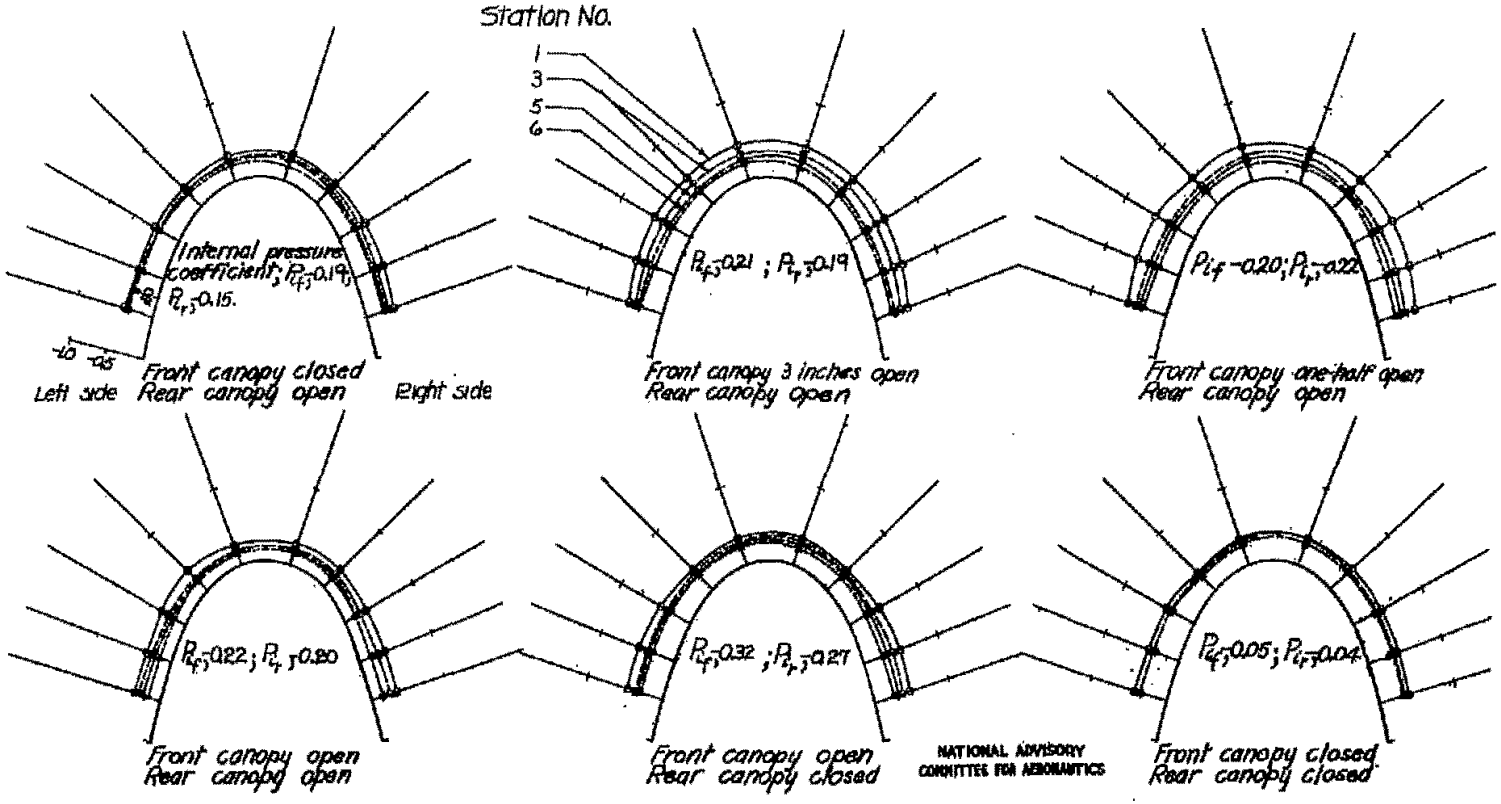

(a) Military power; T_c, 0.04; C_L, 0.17.

Figure 9 – Pressure distributions over the front canopy of the SB2C-4E airplane. ψ, 0 deg.

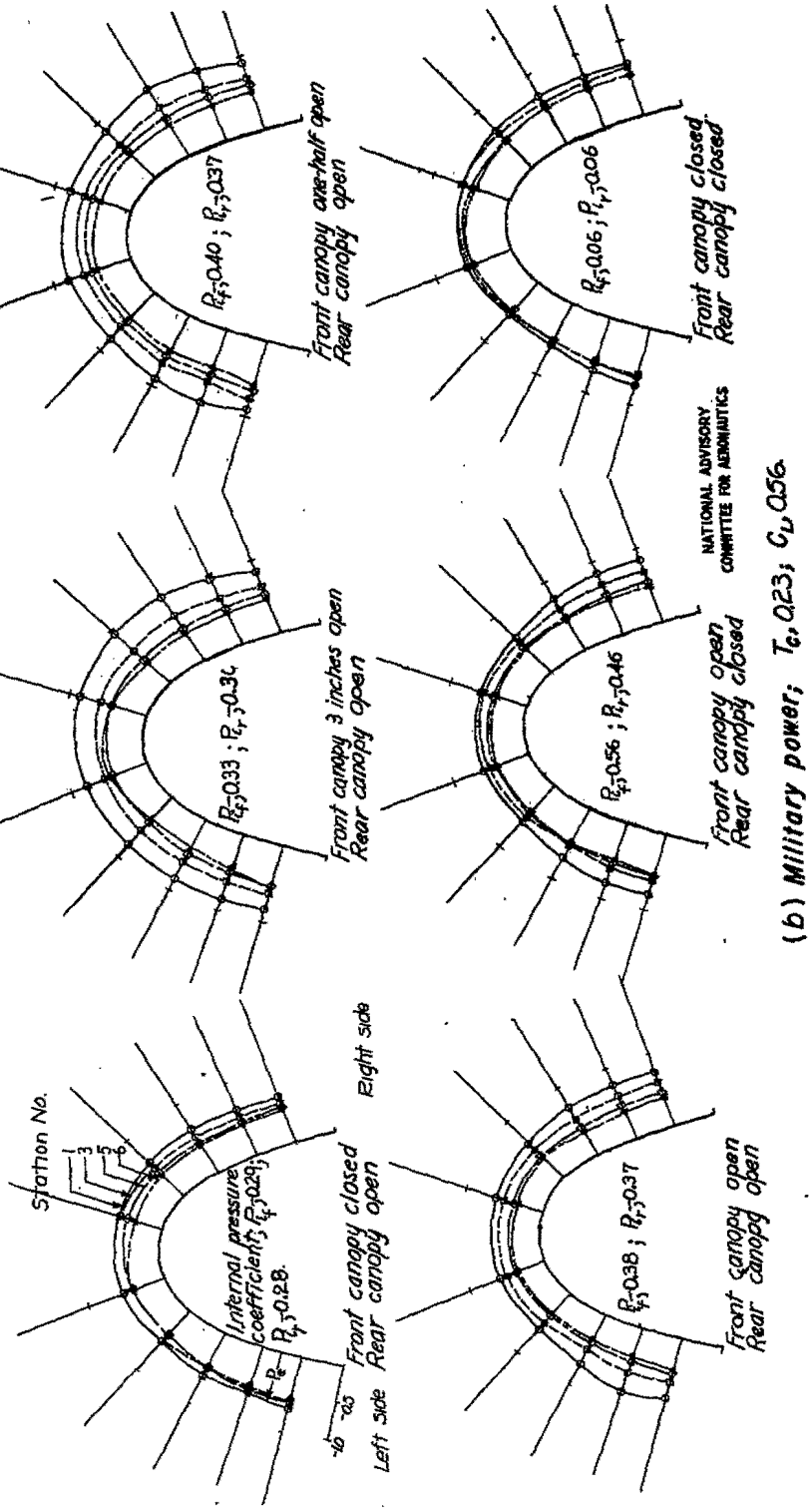

(b) Military power; T_c,0.23; C_L,0.56

Figure 9.- Continued.

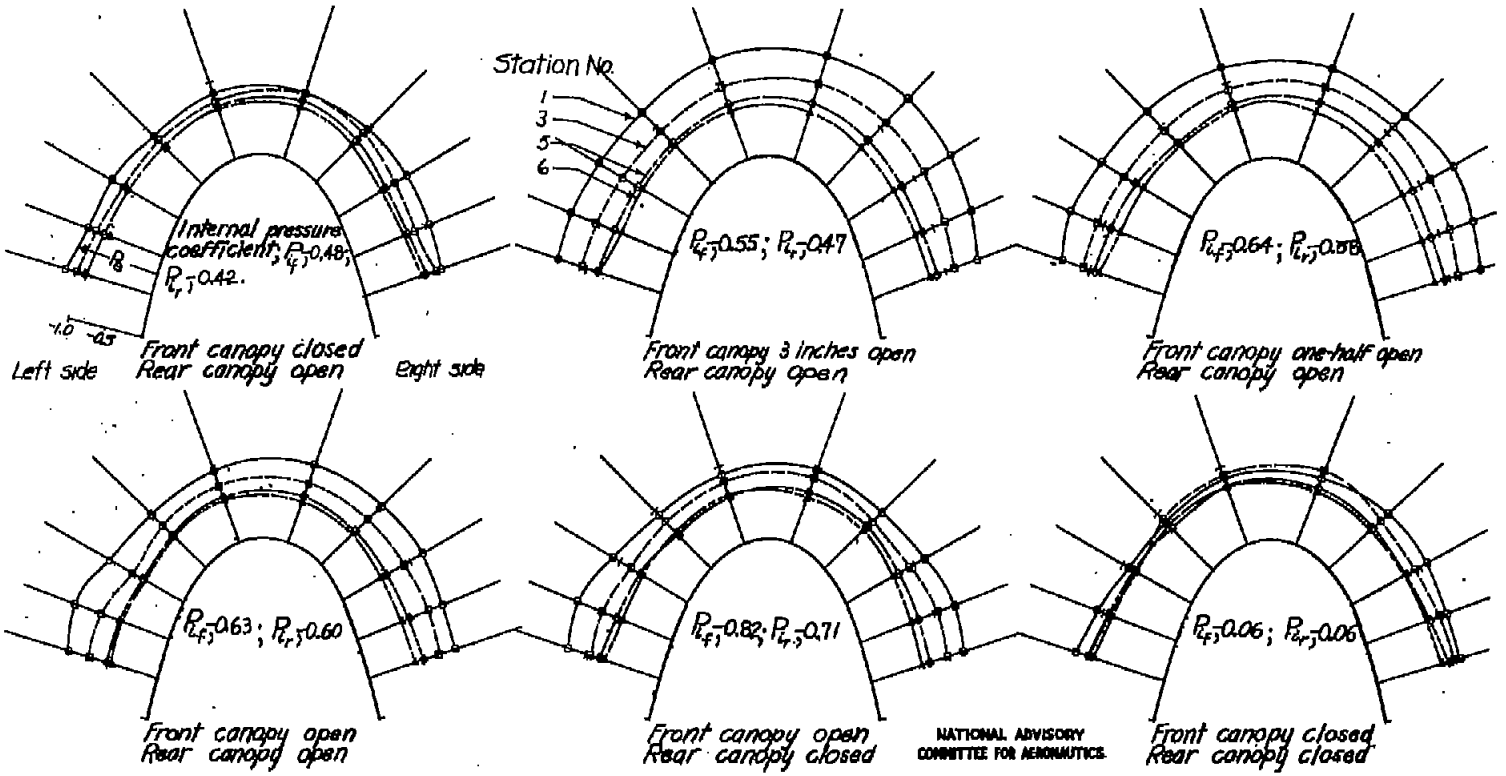

(c) Military power; T_c, 0.45; C_L, 0.98

Figure 9.-Continued.

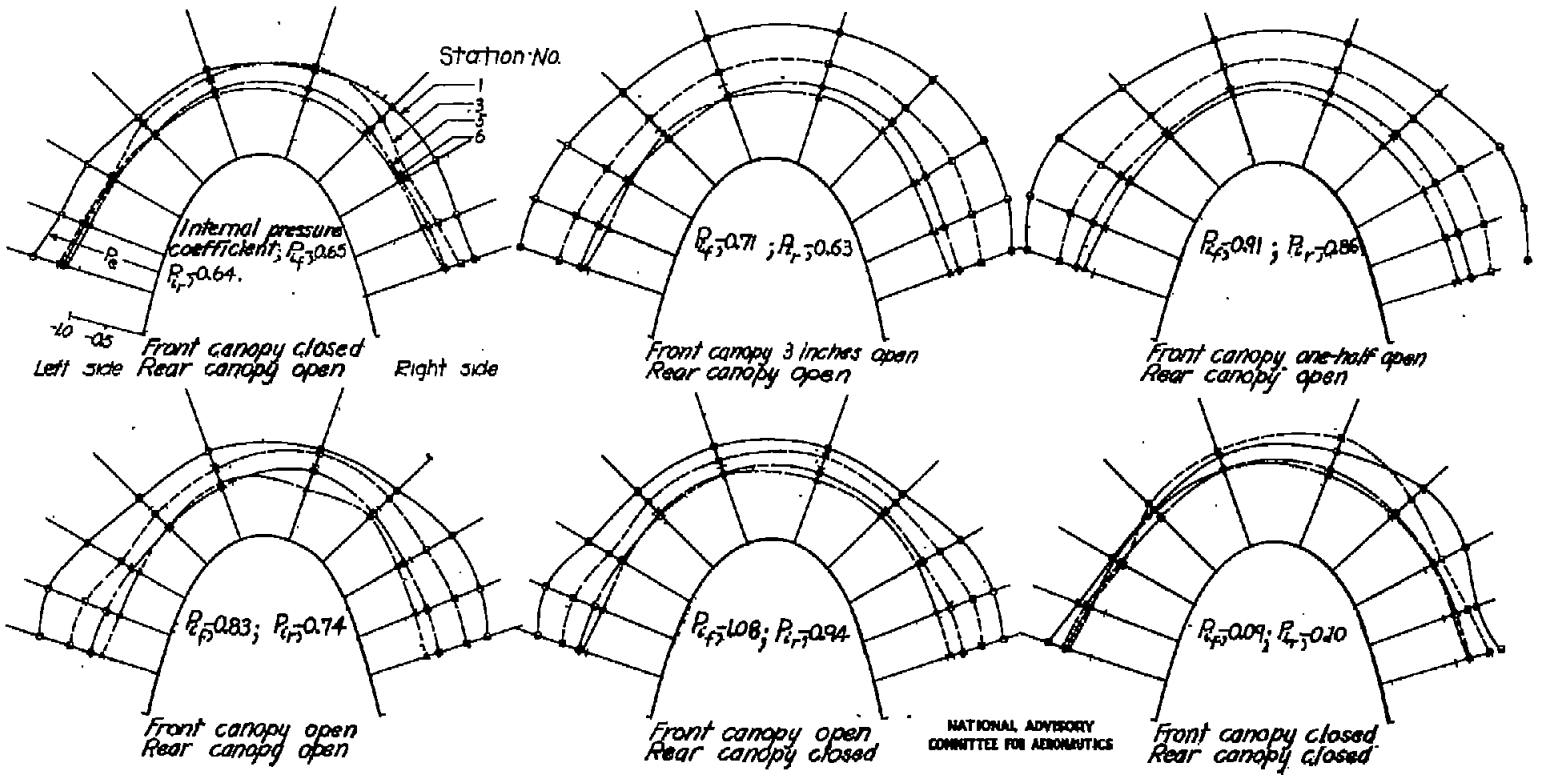

(d) **Military power;** T_c, 0.63; C_L, 1.33.

Figure 9.- Continued.

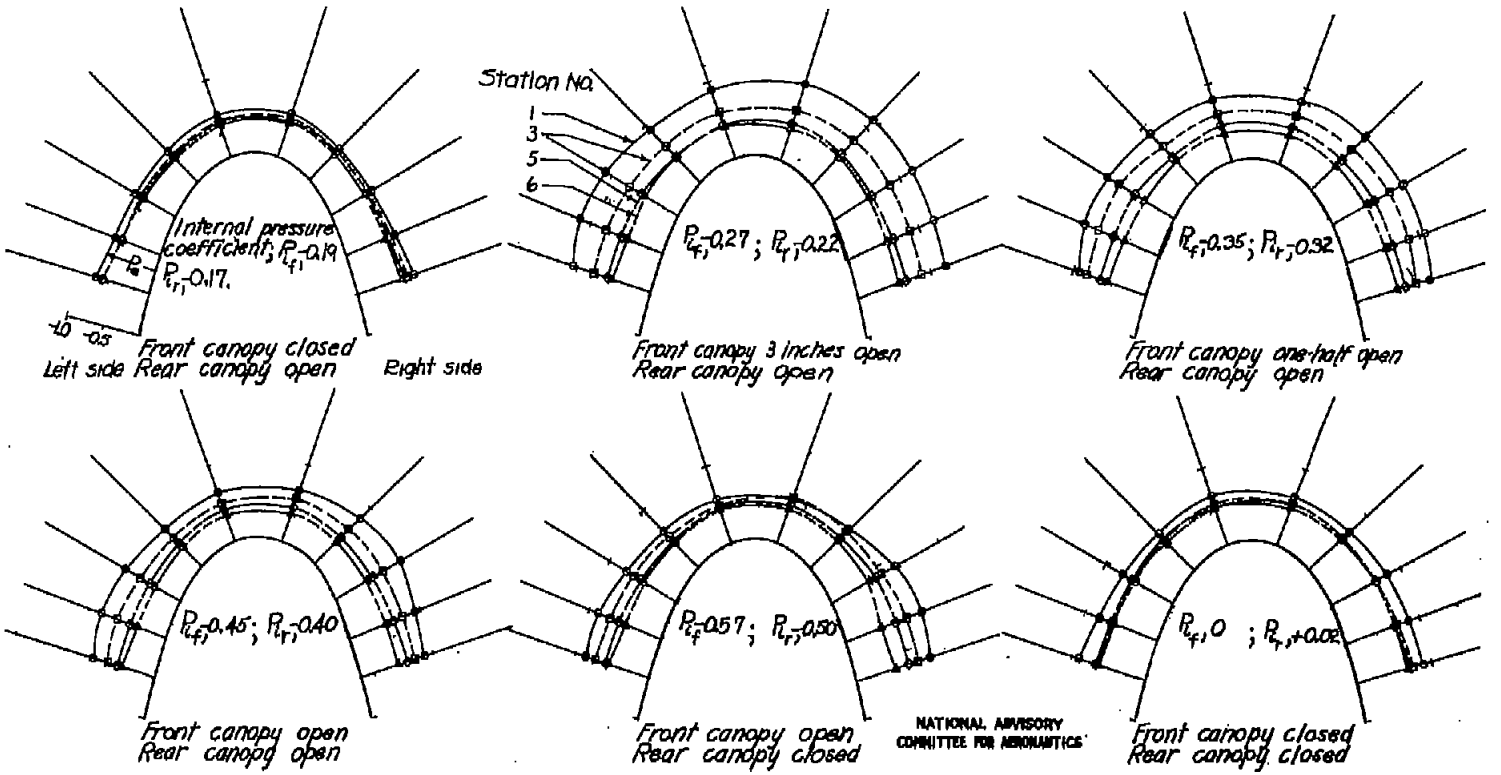

(e) Propeller idling; C_L 1.33.

Figure 9.-Concluded.

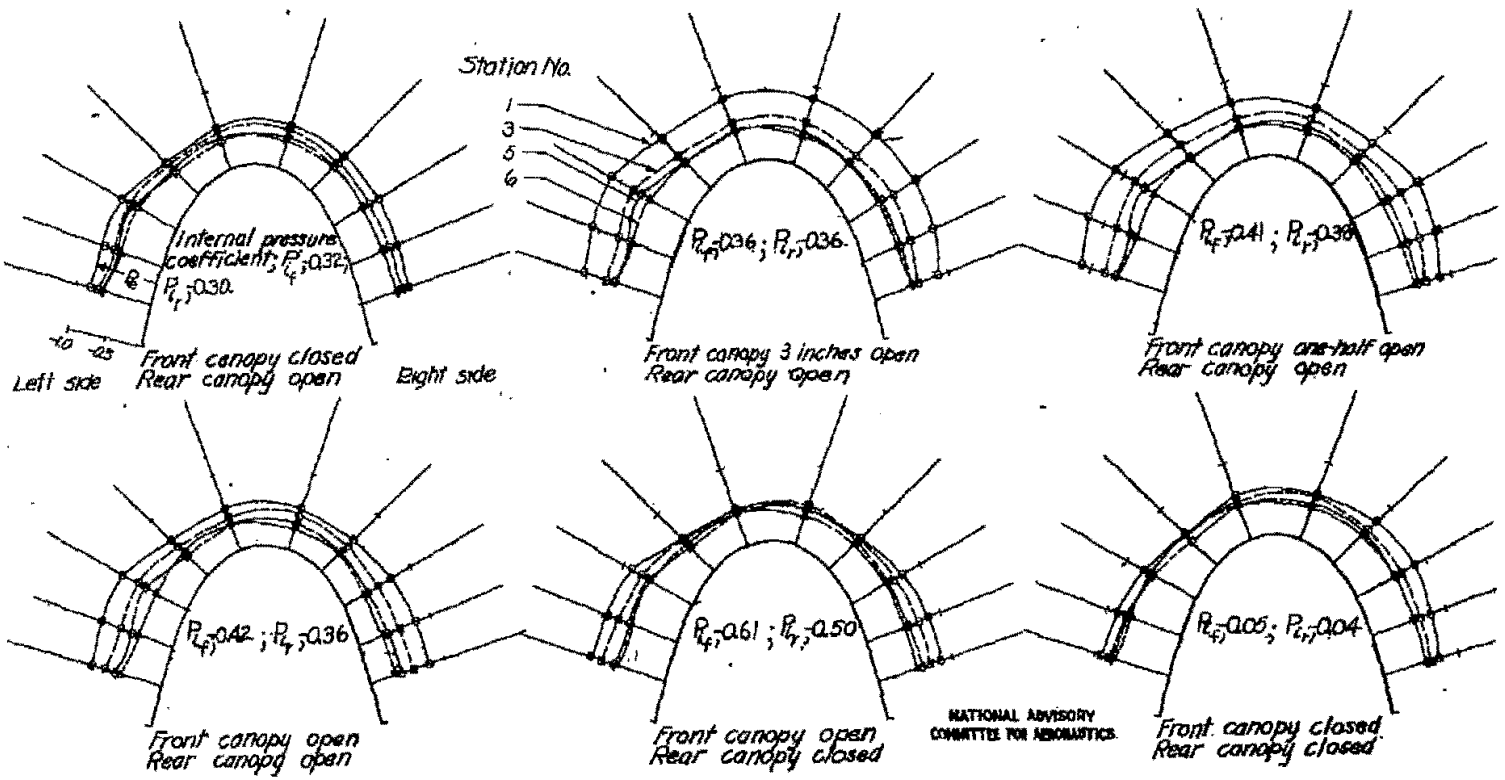

(a) Military power; T_c, 0.23; C_L, 0.56.

Figure 10 .- Pressure distributions over the front canopy of the SB2C-4E airplane. i_t, -7 deg.

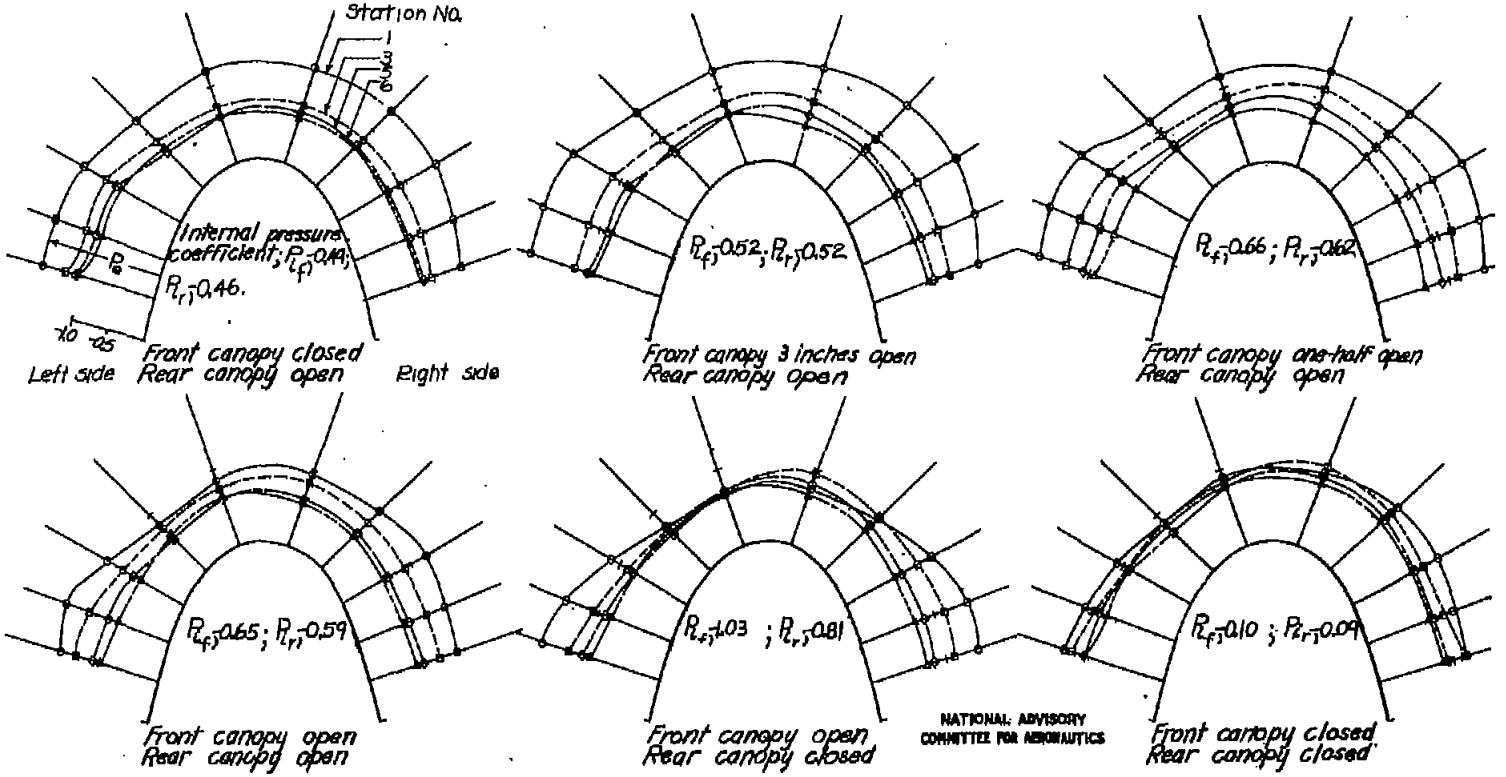

(b) Military power; T_c, 0.45; C_L, 0.98.

Figure 10.- Continued.

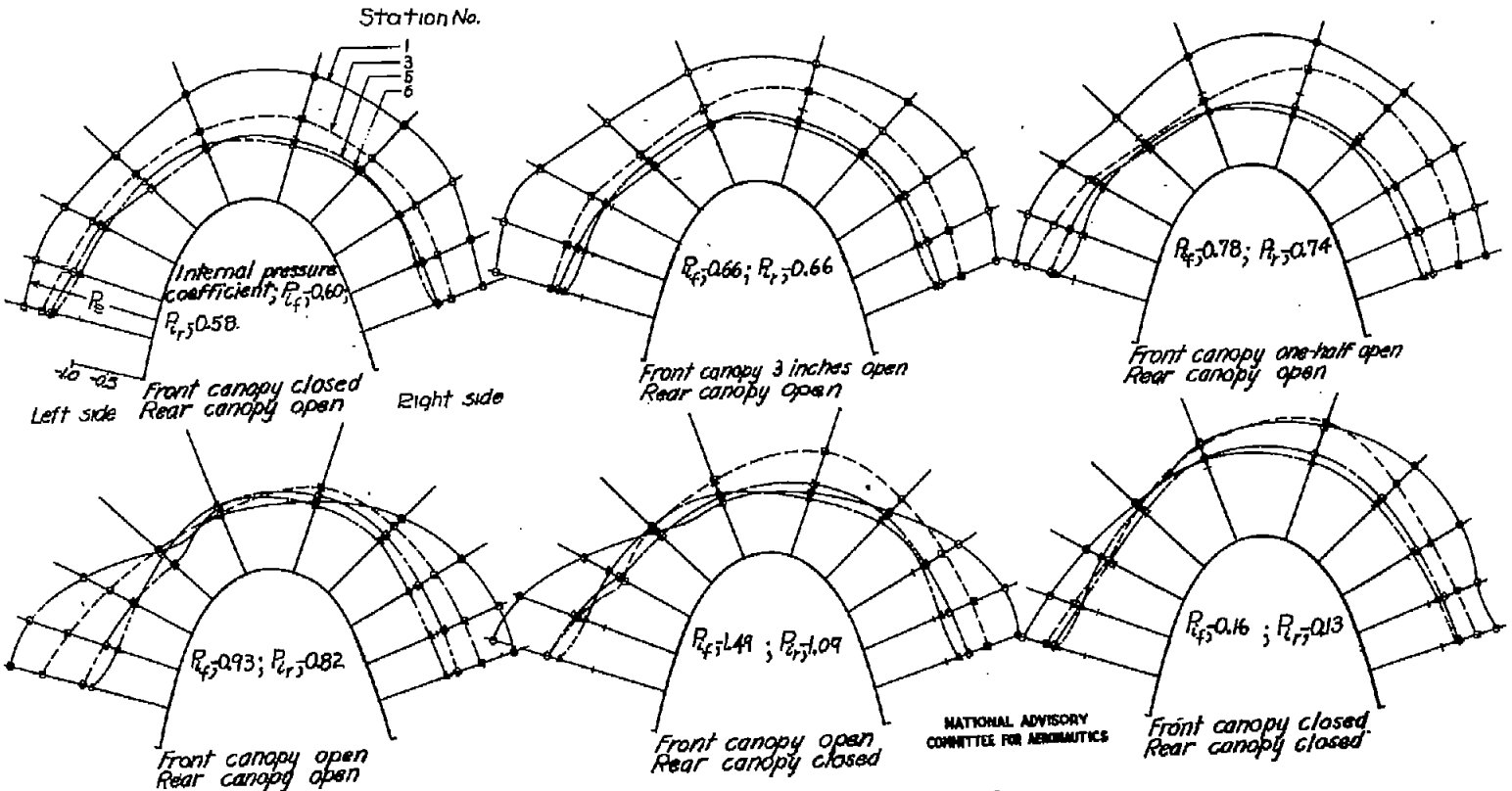

(c) Military power; T_c, 0.63; C_L, 1.33.

Figure 10.- Continued.

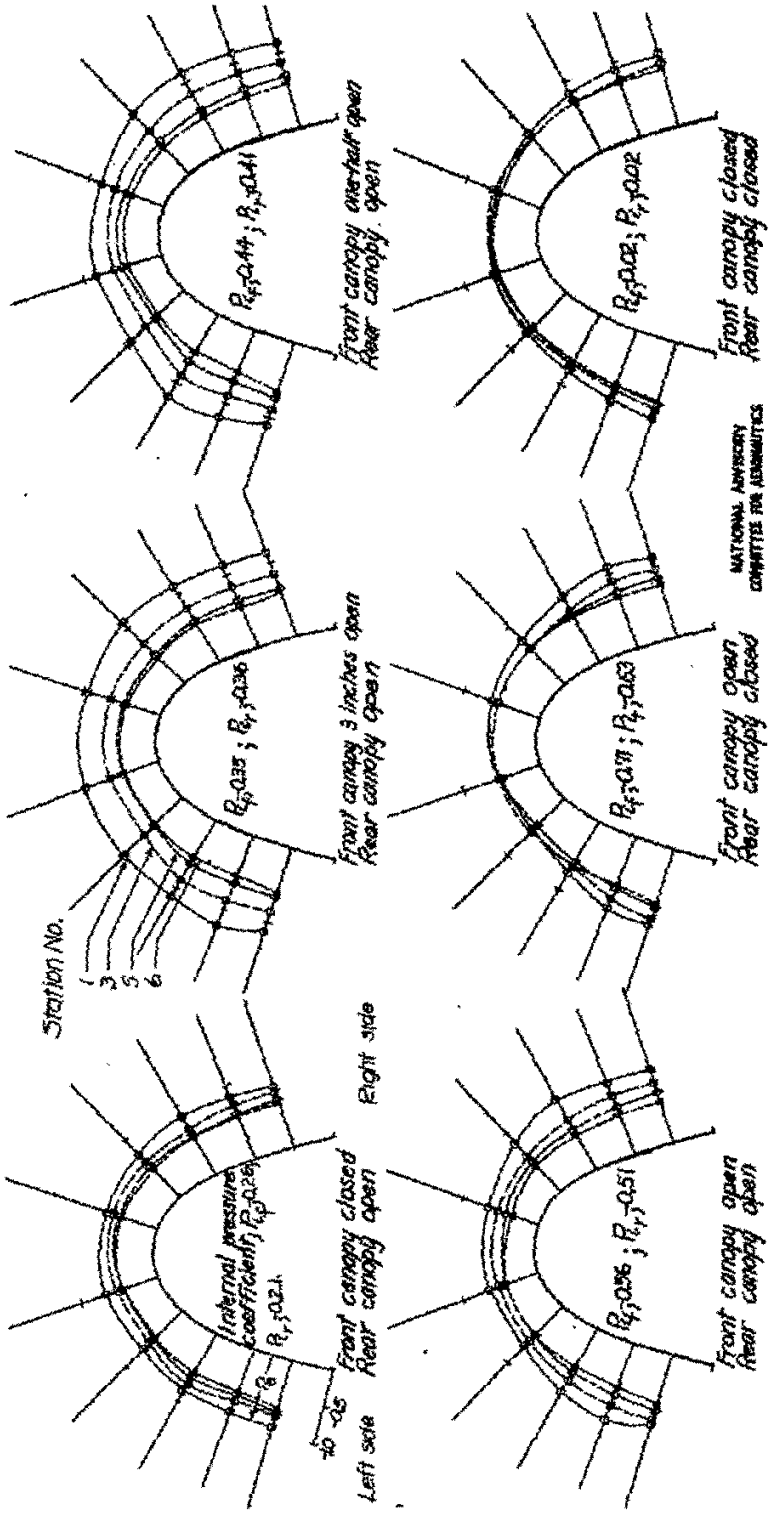

(d) Propeller idling, C_L .133.

Figure 10.- Concluded.

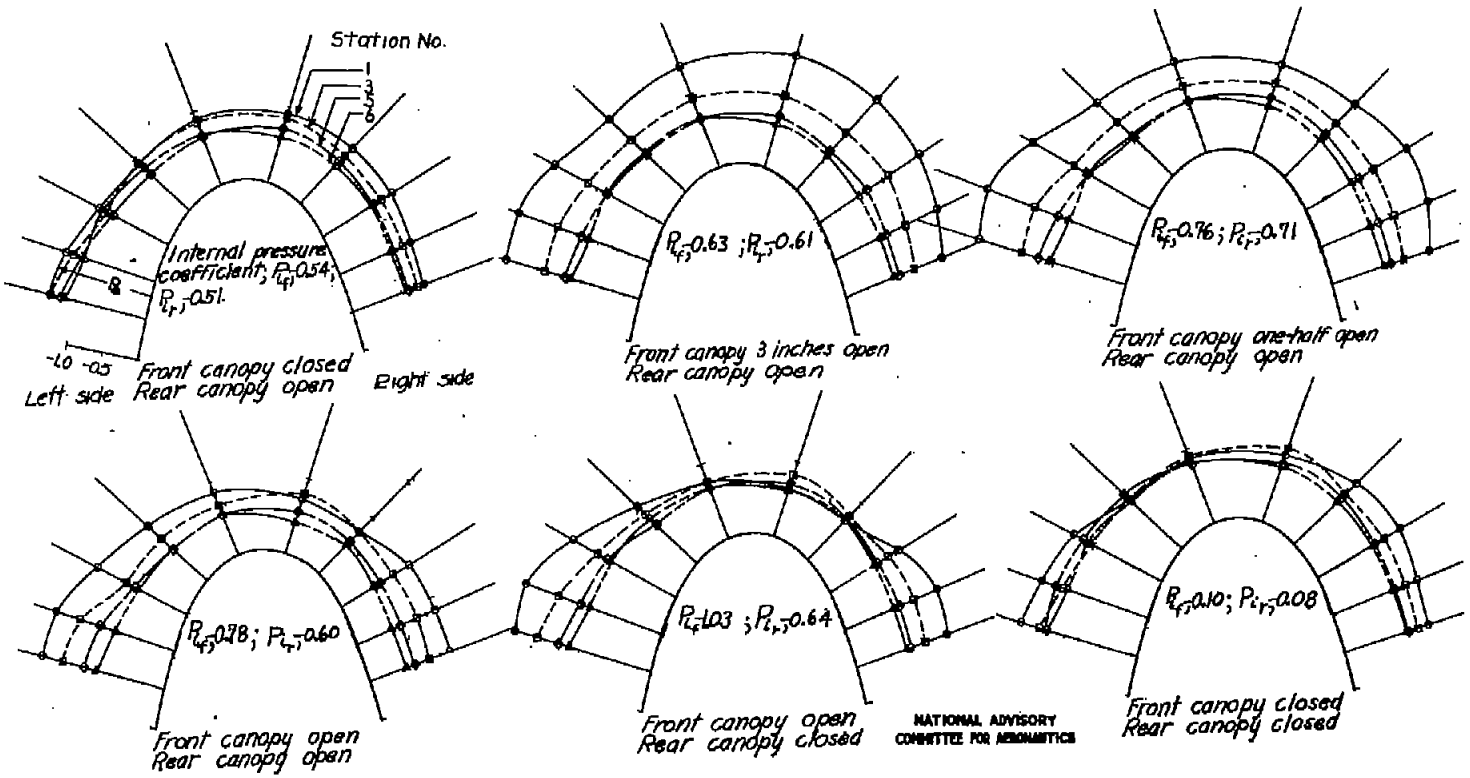

(a) Military power; T_c, 0.45 ; C_L, 0.98.

Figure 11 – Pressure distributions over the front canopy of the SB2C-4E airplane. ψ, -15 deg.

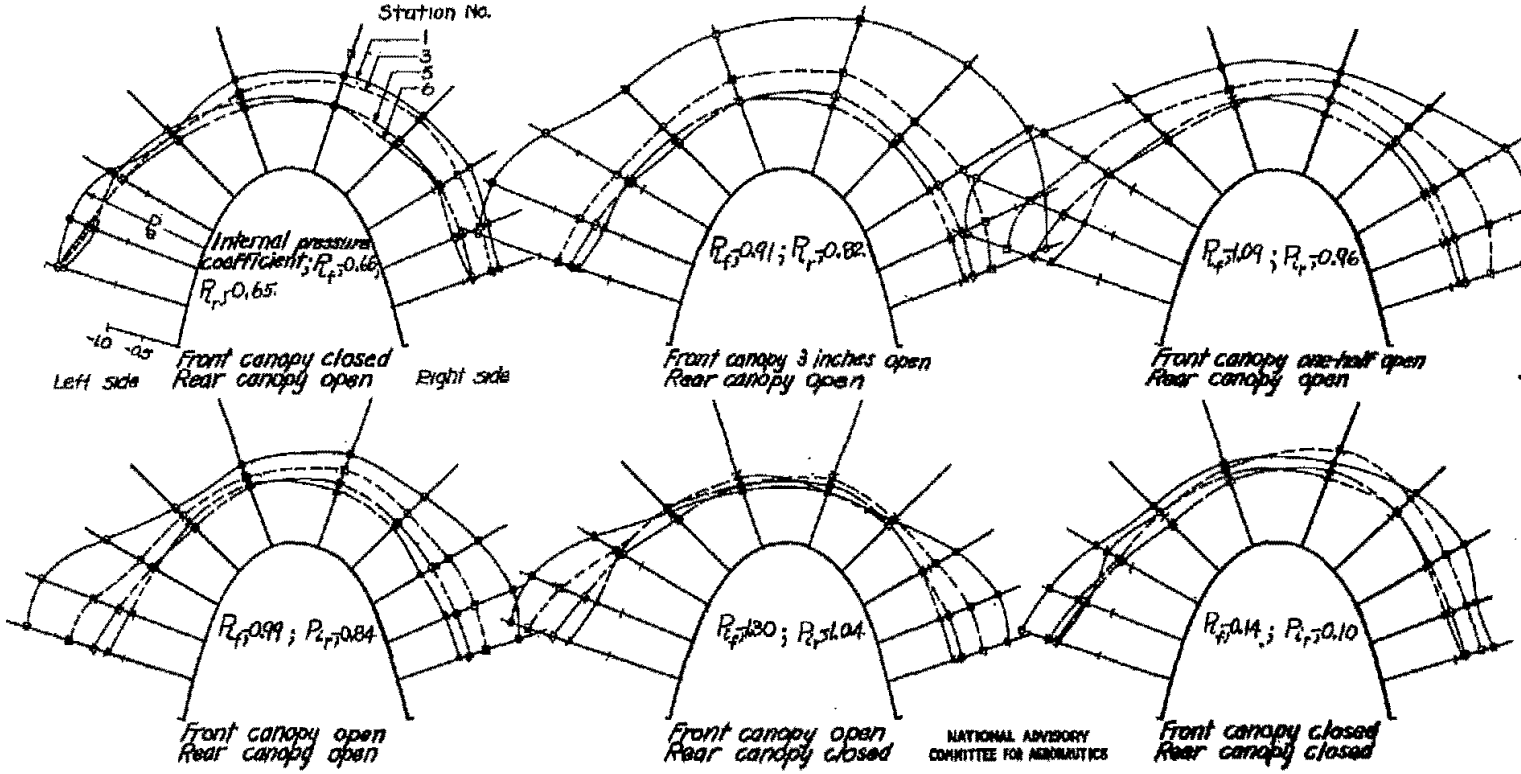

(b) Military power, T_0, 0.63; C_L, 1.33.

Figure 11.- Continued.

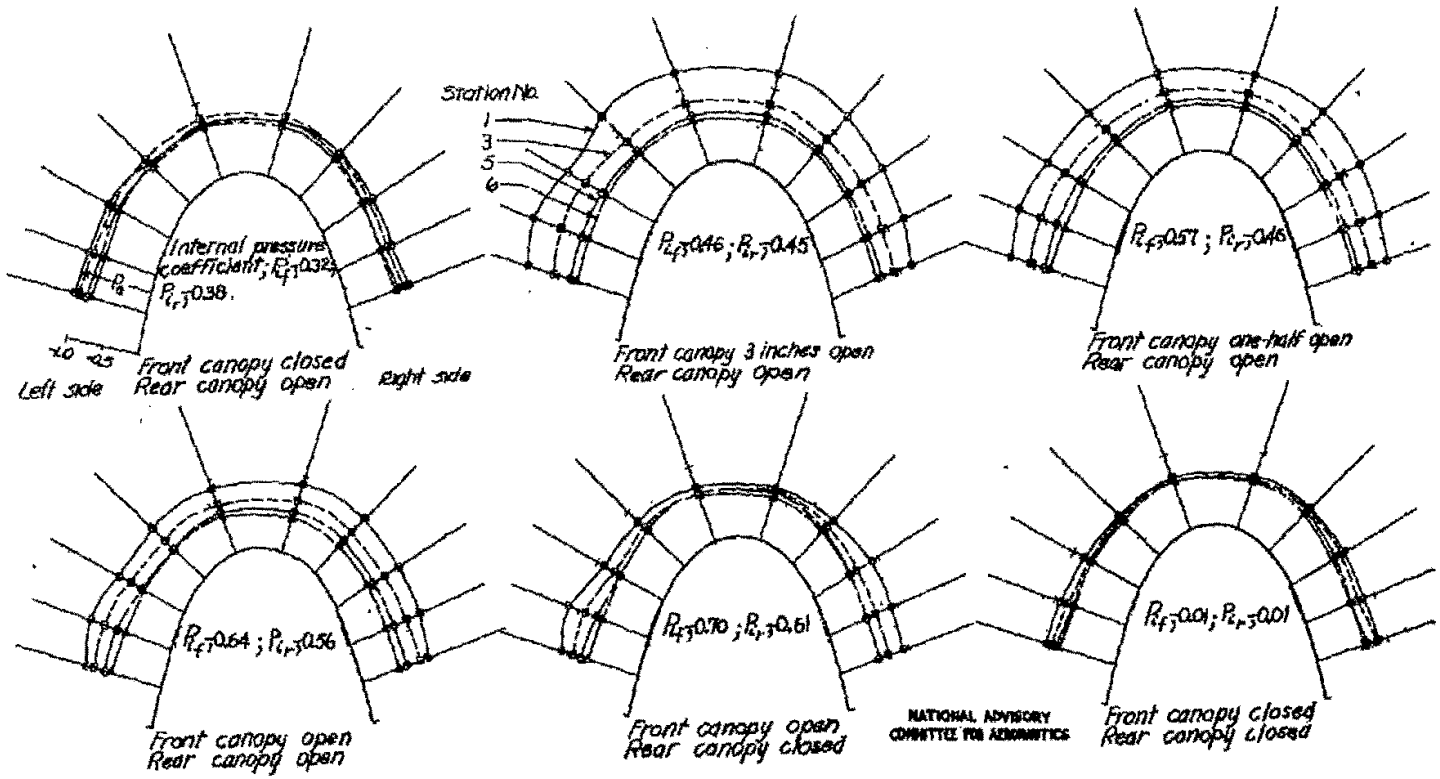

(C) Propeller idling; C_{L_a} 1.33.

Figure 11.-Concluded.

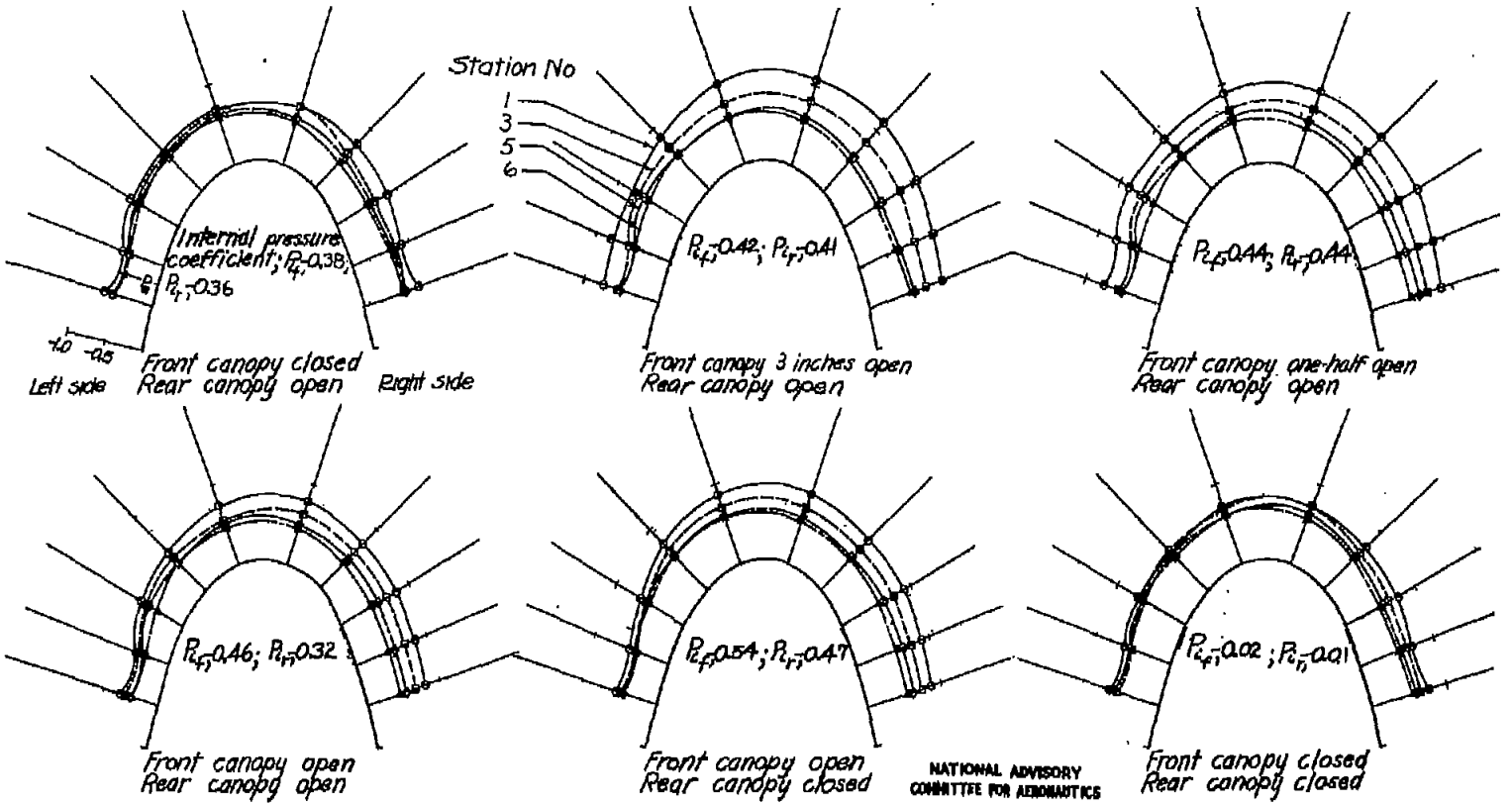

(a) Military power; T_c,023; C_L,056.

Figure 12 .– Pressure distributions over the front canopy of the SB2C-4E airplane. α, 7 deg.

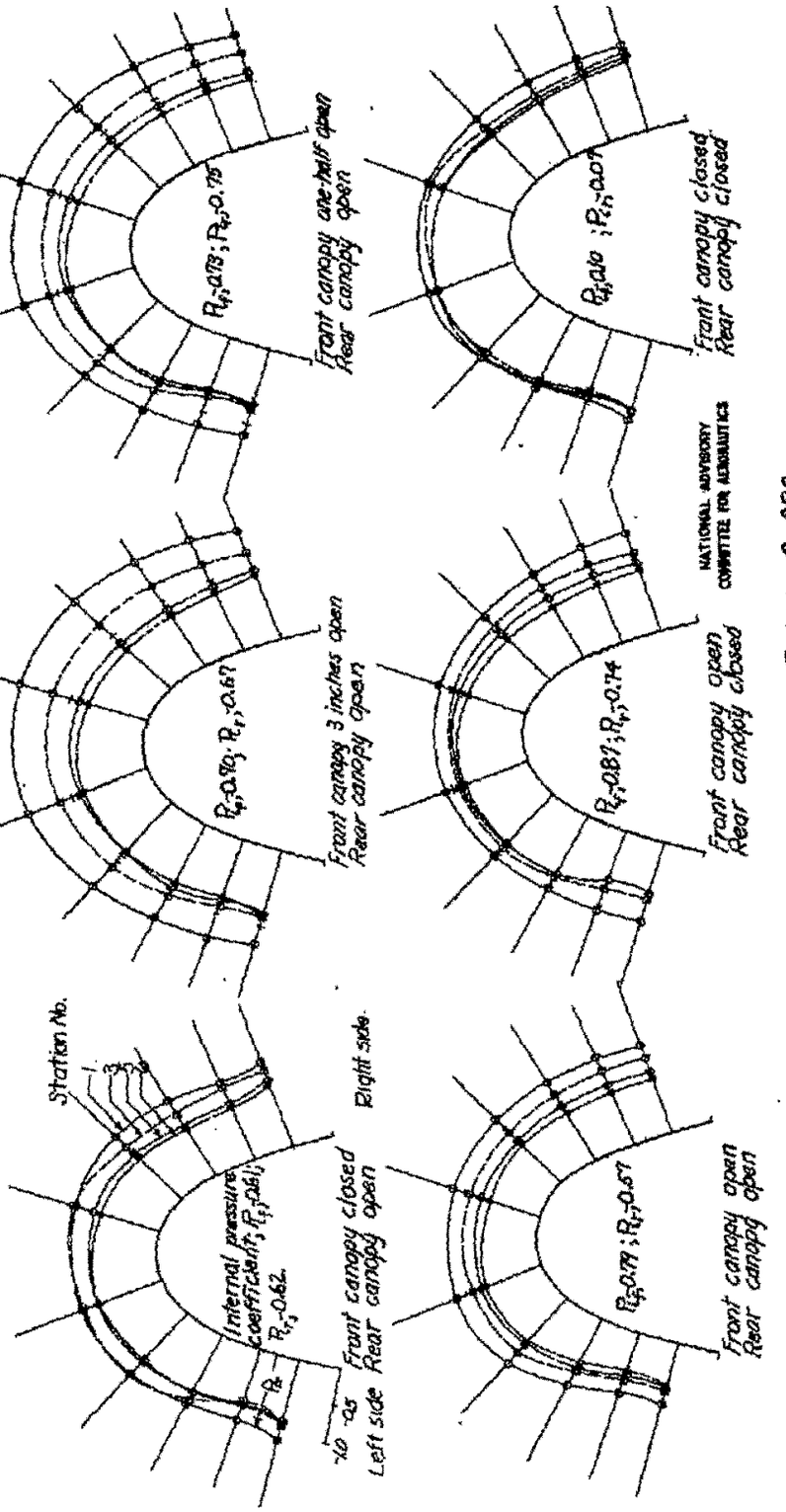

(b) Military power; T_c, 0.45 ; C_L, 0.98.

Figure 12.- Continued.

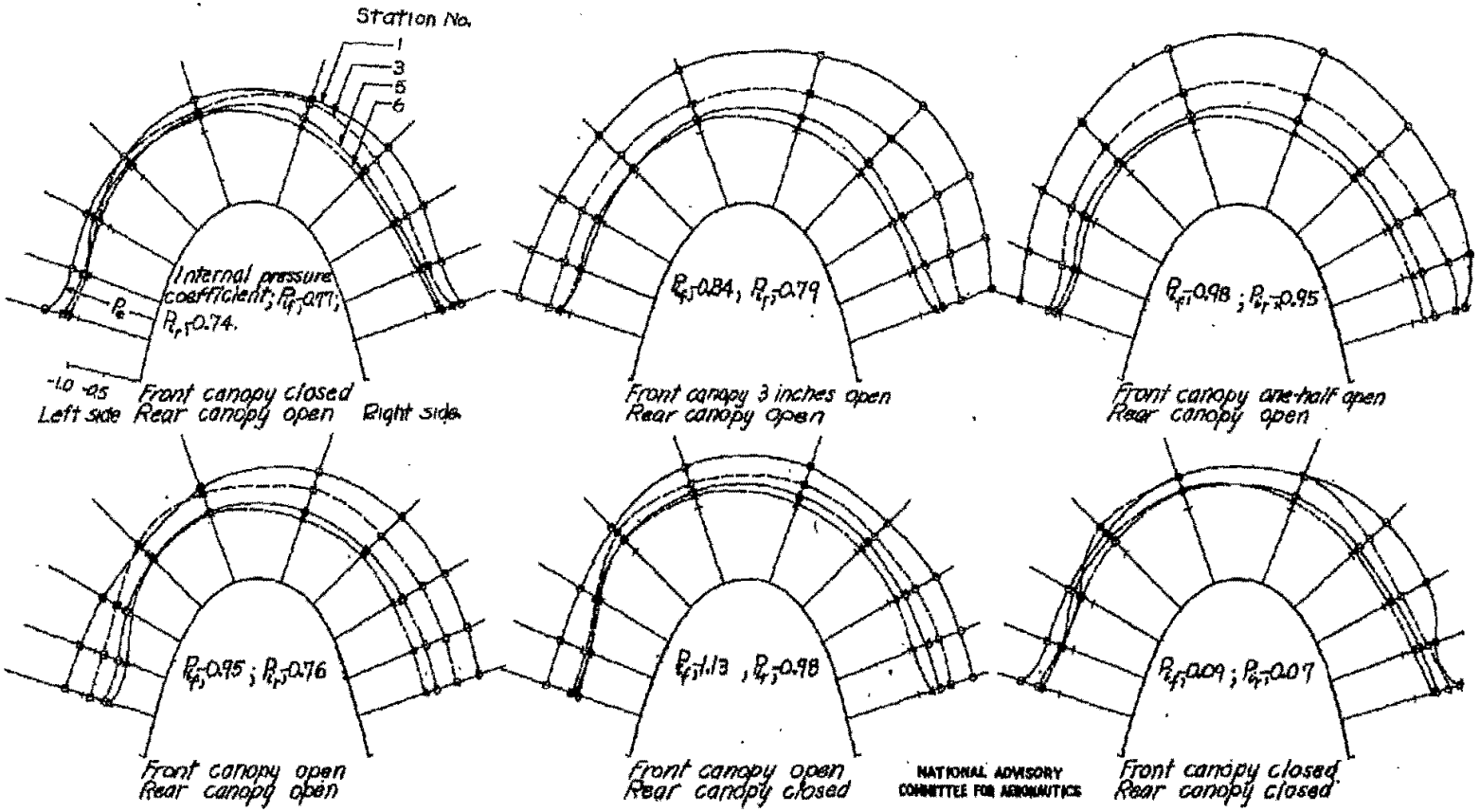

(c) Military power; T_0, 0.63; C_L, 1.33.

Figure 12.- Continued.

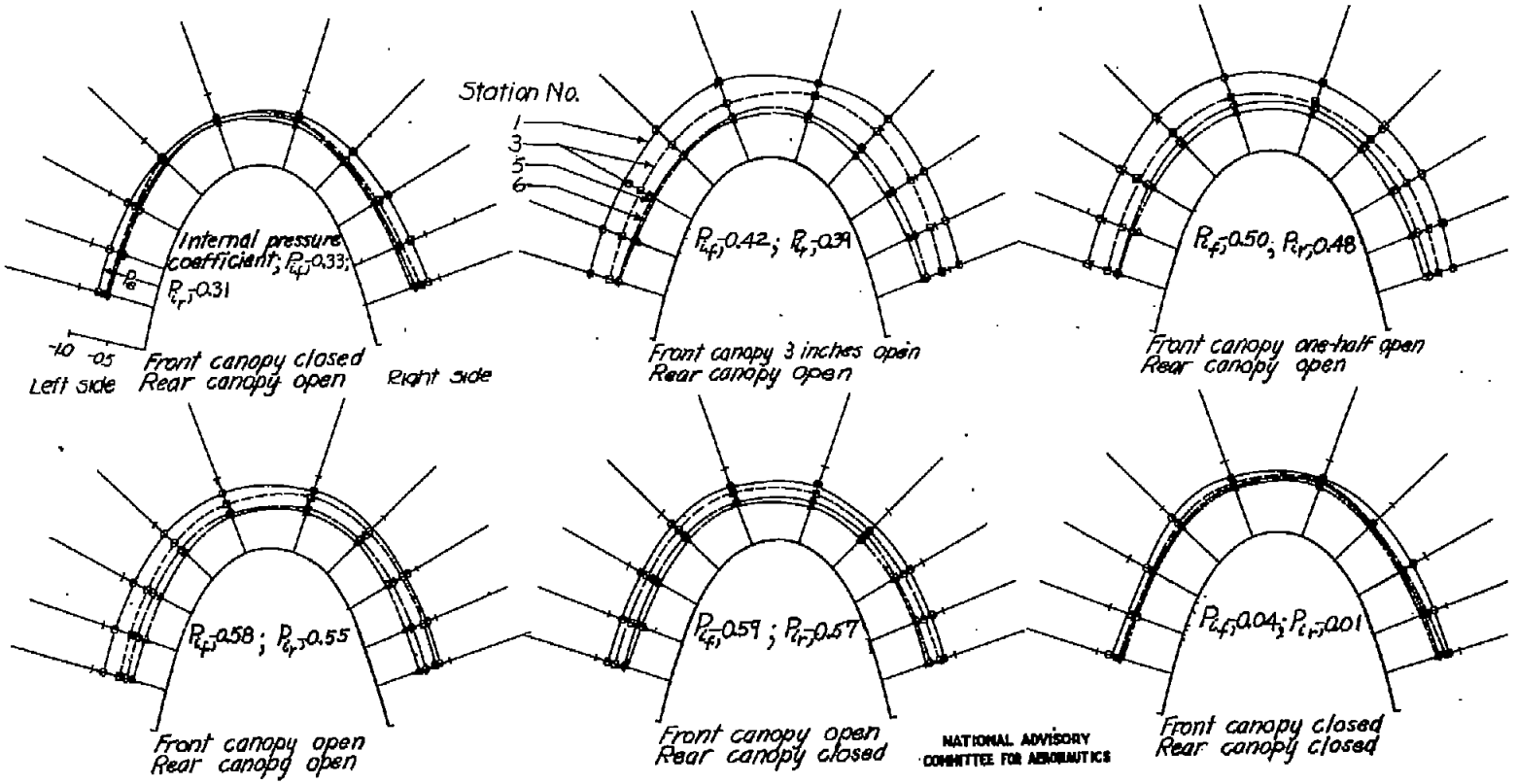

(d) Propeller idling; C_L 1.33

Figure 12.- Concluded.

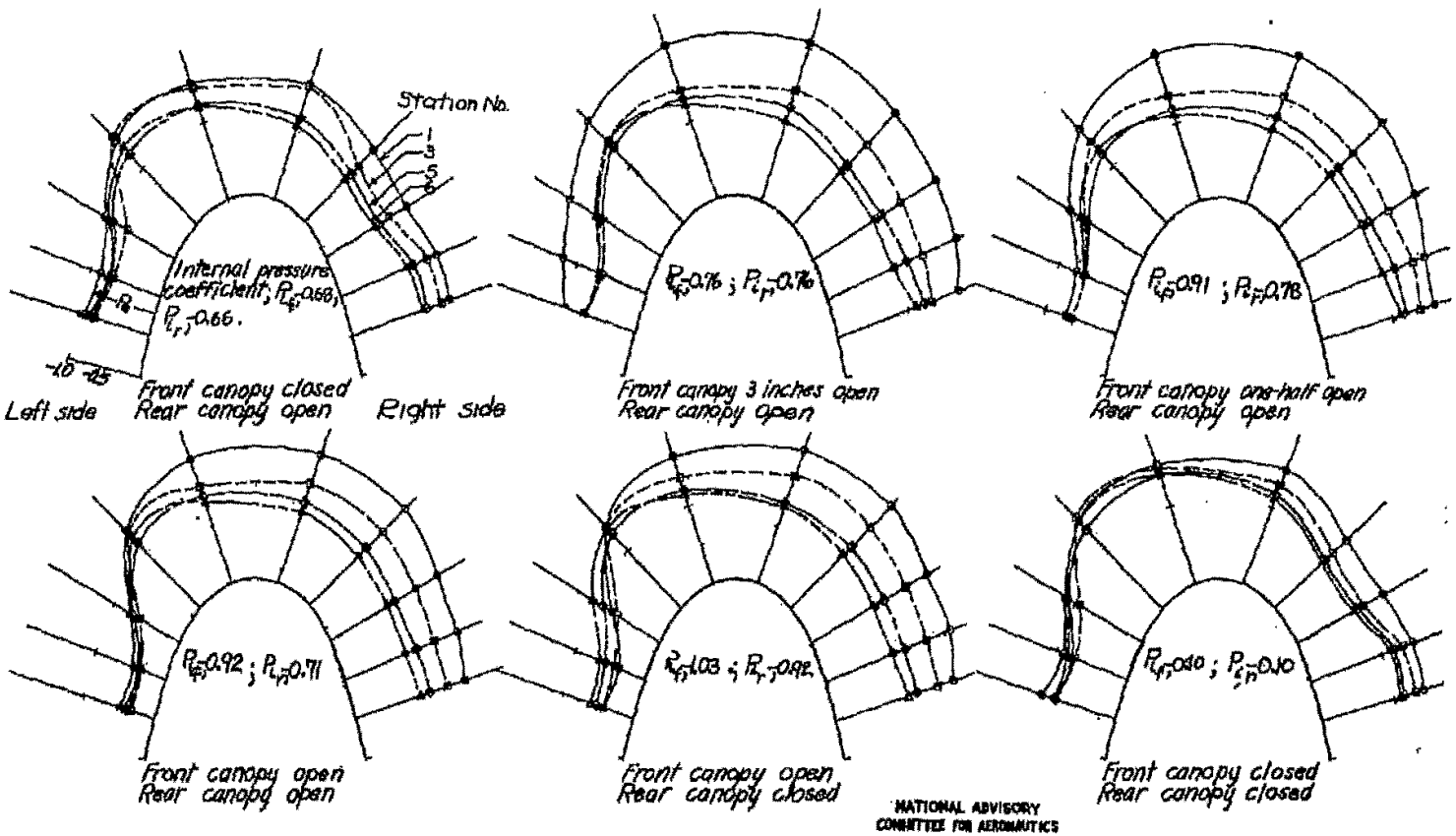

(a) Military power; T_c, 0.45; C_L, 0.98.

Figure 13 .- Pressure distributions over the front canopy of the SB2C-4E airplane. Ψ, 15 deg.

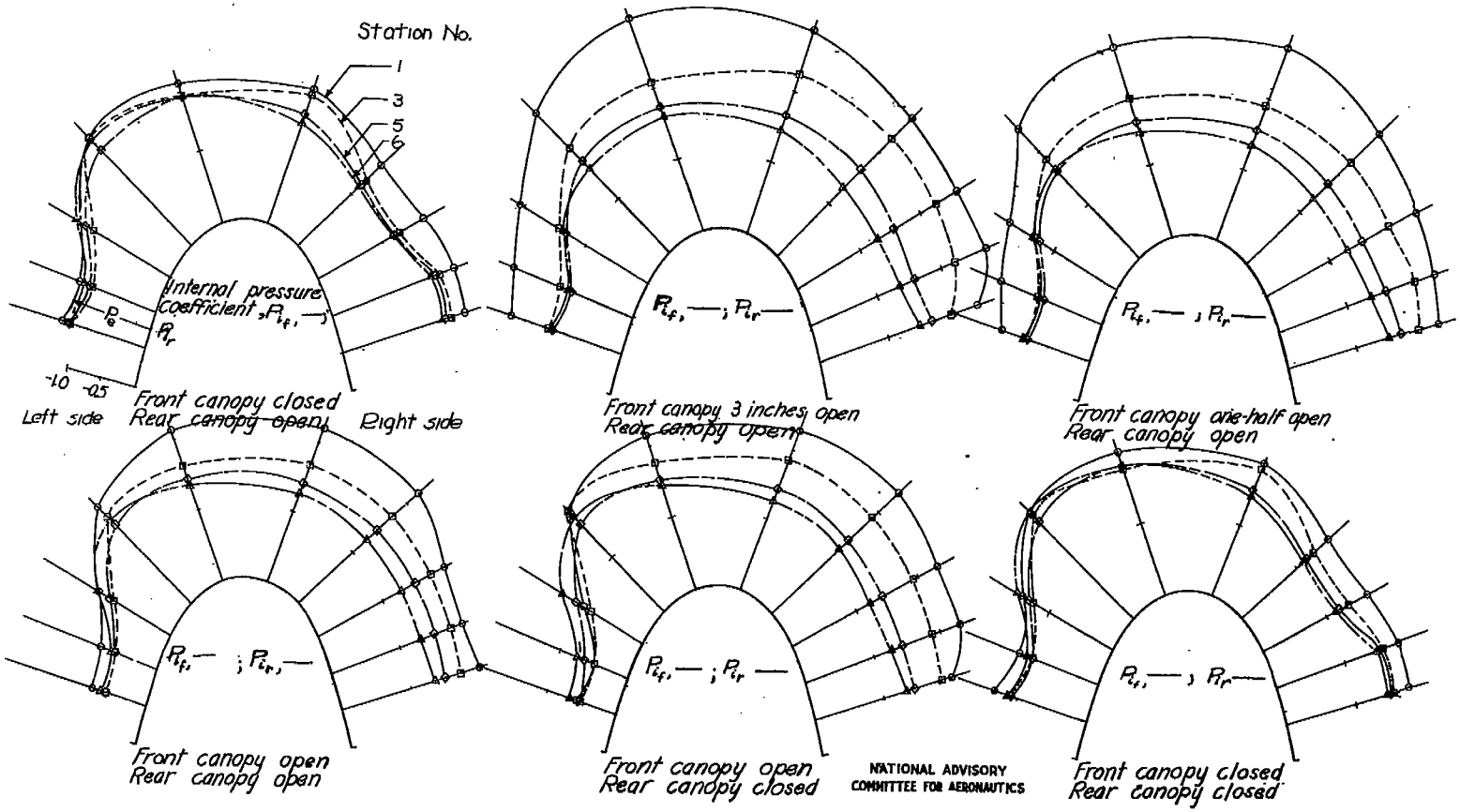

(b) **Military power;** T_c, 0.63; C_L, 1.33

Figure 13.- Continued.

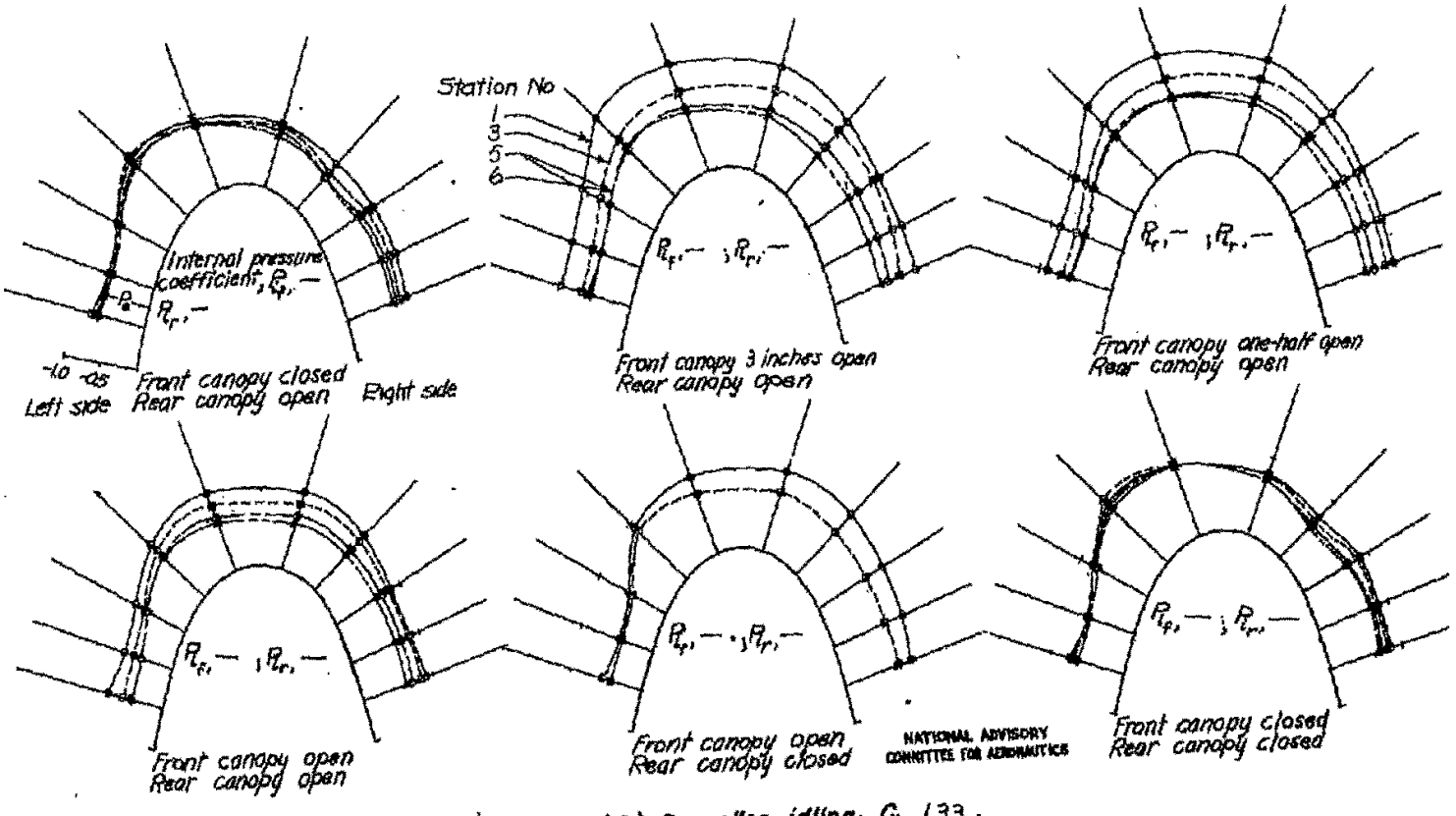

(c) Propeller idling; C_L 1.33.

Figure 13.- Concluded.

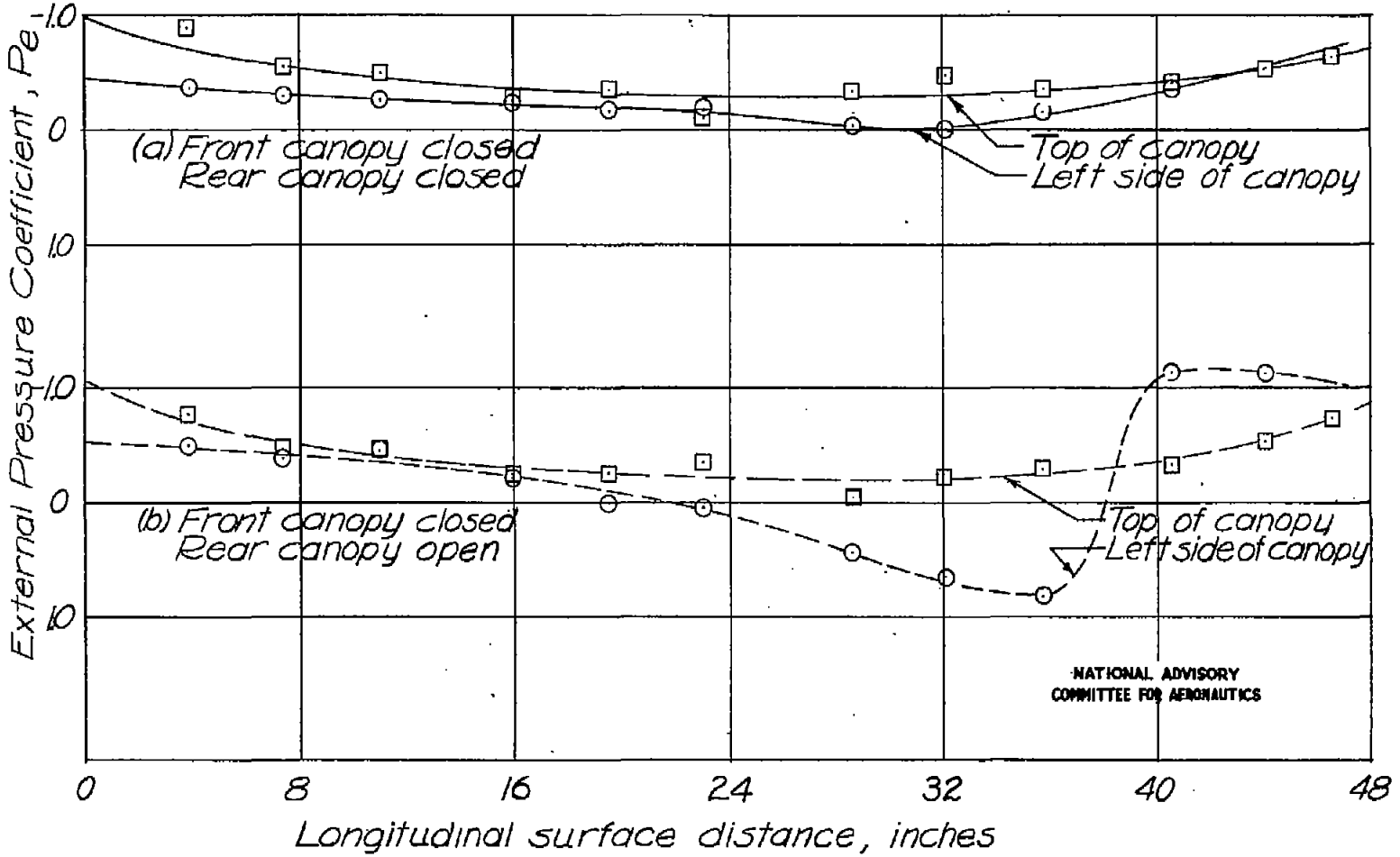

Figure 14.- Typical longitudinal pressure variations on the rear canopy of the SB2C-4E airplane. C_L, 1.33; ψ_f, 0°; Propeller operating; T_c, 0.63

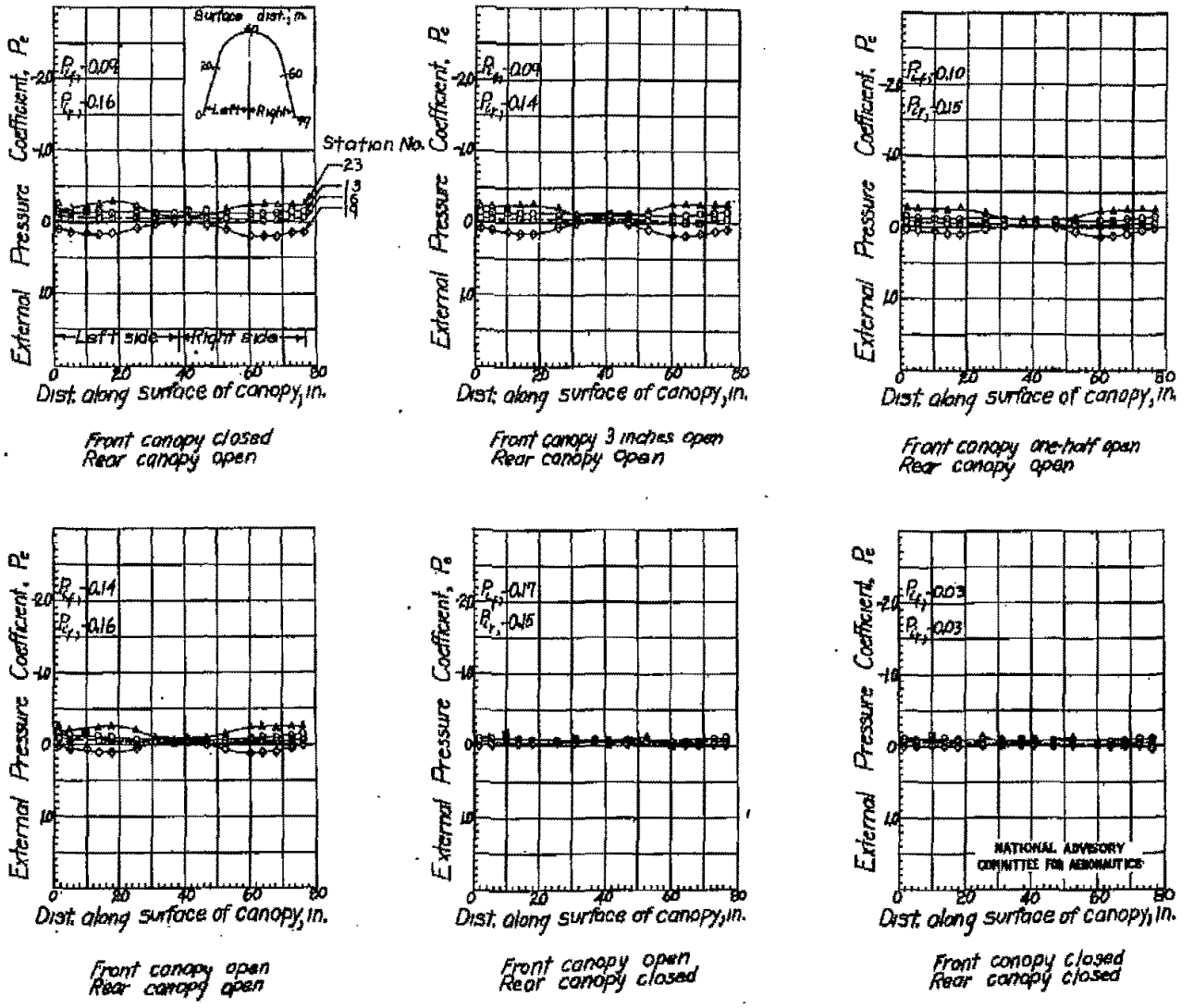

(a) Propeller removed; C_L, 0.17

Figure 15 .- Pressure distributions over the rear canopy of the SB2C-4E airplane. ψ, 0 deg.

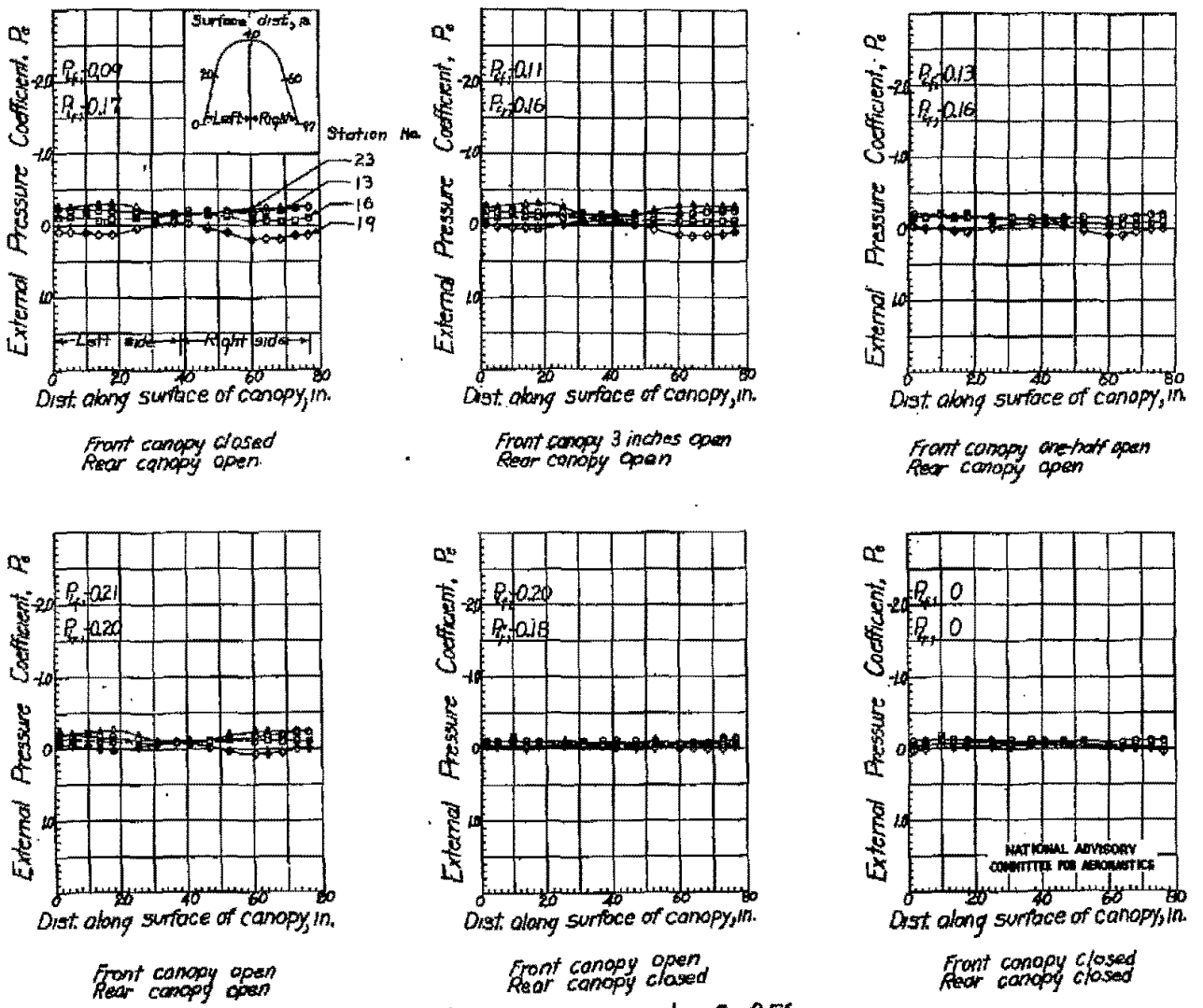

Front canopy closed
Rear canopy open

Front canopy 3 inches open
Rear canopy open

Front canopy one-half open
Rear canopy open

Front canopy open
Rear canopy open

Front canopy open
Rear canopy closed

Front canopy closed
Rear canopy closed

(b) Propeller removed; C_L, 0.56

Figure 15.-Continued.

Fig. 15b

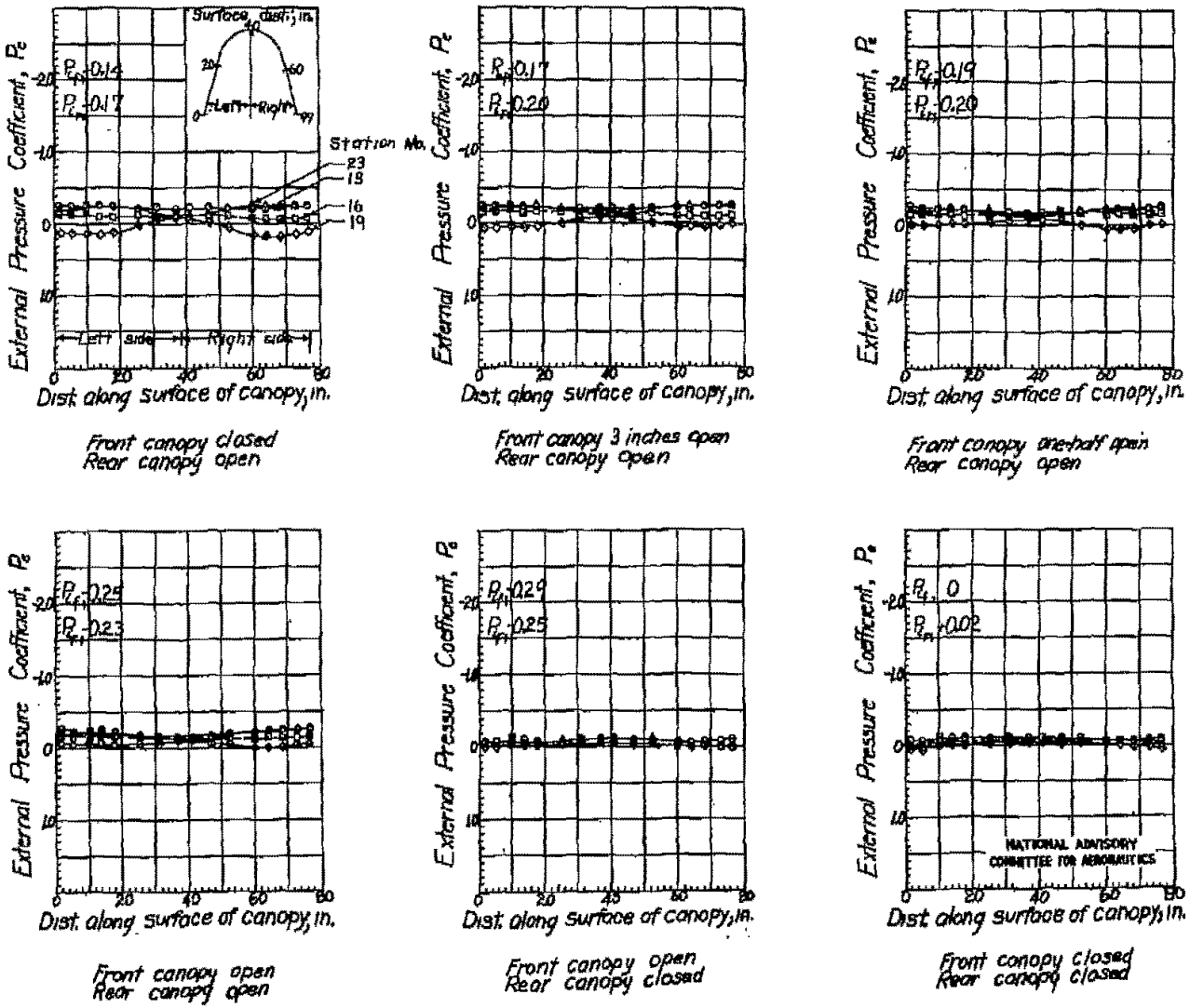

Front canopy closed
Rear canopy open

Front canopy 3 inches open
Rear canopy open

Front canopy one-half open
Rear canopy open

Front canopy open
Rear canopy open

Front canopy open
Rear canopy closed

Front canopy closed
Rear canopy closed

(c) **Propeller removed;** C_{L_1} 0.98

Figure 15. - Continued.

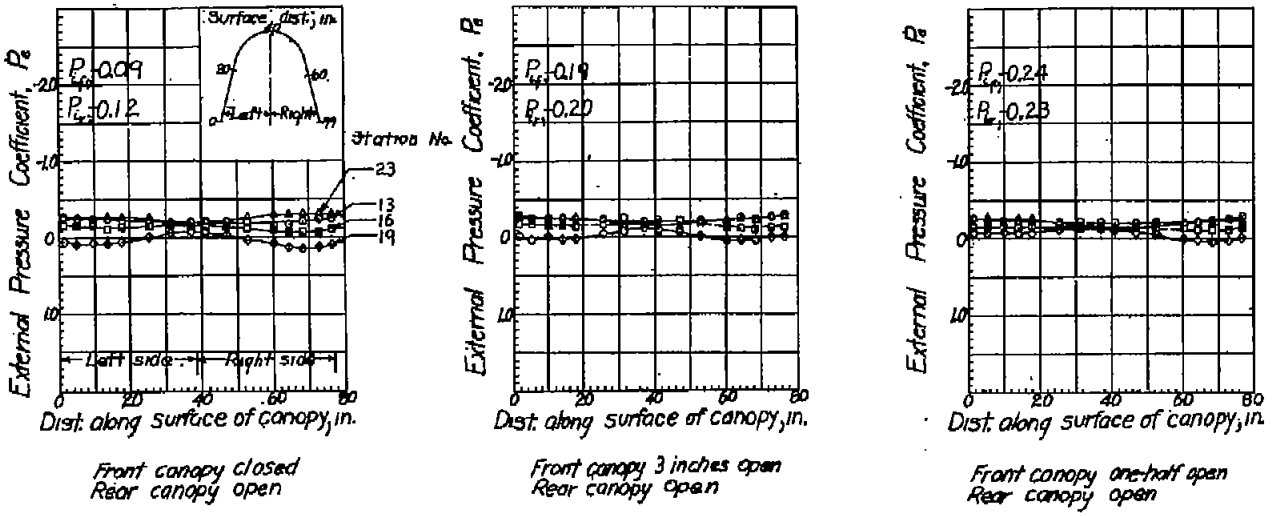

Front canopy closed
Rear canopy open

Front canopy 3 inches open
Rear canopy open

Front canopy one-half open
Rear canopy open

Front canopy open
Rear canopy open

Front canopy open
Rear canopy closed

Front canopy closed
Rear canopy closed

(d) Propeller removed, C_L, 1.33

Figure 15.- Concluded.

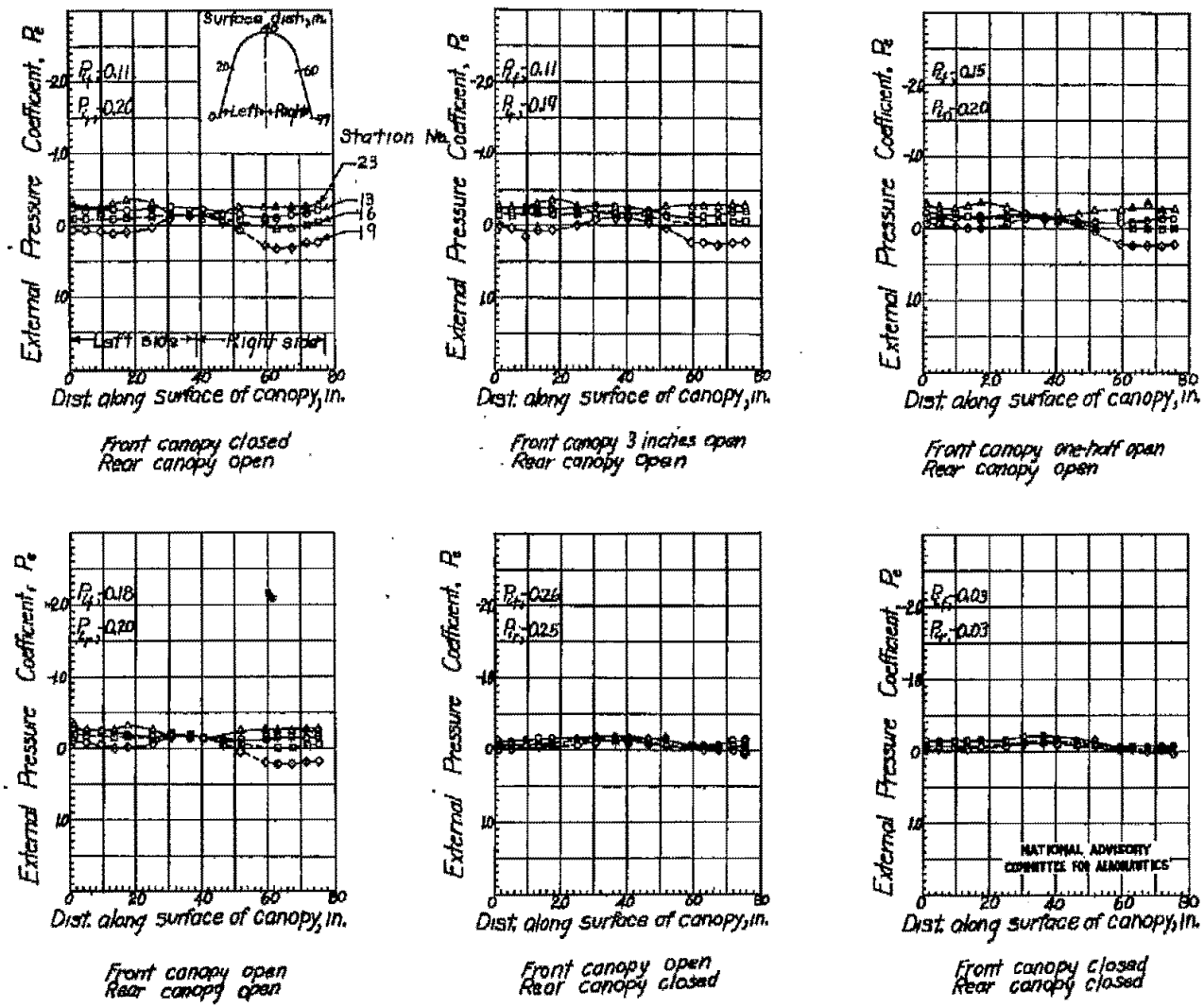

(a) Propeller removed, C_L, 0.56

Figure 16. – Pressure distributions over the rear canopy of the SB2C-4E airplane. ψ, -7 deg.

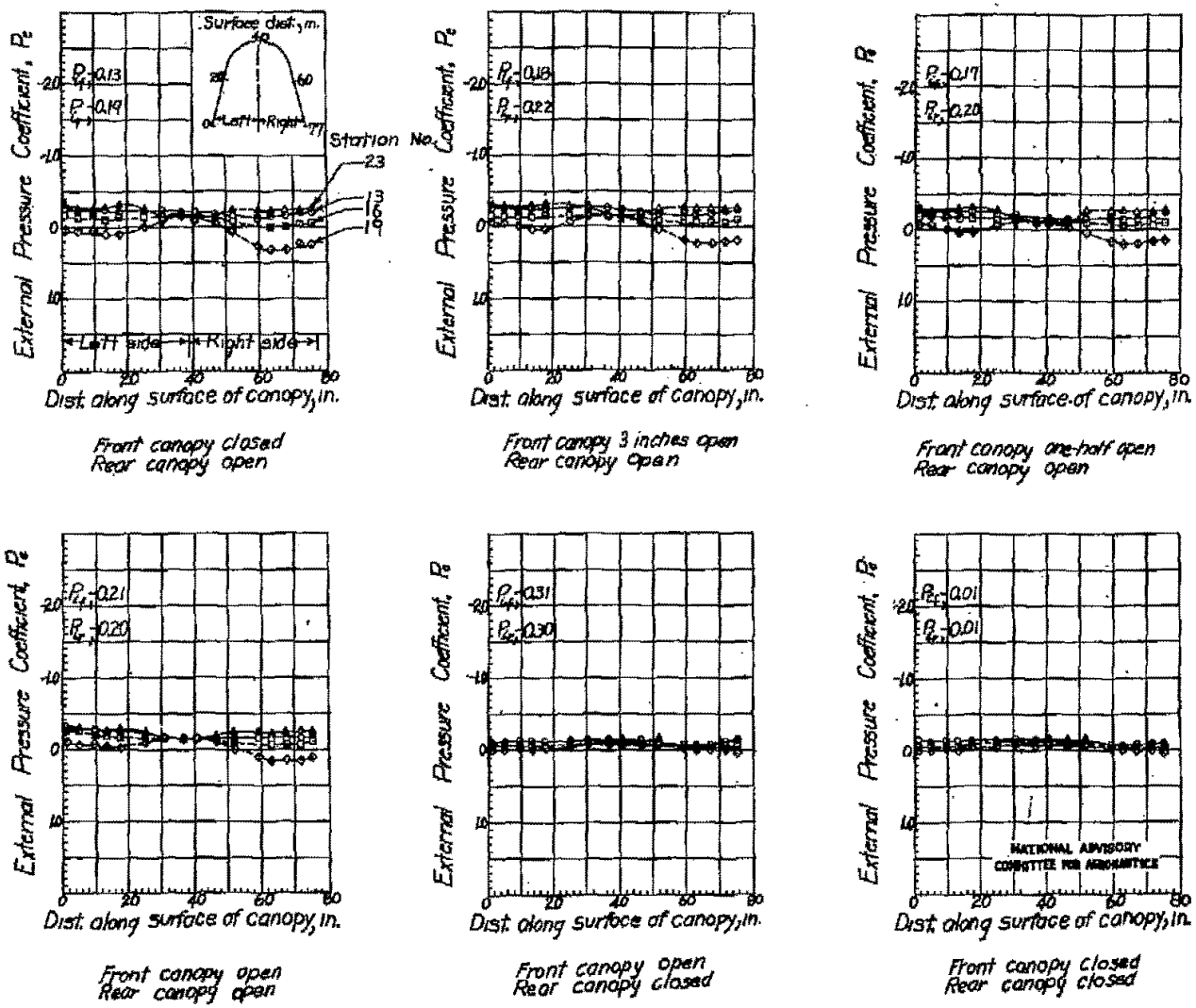

(b) Propeller removed, C_L, 0.98

Figure 16.- Continued.

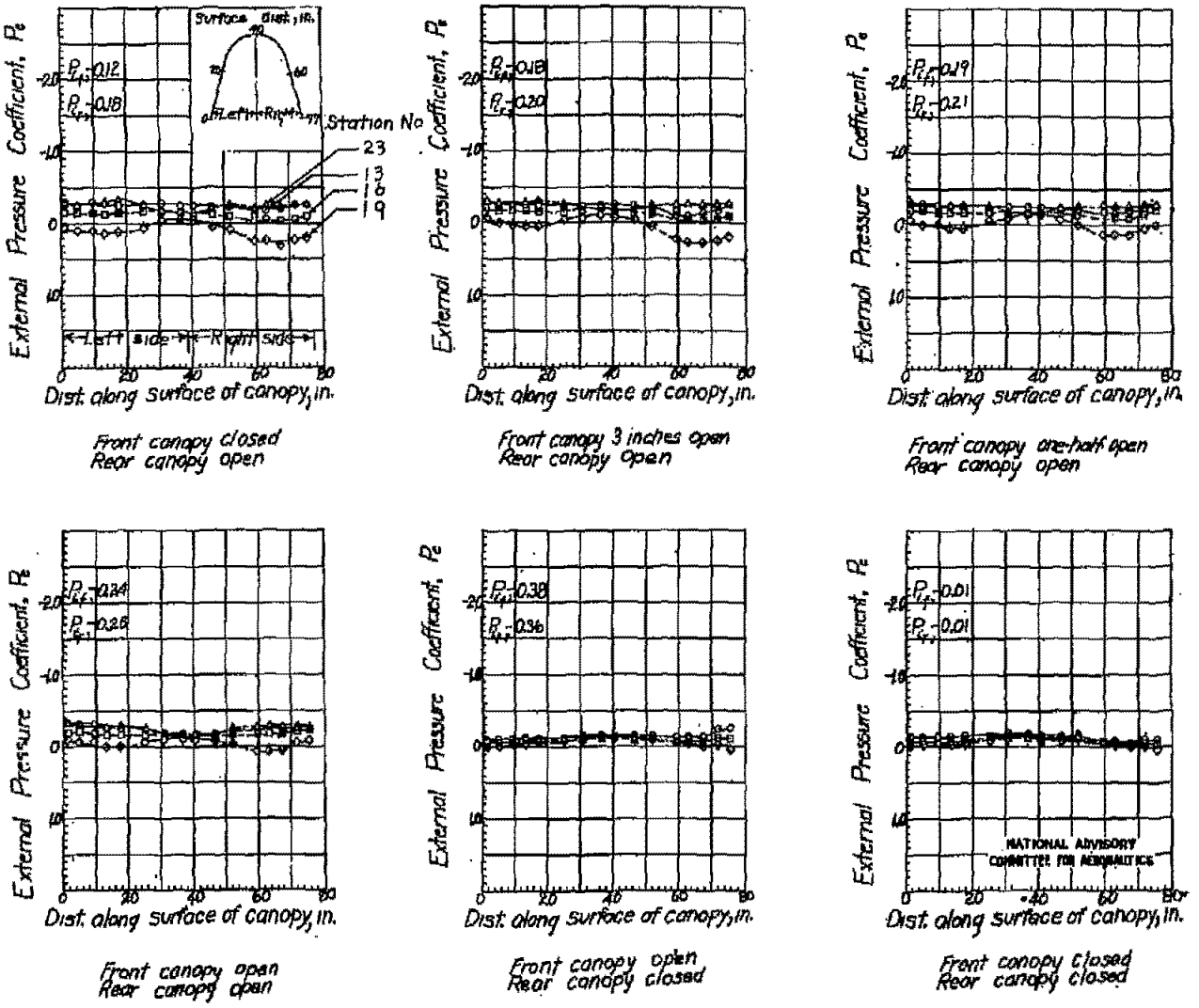

(c) *Propeller removed,* C_L, 1.33

Figure 16.- Concluded.

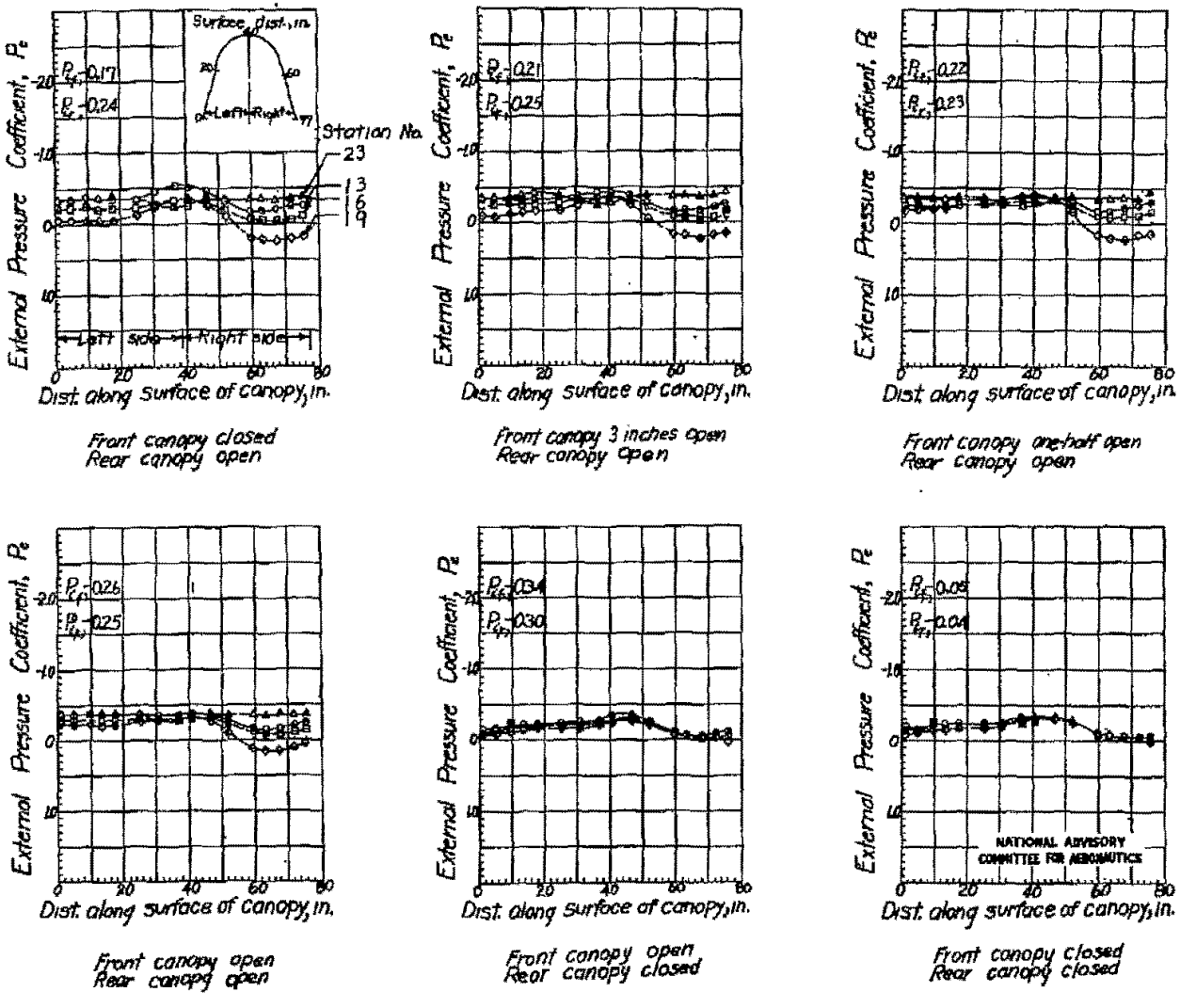

(a) Propeller removed, C_L, 0.96

Figure 17 .– Pressure distributions over the rear canopy of the SB2C-4E airplane. V_i, 115 deg.

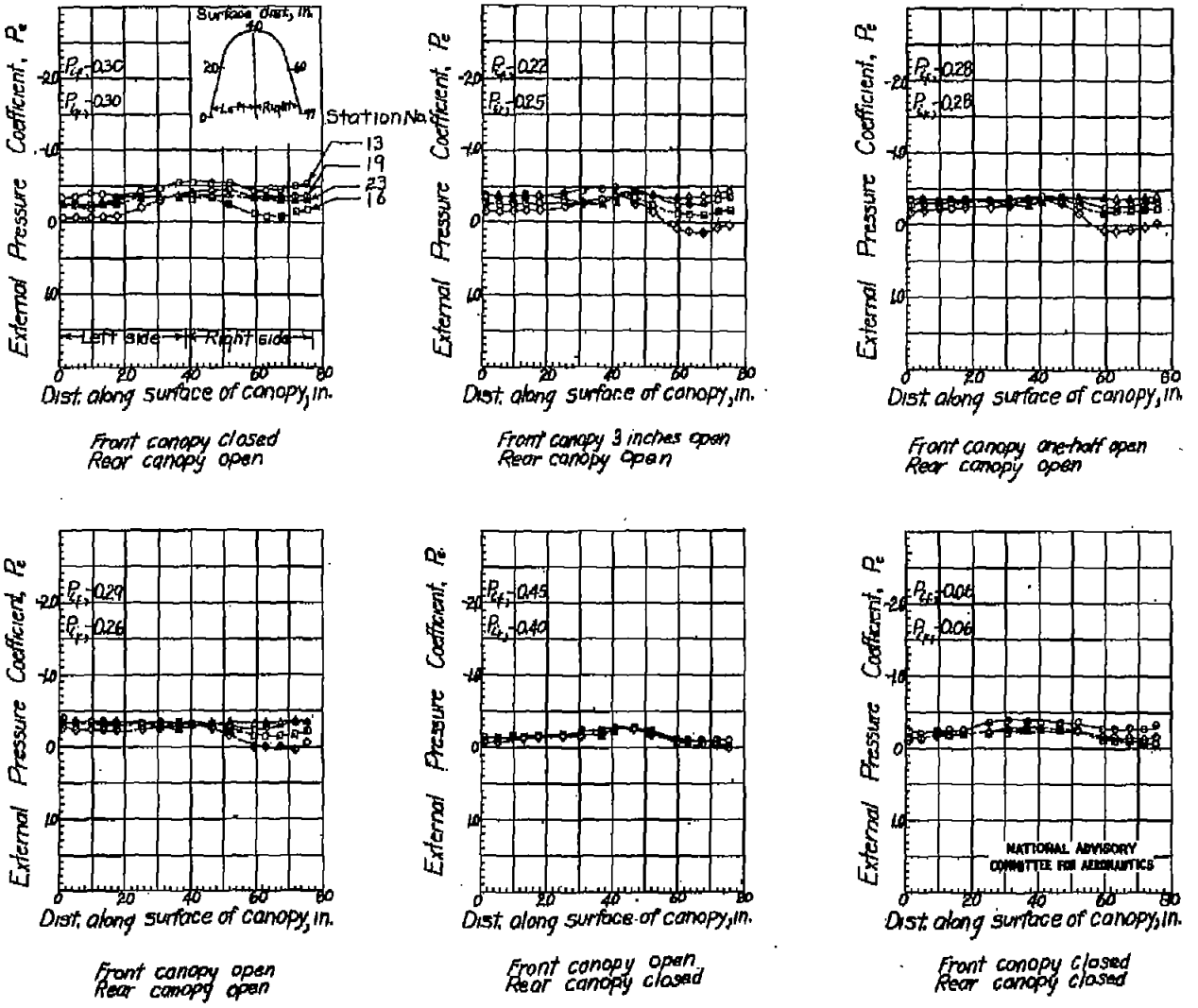

Front canopy closed
Rear canopy open

Front canopy 3 inches open
Rear canopy open

Front canopy one-half open
Rear canopy open

Front canopy open
Rear canopy open

Front canopy open
Rear canopy closed

Front canopy closed
Rear canopy closed

(b) Propeller removed; C_L, 1.33

Figure 17.- Concluded.

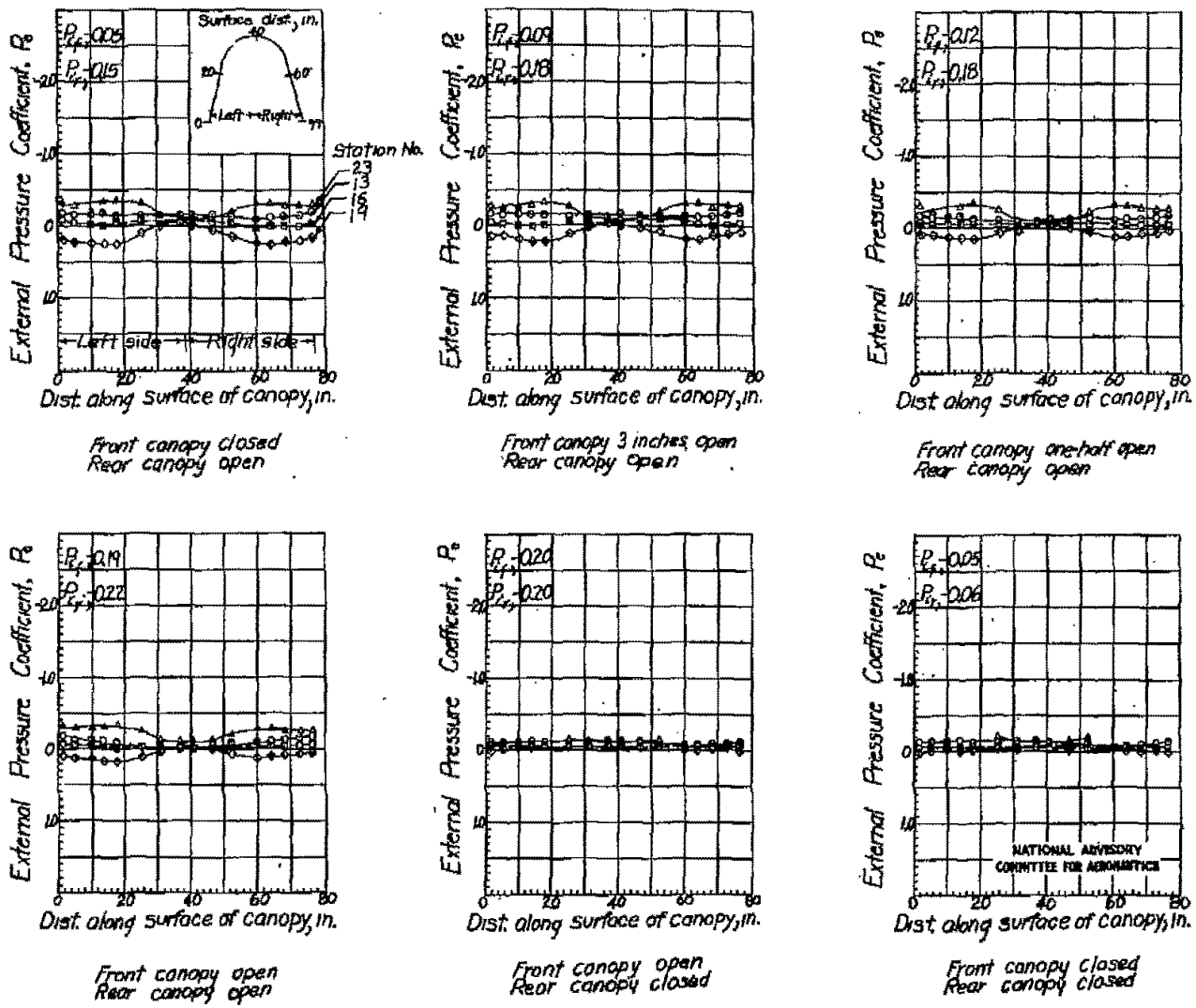

(a) Military power; T_c, 0.04; C_L, 0.17.

Figure 18 .- Pressure distributions over the rear canopy of the SB2C-4E airplane. ψ, 0 deg.

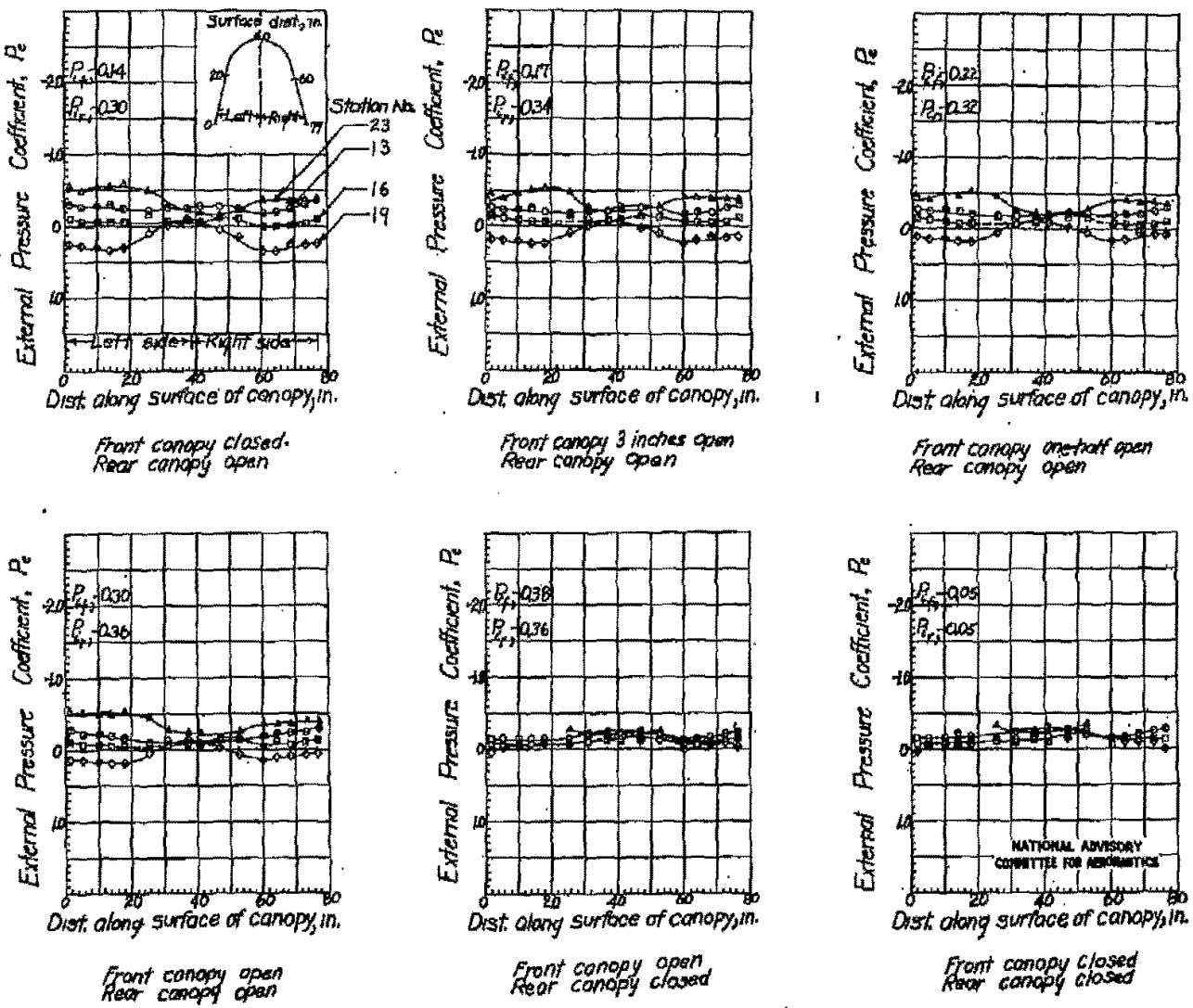

(b) Military power; T_c, 0.23; C_L, 0.56

Figure 18.- Continued.

Fig. 18b

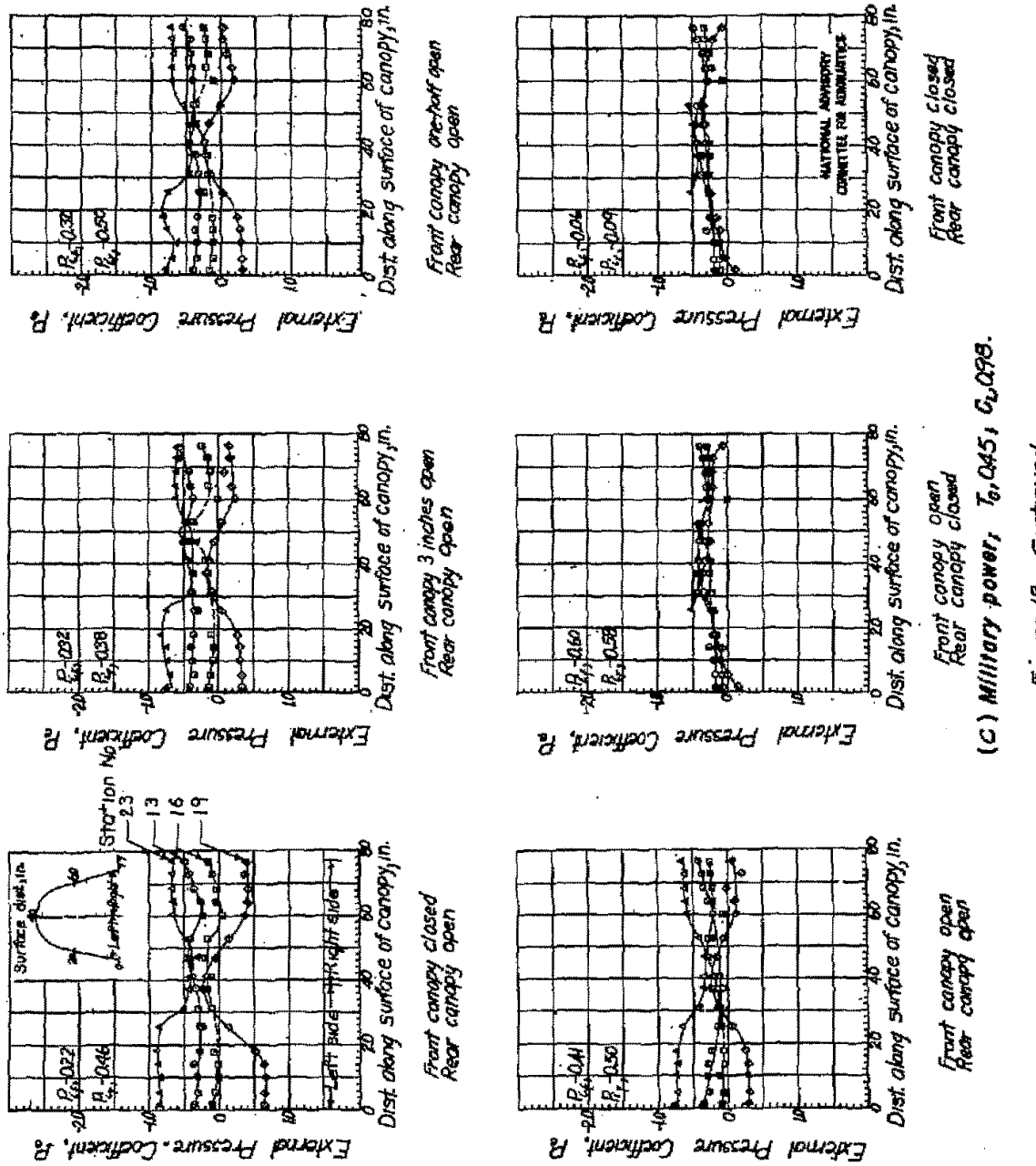

(c) Military power; T_0,045; G_0,098.

Figure 18.- Continued.

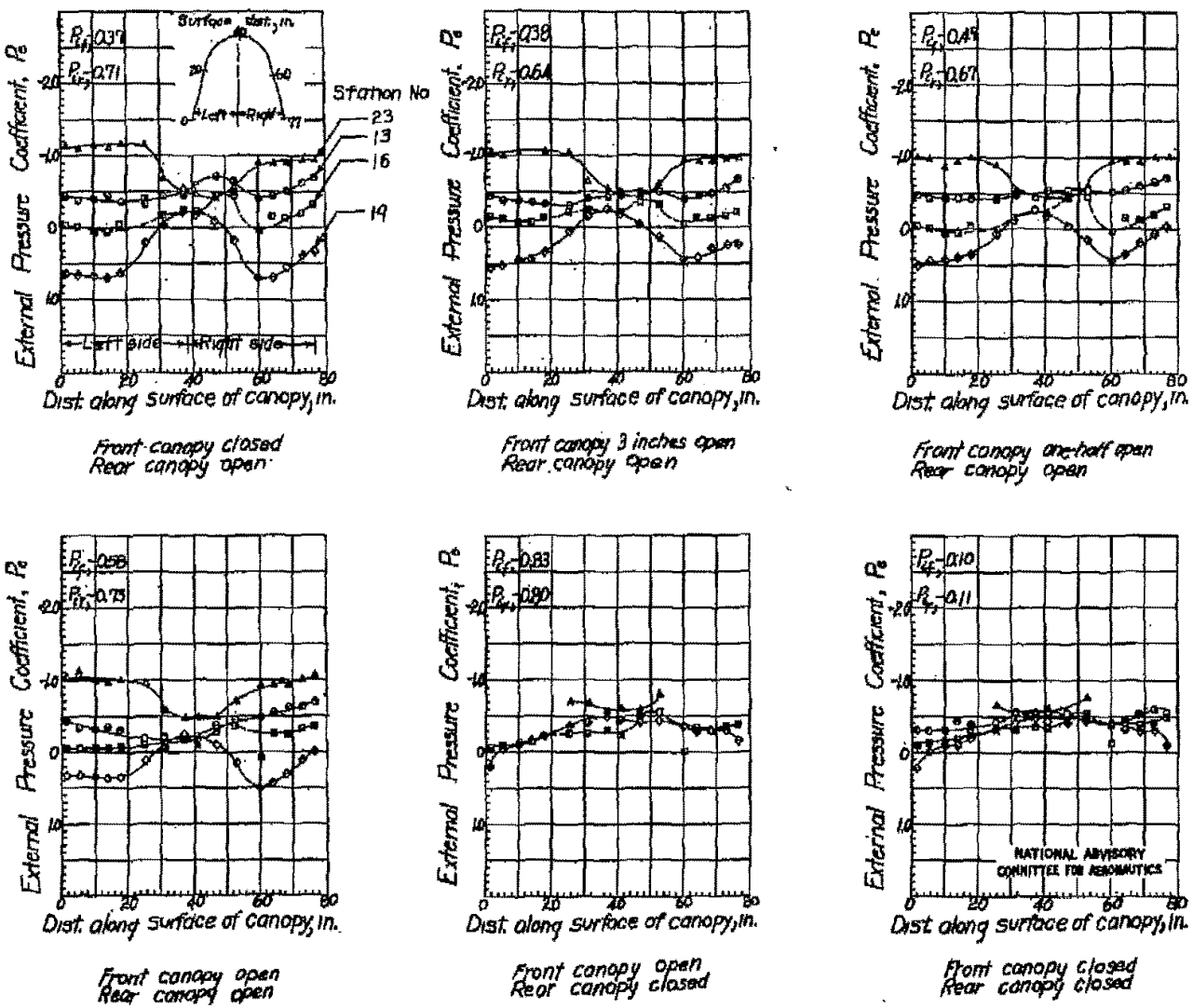

(d) Military power; T_c.063; C_L.133.

Figure 18 - Continued.

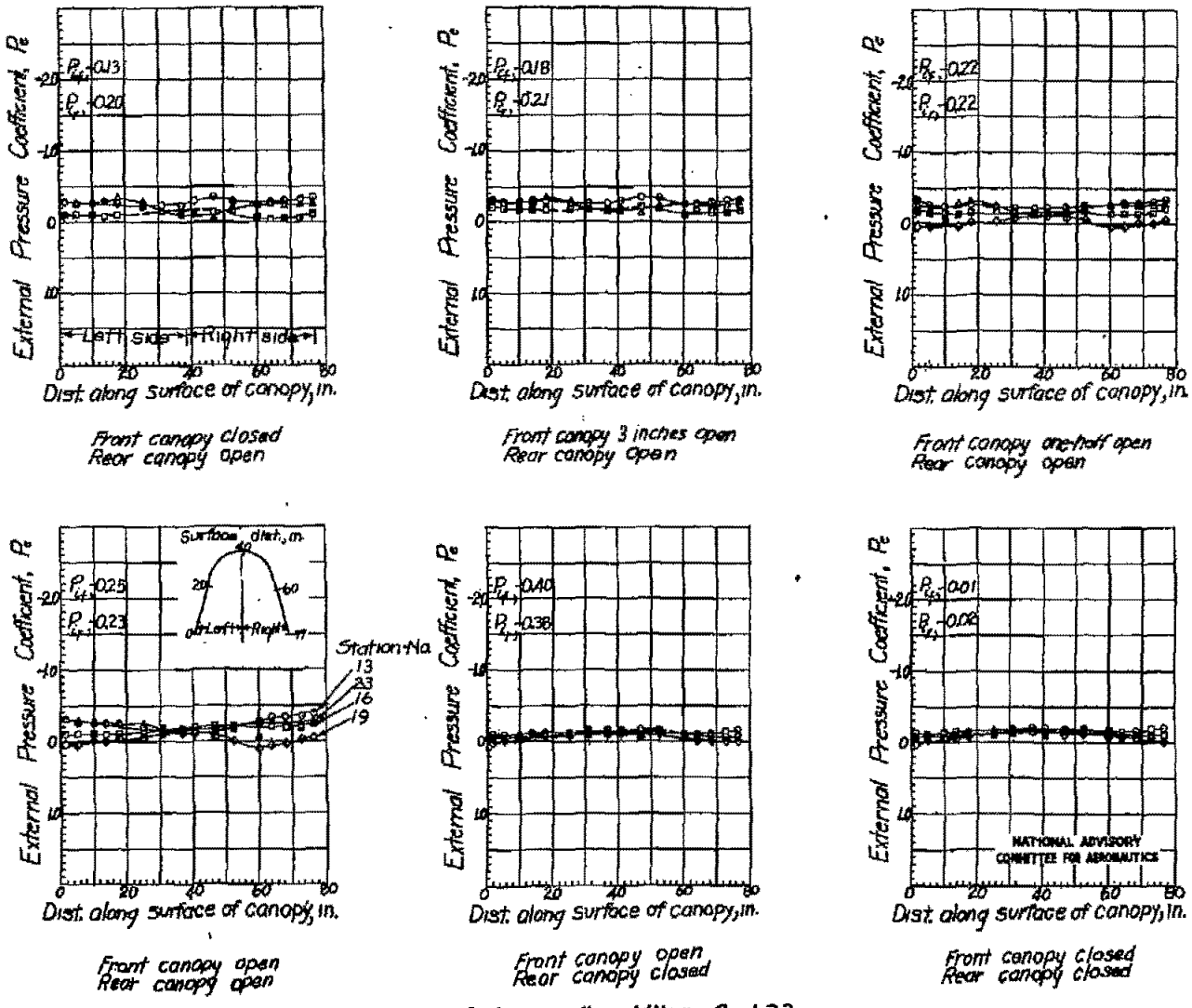

(e) Propeller idling; C_L, 1.33.

Figure 18.- Concluded.

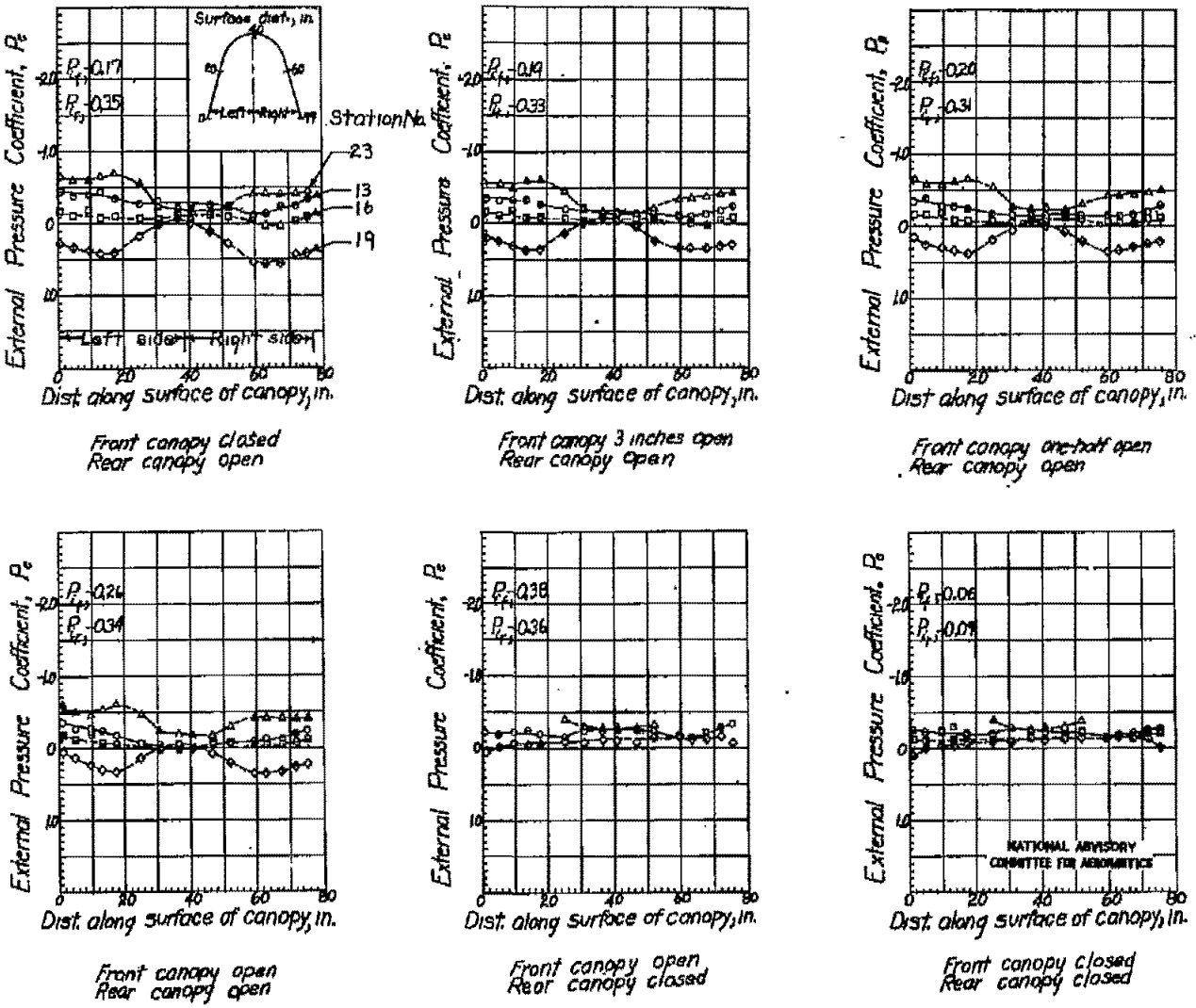

(a) Military power; T_c 0.023 ; C_L 0.56 .

Figure 19 .- Pressure distributions over the rear canopy of the SB2C-4E airplane. ψ, -7 deg.

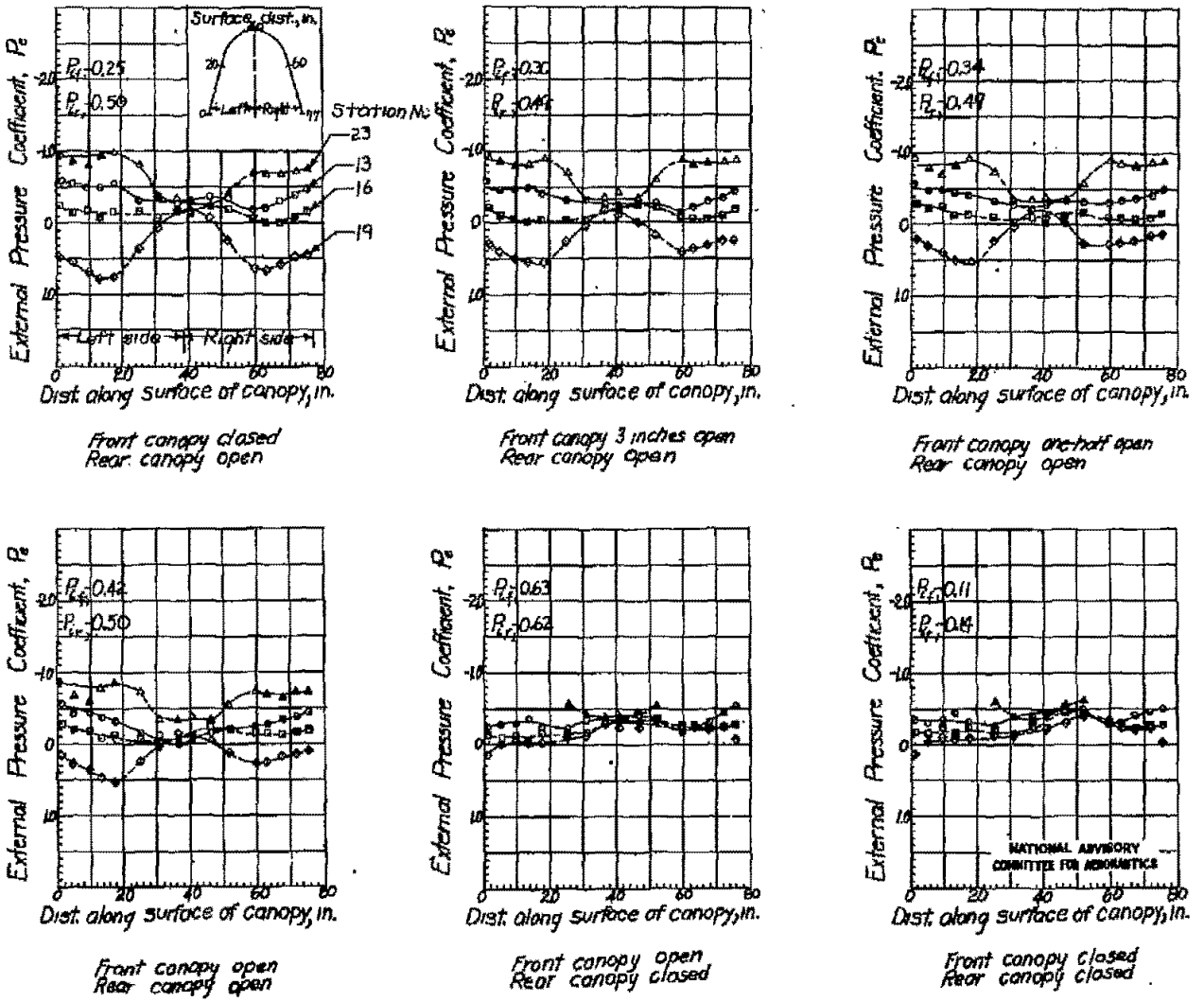

(b) Military power; T_c,045; C_L,098

Figure 19.-Continued.

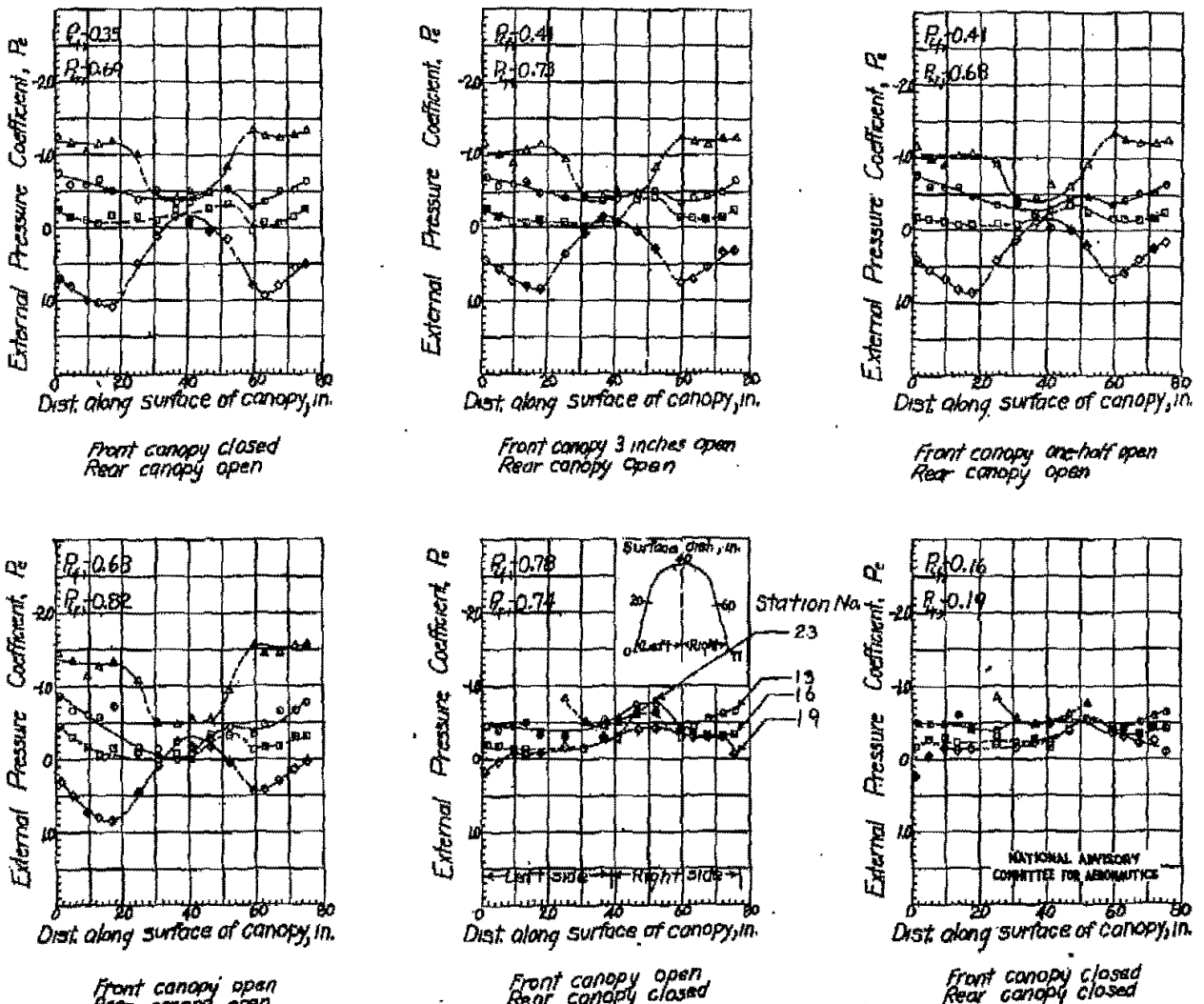

(c) Military power; T_c,063; C_L,1.33

Figure 19.- Continued.

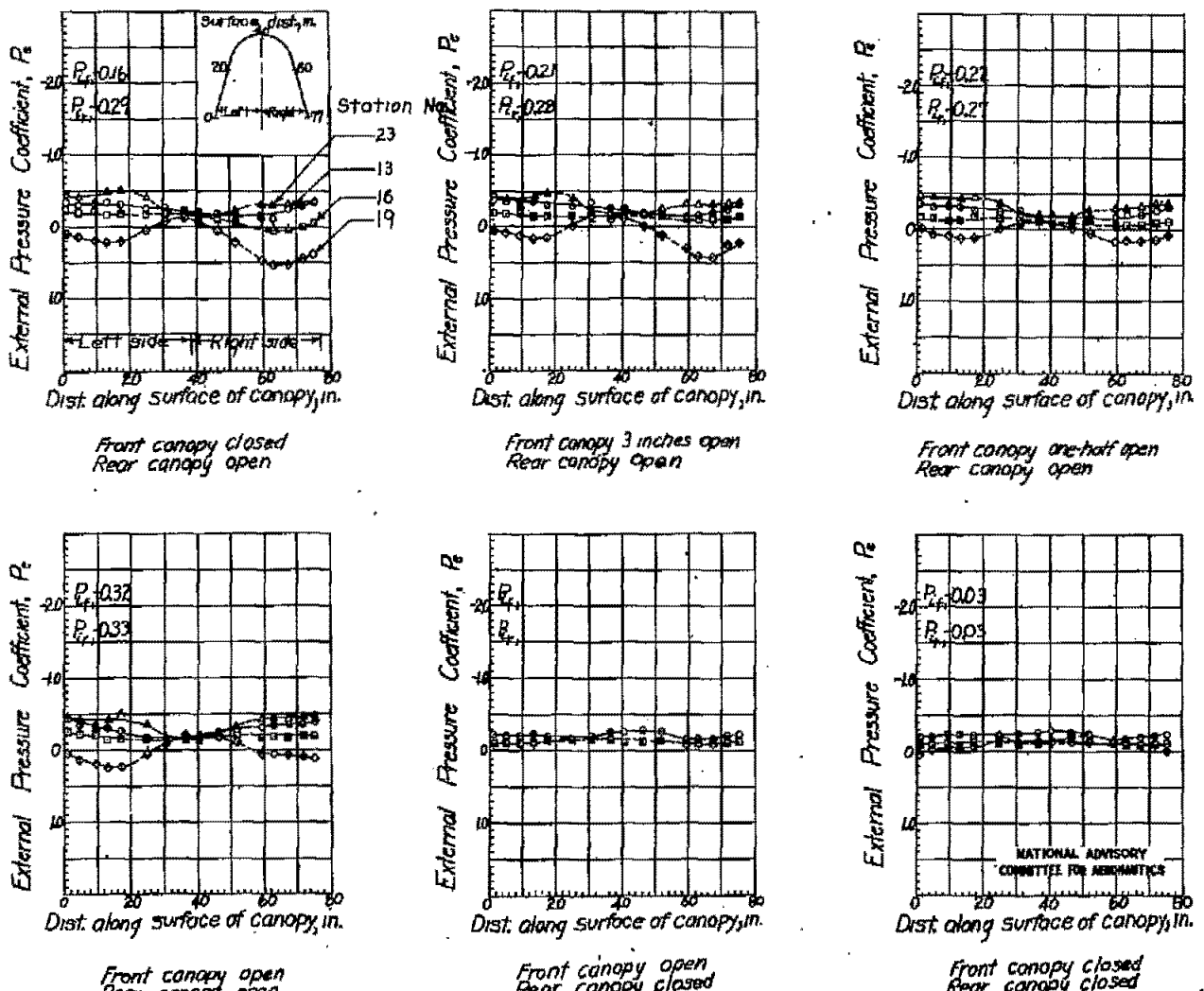

Front canopy closed
Rear canopy open

Front canopy 3 inches open
Rear canopy open

Front canopy one-half open
Rear canopy open

Front canopy open
Rear canopy open

Front canopy open
Rear canopy closed

Front canopy closed
Rear canopy closed

(d) Propeller idling; C_c 1.33.

Figure 19. – Concluded.

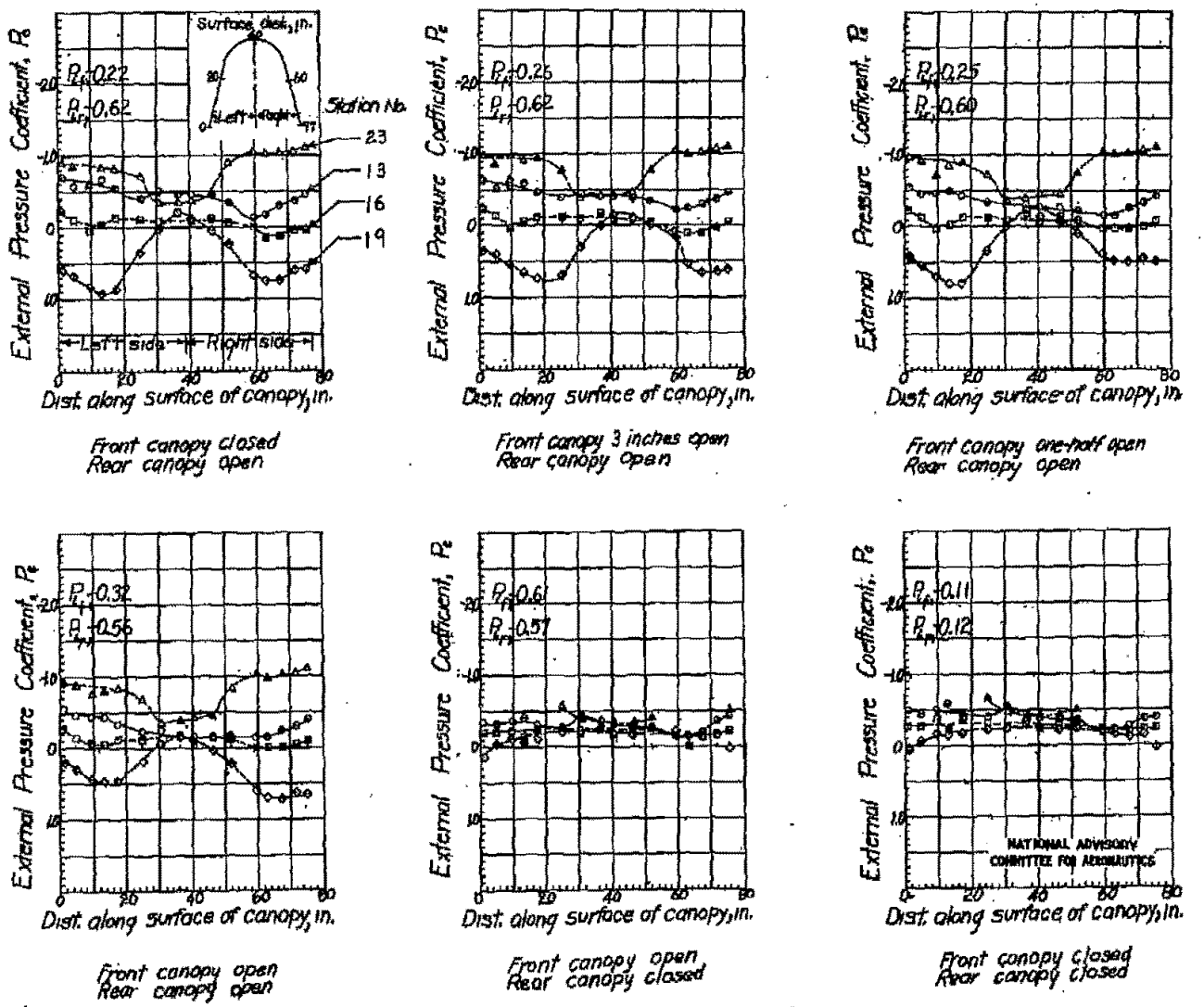

(a) Military power; T_c, 0.45; C_L, 0.98.

Figure 20 .- Pressure distributions over the rear canopy of the SB2C-4E airplane. ψ_t, -15 deg.

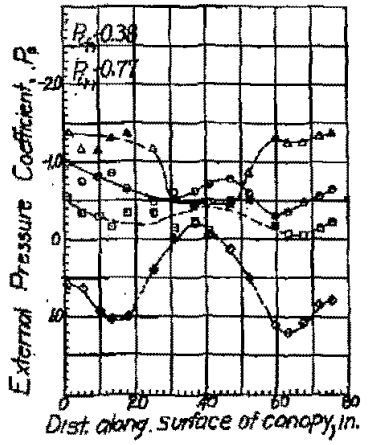

Front canopy closed
Rear canopy open

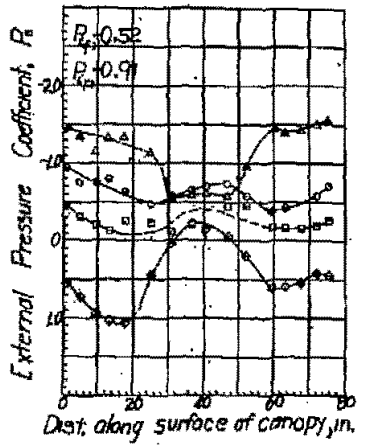

Front canopy 3 inches open
Rear canopy open

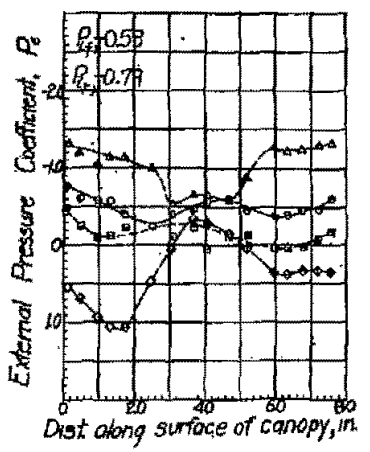

Front canopy one-half open
Rear canopy open

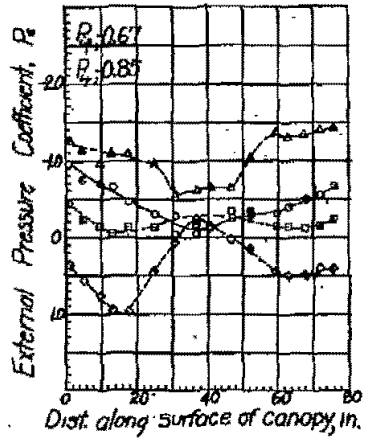

Front canopy open
Rear canopy open

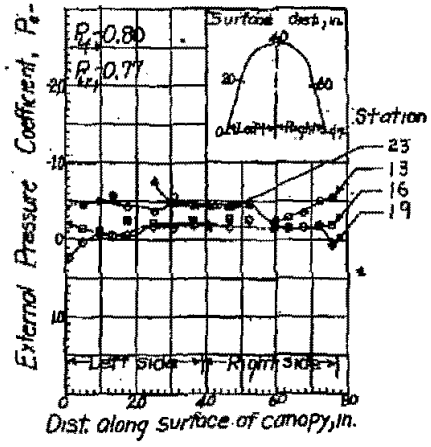

Front canopy open
Rear canopy closed

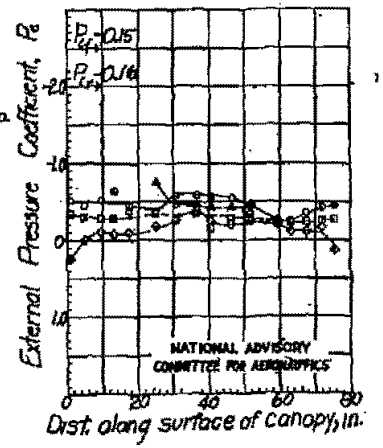

Front canopy closed
Rear canopy closed

(b) Military power; T_c 0.63; C_L 1.33

Figure 20.- Continued.

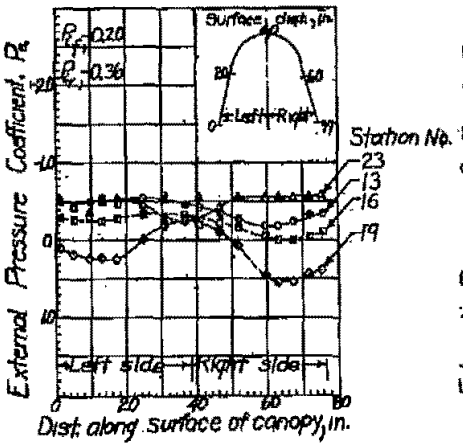

Front canopy closed
Rear canopy open

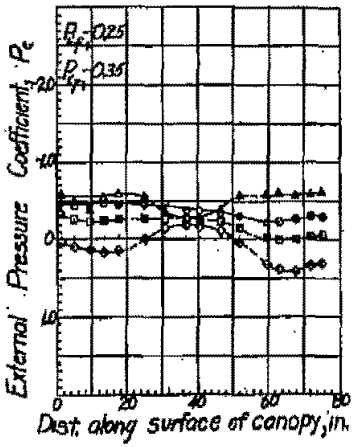

Front canopy 3 inches open
Rear canopy open

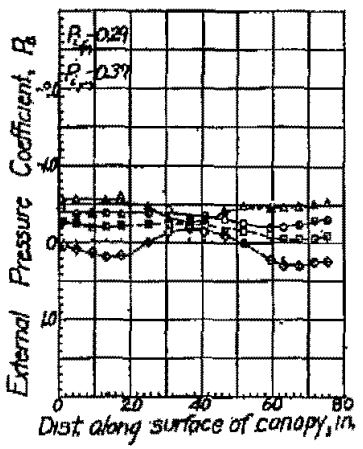

Front canopy one-half open
Rear canopy open

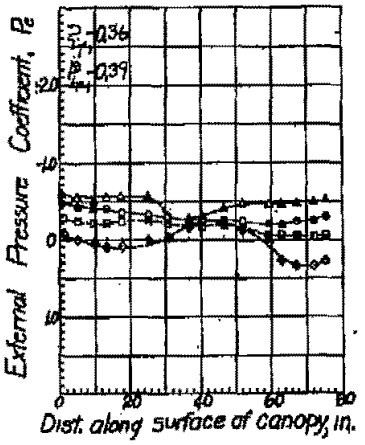

Front canopy open
Rear canopy open

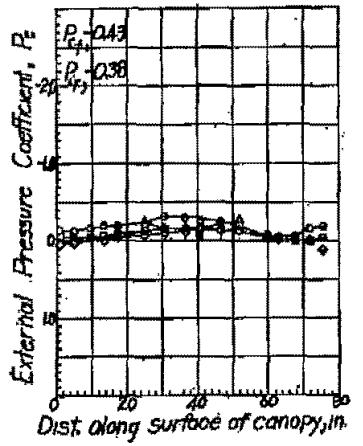

Front canopy open
Rear canopy closed

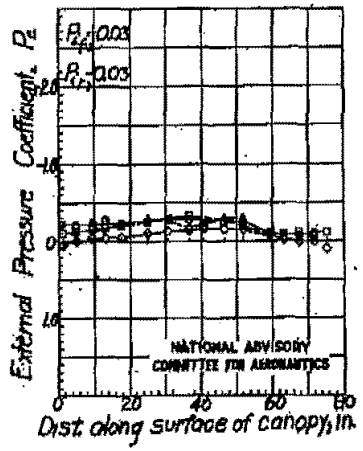

Front canopy closed
Rear canopy closed

(C) **Propeller idling; C_{L_1} 1.33.**

Figure 20.-Concluded.

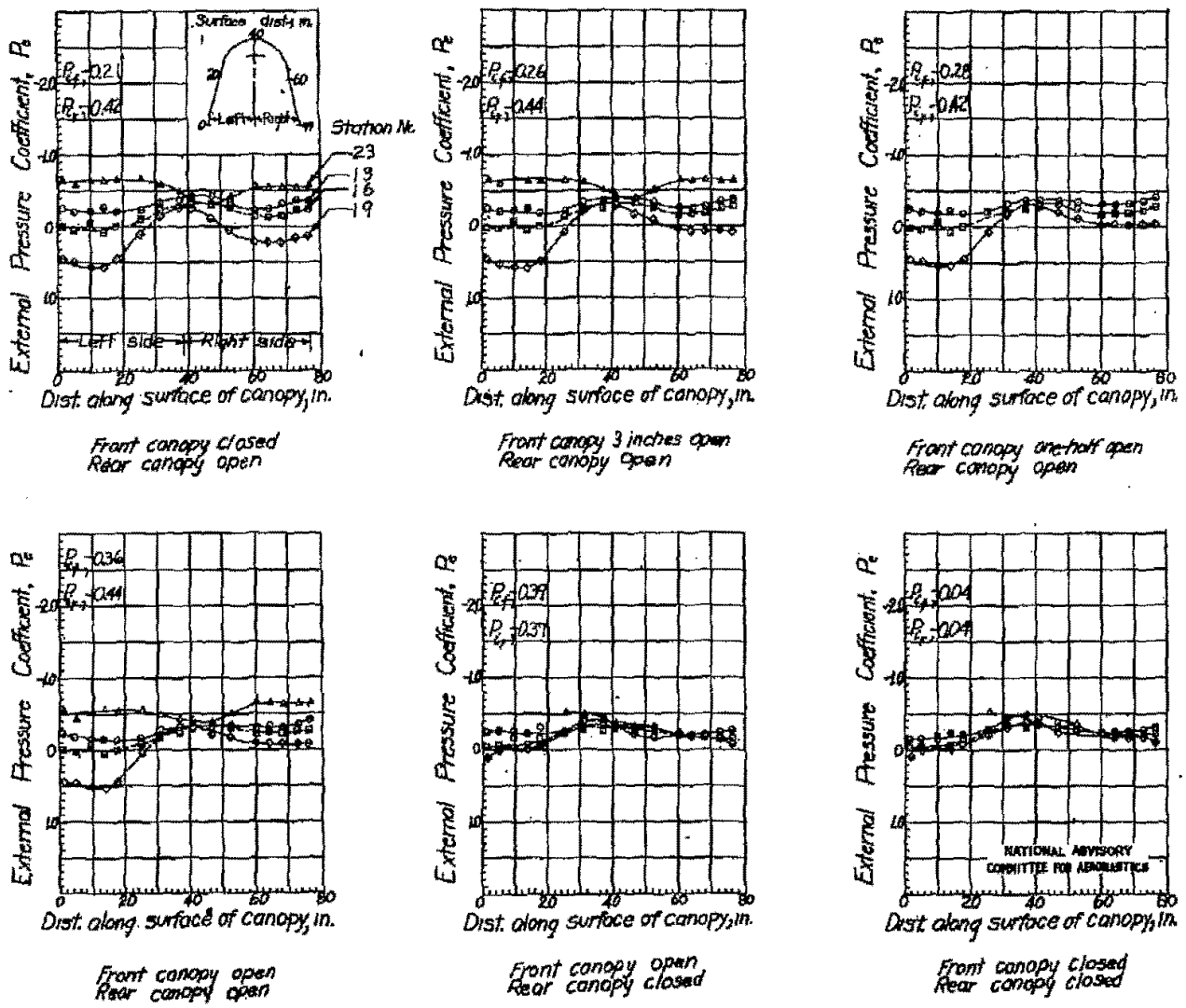

(a) Military power; T_c, 0.23; C_L, 0.56.

Figure 21 .- Pressure distributions over the rear canopy of the SB2C-4E airplane. ψ, 7 deg

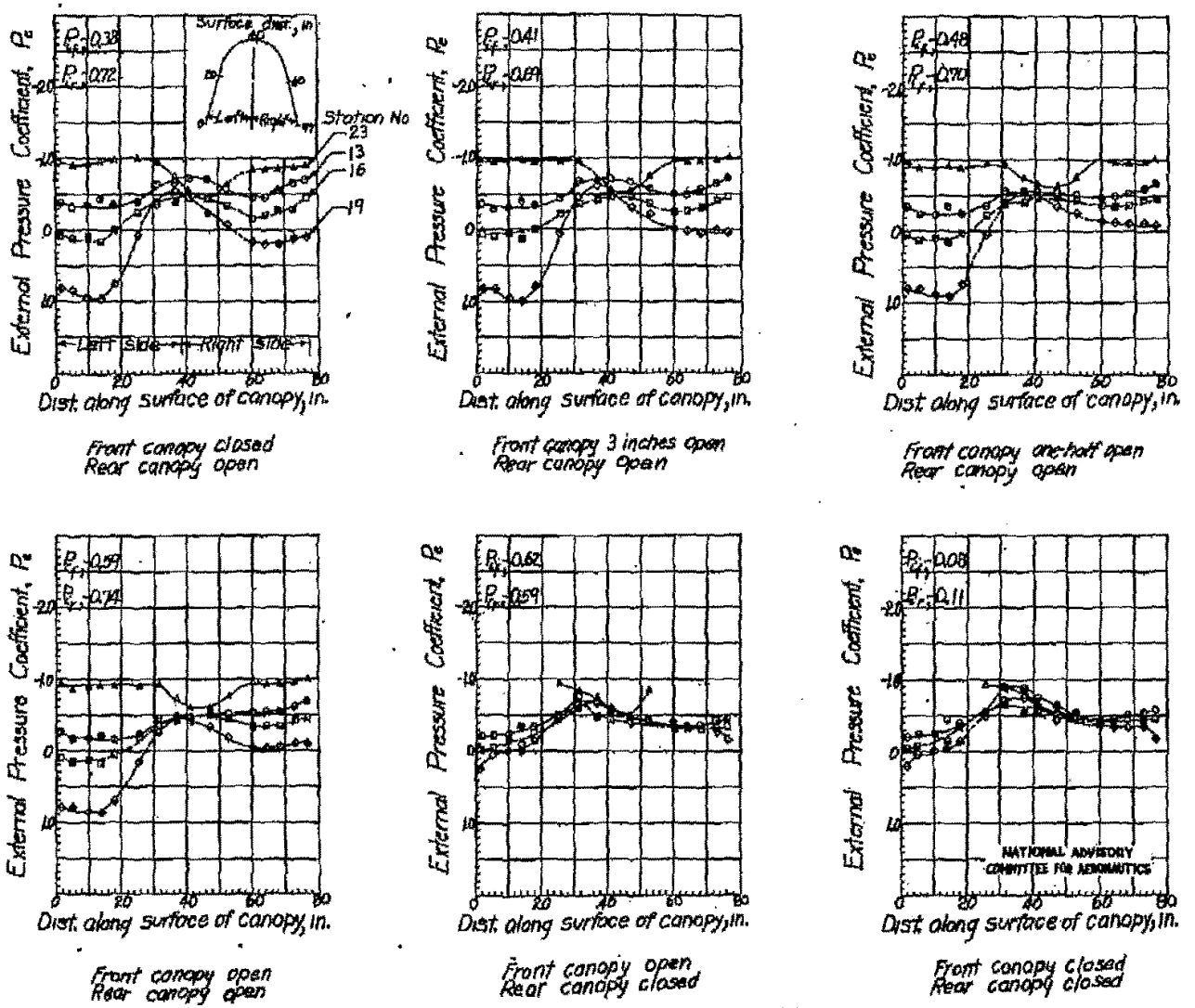

Front canopy closed
Rear canopy open

Front canopy 3 inches open
Rear canopy open

Front canopy one-half open
Rear canopy open

Front canopy open
Rear canopy open

Front canopy open
Rear canopy closed

Front canopy closed
Rear canopy closed

(b) Military power; T_c, 0.45; C_L, 0.98.

Figure 21.- Continued.

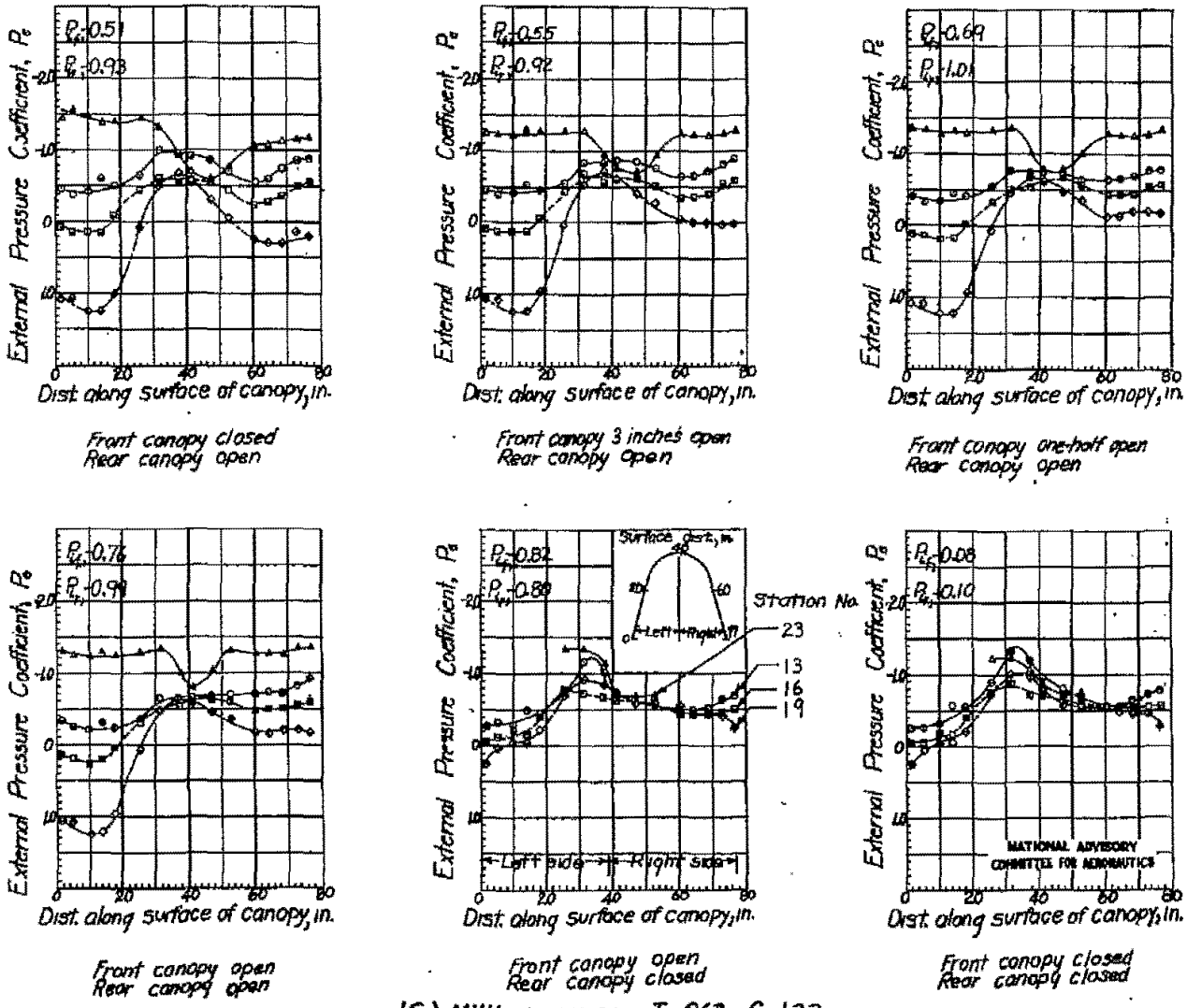

(C) **Military power;** T_c, 0.63; C_L, 1.33.

Figure 21.- Continued.

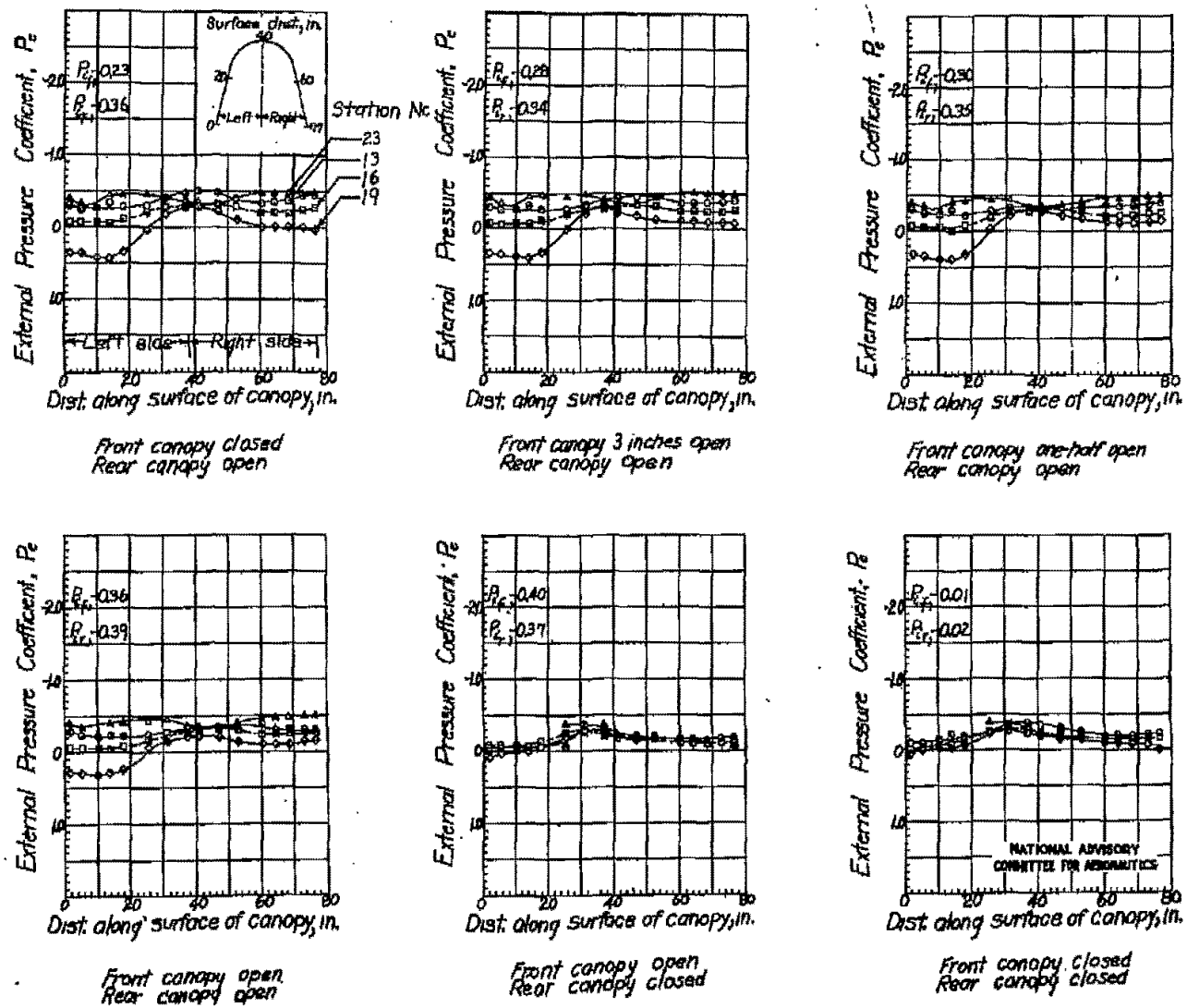

Front canopy closed
Rear canopy open

Front canopy 3 inches open
Rear canopy open

Front canopy one-half open
Rear canopy open

Front canopy open
Rear canopy open

Front canopy open
Rear canopy closed

Front canopy closed
Rear canopy closed

(d) Propeller idling; C_L, 1.33.

Figure 21.- Concluded.

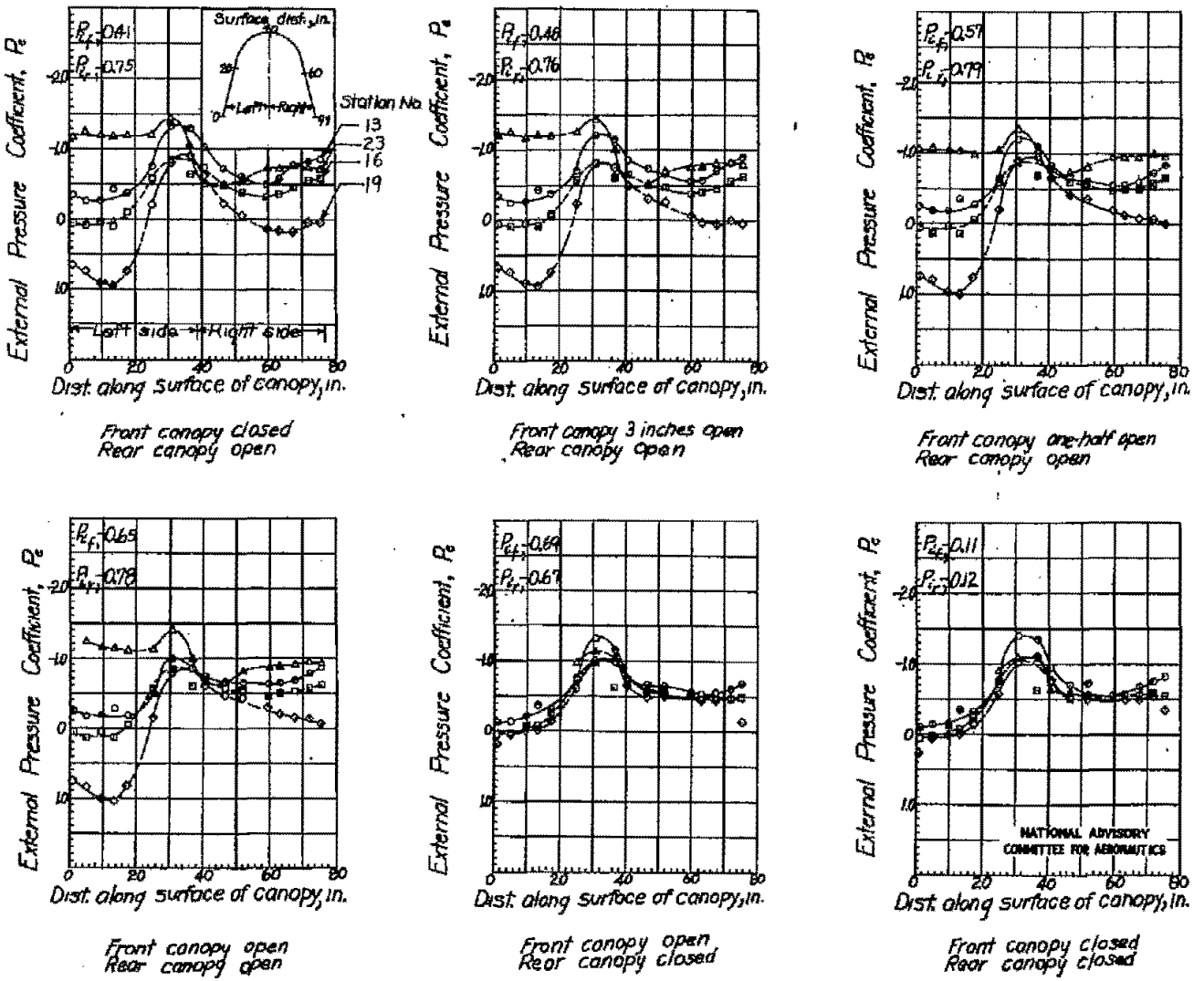

Figure 22.- Pressure distributions over the rear canopy of the SB2C-4E airplane. Ψ, 15 deg., Military power; T_c, 0.45; C_L, 0.98.